Westfälische
Wilhelms-Universität
Münster

Parameter Identification in Medical Imaging

Louise Reips

- 2012 -

WESTFÄLISCHE
WILHELMS-UNIVERSITÄT
MÜNSTER

Parameter Identification in Medical Imaging

Fach: Mathematik

Inaugural-Dissertation zur Erlangung des
Doktorgrades der Naturwissenschaften
im Fachbereich Mathematik und
Informatik der Mathematisch-Naturwissenschaftlichen Fakultät
der Westfälischen Wilhelms-Universität
Münster

vorgelegt von
Louise Reips
aus Ijuí- RS / Brasilien

- 2012 -

Dekan:	Prof. Dr. Martin Stein
Erster Gutachter:	Prof. Dr. Martin Burger (Westfälische Wilhelms-Universität Münster)
Zweite Gutachterin:	Prof. Dr. Barbara Kaltenbacher (Universität Klagenfurt)
Tag der mündlichen Prüfung:	
Tag der Promotion:	

Abstract

PET is an imaging technique applied in nuclear medicine able to produce images of physiological processes in 2D or 3D. The use of ^{18}F-FDG PET is now a widely established method to quantify tumour metabolism, but other investigations based on different tracers are still far from clinical use, although they offer great opportunities such as radioactive water as a marker of cardiac perfusion. A major obstacle is the need for dynamic image reconstruction from low quality data, which applies in particular for tracers with fast decay like $H_2^{15}O$.

Here we present a model-based approach to overcome those difficulties. We derive a set of differential equations able to represent the kinetic behavior of $H_2^{15}O$ PET tracers during cardiac perfusion. In this model one takes into account the exchange of materials between artery, tissue and vein which predicts the tracer activity if the reaction rates, velocities, and diffusion coefficients are known. We then interpretes, the computation of these distributed parameters as a nonlinear inverse problem, which we solve using variational regularization approaches. For the minimization we use the gradient-based methods and Forward-Backward Splitting.

The main advantage of this approach is the reduction of the degrees of freedom, which makes the problem overdetermined and thus allows to proceed to low quality data. Instead of reconstructing the 4D tracer activity distribution (in space and time) we identify a set of 3D parameters (spatially dependent only).

The major contribution of this work in relation to similar studies in the literature is that the differential equations model proposed here involves not only the portions of exchange of materials, but also we take into account the contributions due to diffusion and transport portions, making the proposed model more complex and thus more realistic.

Key words: Parameter Identification, Reaction, Diffusion, Transport, Inverse Problems, Imaging, Image Processing, Poisson Noise, Forward-Backward Splitting, Identifiability, Dynamic Positron Emission Tomography, Regularization Theory.

Acknowledgments

I want to thank

Martin Burger for giving me the opportunity to work on an interesting topic. Throughout the mathematical support for the elaboration of this thesis, for his patience and especially for being the example of Professor I want to follow throughout my professional career.

Barbara Kaltenbacher for co-reviewing this thesis and her sympathy.

Felipe Vieira, my beloved and dear husband, who is always by my side, in happy times and in difficultis also. His care, love and understanding made the development of this thesis and stay here much easier. Surely I can say that my life does not make sense without him.

My colleagues in research group, Ralf Engbers and Martin Benning, for the many mathematical discussions, my questions about the German language and for always opening a space in their agendas for my questions.

My classmate Marcisse, for the decontraction moments and the many conversations.

My colleagues in the 'Imaging' Workgroup: Alex Sawatzky, Jahn Müller, Christoph Brune, Frank Wübbeling, Michael Möller, Felix Lucka, Pia Heins, Hendrik Dirks, for the tips and their assistance in the final elaboration of this thesis and new friendships.

My brothers Lisiane and Jonas and my sister(-in-law) Cristiane that even in the most complicated moments were always pushing me so that I conclude this step more, and my mom Loreci (in memory) that is not even present in the body but always present in my life.

My friends, Gabriela Josko, Wojciech Jary, Varvara Sokolova, Houssaina Dridi, Belisa Zevallos Guarníz, Artem Nikiforov, Hêvron Mohamad, for the decontraction moments and for making these last years very special.

And all those that deserve to be mentioned here but I have been forgotten. Thanks!!!

“ The LORD is my shepherd, I shall not be in want.”
Psalm 23:1

Contents

List of Tables

Nomenclature

$\mathbb{N}$	The set of natural numbers
$\mathbb{N}_0$	The set of natural numbers and zero
$\mathbb{Z}$	The set of integer numbers
$\mathbb{R}$	The set of real numbers
$\mathbb{R}_{>0}$	The set of positive real numbers
$\mathbb{R}_{\geq 0}$	The set of nonnegative real numbers
$\mathbb{R}^n$	The n-dimensional vector space with elements in $\mathbb{R}$
$\mathcal{X}$	A (real) Banach space
$\|\|u\|\|_{\mathcal{X}}$	The norm mapping for $u \in \mathcal{X}$
$\mathcal{K}(\mathcal{X}, \mathcal{Y})$	The space of all linear operators $M : \mathcal{X} \to \mathcal{Y}$
$\mathcal{X}^*$	The dual space of $\mathcal{X}$
$\mathcal{H}$	A Hilbert space
$dom(P)$	The effective domain of a functional $P : \mathcal{X} \to \mathbb{R} \cup \{+\infty\}$
$d_y P(x)$	The directional derivative of P at x in direction y
$d^2_{y,w} P(x)$	The second directional derivative of P at x in direction w
$dP(x)$	The Gâteaux-derivative of P
$P^{'}$	The Fréchet-derivative of P
$\rightharpoonup$	Convergence in the weak topology
$\rightharpoonup^*$	Convergence in the weak-* topology
H^1	A Hilbert space
H^{-1}	The dual space of H^1
L^2	A Hilbert space
L^{-2}	The dual space of L^2
$\hookrightarrow$	Injection
ξ	Poisson statistics
K	Linear operator
$\mathcal{R}$	The regularization functional
V	A vector space
$\langle p, x \rangle_{\mathcal{X}}$	The dual product, see e.q (2.2)

$L^p(\Omega)$	The space of Lebesgue measurable functions such that $\|\|f\|\|_{L^p(\Omega)} < \infty$ holds
$W(a, b; H^1, H^{-1})$	The space of Sobolev functions
$L^p_{\geq 0}(\Omega)$	All positive functions $f \in L^p(\Omega)$
$C_{\mathcal{A}}$	The radioactive concentration in the artery
$C_{\mathcal{T}}$	The radioactive concentration in the tissue
$C_{\mathcal{V}}$	The radioactive concentration in the vein
$V_{\mathcal{A}}$	The velocity parameter in the artery
$V_{\mathcal{T}}$	The velocity parameter in the tissue
$V_{\mathcal{V}}$	The velocity parameter in the vein
$D_{\mathcal{A}}$	The diffusion parameter in the artery
$D_{\mathcal{T}}$	The diffusion parameter in the tissue
$D_{\mathcal{V}}$	The diffusion parameter in the vein
k_1	The exchange of fluids from artery to the tissue
k_2	The exchange of fluids from tissue to the vein
k_3	The exchange of fluids from vein to the artery
$k_0 C_{\mathcal{A}}$	The radioactive decay in the artery
$k_0 C_{\mathcal{T}}$	The radioactive decay in the tissue
$k_0 C_{\mathcal{V}}$	The radioactive decay in the vein
$const$	Constant
p	Vector containing all physiological parameters
$IM(u)$	The image reconstruction process of u
$D(A)$	A subspace of H^1
$\mathfrak{V}$	A dense subspace of H^1
H^1_m	The Galerkin approximation or order m of H^1
λ	The Lagrange multiplier ($\lambda \geq 0$)
$KL(f, F(p))$	The Kullback - Leibler functional
$V_\mu(\Omega)$	A Banach space of functions with respect to the measure μ
I	The functional I, see (4.15)
$\mathcal{D}(I)$	The effective domain of I
$\mathcal{S}_{\mathcal{R}}$	The sub-level sets of the regularization functional $\mathcal{R}$
$L^2_\mu(\Omega)$	The Lebesgue spaces $L^2(\Omega)$ with respect to the measure μ
α	The a-priori regularization parameter
ξ	The gradient regularization parameter
iff	If and only if

1 Introduction

Inverse Problems are focus of current research interest in industrial applications (as the identification of parameters in industrial processes) **[37, 46, 55]**, applications to geophysics **[64, 101]**, tomography and medical sciences (detection of tumors and fractures) **[12, 74, 81, 82]**. They are systems that, based on observed measurements, allow us to obtain information about a physical object or system which we are interested in.

Here we will focus on the use of inverse problems involving image reconstruction. The reconstruction of images has a significant impact in several areas of applied sciences, such as astronomy, microscopic imaging and especially in medical imaging techniques have a high diagnostic value because they allow the visualization of anatomical information and physiological effects.

The main objective of this thesis is the reconstruction of kinetic behavior of radioactive water $H_2^{15}O$ during cardiac perfusion based on real PET-data. We want also formulate the parameter identification problem associated with the inverse problem in question and solve it in order to reconstruct the kinetic parameters that compose the model of differential equations (which represents the kinetic behavior of $H_2^{15}O$) proposed in this work. The disadvantages arising from the short radioactive half-life (for $H_2^{15}O \approx 2$ min) are noise and low-resolution reconstructions. We present here the tools which allow the reconstruction of biological parameters in question.

In the following section, we want to recall the basic motivations and the contributions of this thesis. Finally, we provide a sketch of how this thesis is organized.

Figure 1.1: Image of a typical positron emission tomography (PET). © Wikipedia

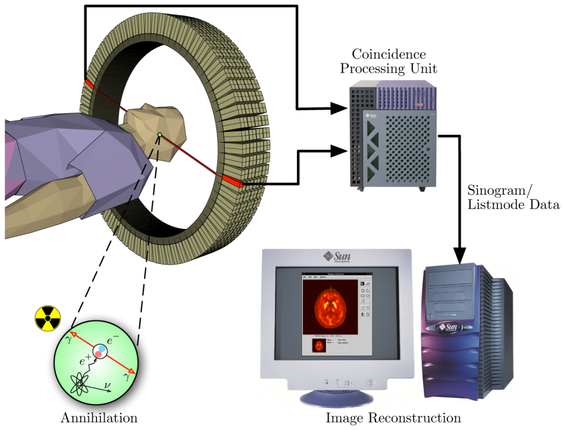

Figure 1.2: Schema of a PET acquisition process. © Wikipedia

1.1 Motivation

Positron Emission Tomography is an imaging technique applied in nuclear medicine able to produce images of physiological process in 2D or 3D. In comparison to other imaging techniques with higher spatial resolution, the major advantage of the PET procedure is the high sensitivity and ability for quantitative measurement, making it possible to visualize and to examine specific physiological effects inside the body.

Besides from being a minimally invasive examination and therefore causing less patient discomfort, PET allows the development of better diagnostic imaging, detecting and monitoring the activity of malignant tumors, as well as a better treatment of patients. Many methods to analyze PET data have been developed based on compartmental models such as cerebral oxygen utilization [**78**], neuroreceptor ligand binding [**77**] and the quantification of blood flow [**2, 10, 11, 68, 70**].

The procedure is simple and PET will be explained below. Usually glucose connected to a radioactive element is injected into the patient (normally into the blood circulation). The radioactive tracer then spreads through the blood circulation and the regions that metabolize the excess of glucose, such as tumors, are highlighted in the image created by the computer. Figure 1.1[1] shows an example for a typical PET-scanner that produces data to process images.

The emission of positrons occurs when the radioactive tracer isotope decays. These positrons are the antimatter counterparts of electrons. Thus, the electrons annihilate with positrons and produce a pair of gamma photons that travel into opposite directions. The photons are detected during the

[1] http://upload.wikimedia.org/wikipedia/commons/b/b8/ECAT-Exact-HR–PET-Scanner.jpg

PET-scan. Each pair of detectors defines a line along which the intensity of the annihilation is measured. This intensities along lines can be described via line integrals and the data are stored by a sinogram before the reconstruction. The process is schematically described in Figure 1.2[2].

With the given PET sinogram data $f(\theta, y)$ the inverse problem of generating an image $u(x)$ from this data is to compute u from

$$f = \xi(Ku) \tag{1.1}$$

where ξ represents the Poisson statistics and K denotes the X-ray transform, defined by

$$Ku(\theta, x) = \int_{\mathbb{R}} u(x + t\theta)dt, \quad x + t\theta \subseteq \Omega \tag{1.2}$$

In the 2D case the X-Ray transform is equivalent to the more popular Radon Transform.

The biggest disadvantage of working with inverse problems is that the data f are corrupted by noise, especially, because the problem is usually ill-posed in the sense of Hadamard **[49]**. One problem is called well-posed if it satisfies the conditions of existence, uniqueness and continuous dependence on data. If any of these requirements is not satisfied, the problem is called ill-posed. This instability and ill-conditioning must be overcome if we want to solve the inverse problem satisfactorily. This problem is also transferred to a nonlinear parameter identification problem which we add regularization methods to each biological parameters (that we want to reconstruct) independently and to transform the ill-posed problem in a well-posed.

A solution for this inverse problem is given via the minimization below

$$\begin{aligned} & u \in \arg\min_{u\in\Omega} \left\{ \int_{\Omega} Ku - flog(Ku)d\sigma(\theta, y) + \alpha\mathcal{R}(u) \right\} \\ \Rightarrow & u \in \arg\min_{u\in\Omega} \left\{ \int_{\Omega} flog\left(\frac{f}{Ku}\right) + Ku - fd\sigma(\theta, y)d\sigma(\theta, y) + \alpha\mathcal{R}(u) \right\} \end{aligned} \tag{1.3}$$

where $\mathcal{R}$ is a regularization fuctional (gradient and a-priori regularization) and penalizes the deviation from a ideal (smooth) solution u.

The solution of the minimization problem presented above as well as the calculation of all physiological parameters involved in this process with application in medical science, more specifically in positron emission tomography, is the biggest motivation of this thesis. Based on the statements

[2] http://upload.wikimedia.org/wikipedia/commons/c/c1/PET-schema.png

above we summarize the contribuitions of this work in the following section.

1.2 Contributions

We propose in this thesis a set of differential equations to represent the kinetic behavior of PET-data during cardiac perfusion. This model is flexible in the sense that one can consider only two differential equations that take into account only the exchange of materials between artery and tissue

$$\frac{\partial C_{\mathcal{A}}}{\partial t} = -(l_0(x)+l_1(x))C_{\mathcal{A}}(x,t)+l_3(x)C_{\mathcal{T}}(x,t)+\nabla\cdot(V_{\mathcal{A}}(x)C_{\mathcal{A}}(x,t))+\nabla\cdot(D_{\mathcal{A}}(x)\nabla C_{\mathcal{A}}(x,t)) \quad (1.4)$$

$$\frac{\partial C_{\mathcal{T}}}{\partial t} = -(l_0(x)+l_2(x))C_{\mathcal{T}}(x,t)+l_1(x)C_{\mathcal{A}}(x,t)+\nabla\cdot(V_{\mathcal{T}}(x)C_{\mathcal{T}}(x,t))+\nabla\cdot(D_{\mathcal{T}}(x)\nabla C_{\mathcal{T}}(x,t)) \quad (1.5)$$

Or even with the aid of a third equation, we can represent a more complex system involving artery, tissue and vein:

$$\frac{\partial C_{\mathcal{A}}}{\partial t} = -(k_0(x)+k_1(x))C_{\mathcal{A}}(x,t)+k_3(x)C_{\mathcal{V}}(x,t)+\nabla\cdot(V_{\mathcal{A}}(x)C_{\mathcal{A}}(x,t))+\nabla\cdot(D_{\mathcal{A}}(x)\nabla C_{\mathcal{A}}(x,t)) \quad (1.6)$$

$$\frac{\partial C_{\mathcal{T}}}{\partial t} = -(k_0(x)+k_2(x))C_{\mathcal{T}}(x,t)+k_1(x)C_{\mathcal{A}}(x,t)+\nabla\cdot(V_{\mathcal{T}}(x)C_{\mathcal{T}}(x,t))+\nabla\cdot(D_{\mathcal{T}}(x)\nabla C_{\mathcal{T}}(x,t)) \quad (1.7)$$

$$\frac{\partial C_{\mathcal{V}}}{\partial t} = -(k_0(x)+k_3(x))C_{\mathcal{V}}(x,t)+k_2(x)C_{\mathcal{T}}(x,t)+\nabla\cdot(V_{\mathcal{V}}(x)C_{\mathcal{V}}(x,t))+\nabla\cdot(D_{\mathcal{V}}(x)\nabla C_{\mathcal{V}}(x,t)) \quad (1.8)$$

Then we consider in this work the elaboration of the parameter identification problem that, by solving a minimization problem, allows the reconstruction of a sequence of images and dynamic parameters in positron emission tomography or fluorescence recovery after photobleaching (FRAP) [**23**].

As a further contribution in this thesis, we present also the results of the computational simulation of the equations that describe the model to real PET-data.

1.3 Organization of this Work

The *Chapter 2* is designed to provide the mathematical tools needed in the course of this work. We present here basic concepts of functional analysis and variational calculus, as also the definition of ill-posed problems.

In *Chapter 3* we discuss the model proposed here, consisting of three differential equations, with the objective to reconstruct kinetic behavior of radioactive water $H_2^{15}O$ during cardiac perfusion. We also present a section devoted specifically to the existence and uniqueness of solution of the problem.

In *Chapter 4* we work on the parameter identification problem associated with the proposed model. This section involves basic concepts of inverse problems, Expectation Maximization algorithms and Regularization.

The *Chapter 5* consists of a discussion about the identifiability of constant parameters in the system described by the parabolic differential equations proposed here.

The *Chapter 6* is intended for the numerical solution with a brief discussion involving the combination of EM-algorithm with the parameter identification problem to the resolution of the problem. We also discuss how the discretization of the differential equations is made and also we discuss methods used to solve the minimization problem.

Finally, in *Chapter 7* we present the computational results with the reconstruction of all parameters and of the image that represents the physiological process on synthetic and real data in positron emission tomography.

2

Mathematical Foundations

This chapter is designed to provide the basic mathematical tools needed in the course of this work. *Section 2.1*, *2.2* consist of basic concepts of linear spaces (Banach, Hilbert and Sobolev Spaces) and their properties. Below we approach some basic concepts about ill-posed problems. Therefore we present questions involving Variational Calculus and Lebesgue Spaces with concepts widely used in *Chapter 5*. Finally the last section is designed to Sobolev Space and their properties.

2.1 Banach Spaces

We present here some definitions involving the Banach and Hilbert Spaces and also dual spaces, based on **[51]**.

Definition 2.1.1 *Let V be a (real or complex) vector space. A norm on V is a real - valued function, written $||x||$ such that*

1.) $||x|| > 0$ *for all* $x \in V$ *and* $||x|| = 0$ *implies* $x = 0$.

2.) $||\alpha x|| = |\alpha|||x||$ *for all scalar* α *and vector* x.

3.) $||x + y|| \leq ||x|| + ||y||$ *(triangle inequality).*

A vector space with a norm is called a normed space.

Definition 2.1.2 *A Banach space is a complete, normed linear space.*

Definition 2.1.3 *If a normed real vector space $\mathcal{X}$ is complete, it is called (real) Banach space, i.e,* *if any Cauchy sequence $(x_n)_{n\in\mathbb{N}}$ has a limit $x \in \mathcal{X}$, more specifically if*

$$\lim_{m,n\to\infty} ||x_m - x_n||_{\mathcal{X}} = 0$$

holds, then exists a function $x \in \mathcal{X}$ with $\lim_{n\to\infty} ||x_n - x||_{\mathcal{X}} = 0$.

Definition 2.1.4 *Let $\mathcal{K}(\mathcal{X}, \mathcal{Y})$ be the space of all linear operators $M : \mathcal{X} \to \mathcal{Y}$ that are bounded in the sense that*

$$||M||_{\mathcal{X},\mathcal{Y}} := \sup_{||x||_{\mathcal{X}}=1} ||Mx||_{\mathcal{Y}} < \infty \tag{2.1}$$

holds. The space $\mathcal{K}(\mathcal{X}, \mathcal{Y})$ is a normed space with operator norm $||\cdot||_{\mathcal{X},\mathcal{Y}}$.

Theorem 2.1.5 *If $\mathcal{Y}$ is a Banach space then $\mathcal{K}(\mathcal{X}, \mathcal{Y})$ is a Banach space.*

2.1.1 Dual Spaces

The dual space of a linear space consists of the scalar-valued linear maps on the space. Duality methods play a crucial role in many parts of analysis.

Definition 2.1.6 *(Dual Space) Let $\mathcal{X}$ be a Banach space. The space $\mathcal{X}^* : \mathcal{K}(\mathcal{X}, \mathbb{R})$ bounded of linear functionals on $\mathcal{X}$ is called dual space of $\mathcal{X}$. Due to Theorem 2.1.5 we know that $\mathcal{X}^*$ is a Banach space equipped with the operator norm*

$$||p||_{\mathcal{X}^*} := \sup_{||x||_{\mathcal{X}}=1} |p(x)| = \sup_{x\in\mathcal{X}\setminus\{0\}} \frac{|p(x)|}{||x||_{\mathcal{X}}} = \sup_{||x||_{\mathcal{X}}\leq 1} |p(x)|; \tag{2.2}$$

for $p(x)$ defined as the fuctional dual product

$$\langle p, x\rangle_{\mathcal{X}^*\times\mathcal{X}} := p(x) \tag{2.3}$$

We are going to write $\langle p, x\rangle_{\mathcal{X}}$ respectively $\langle p, x\rangle_{\mathcal{X}^*}$ instead of $\langle p, x\rangle_{\mathcal{X}^*\times\mathcal{X}}$ for simplicity.

Definition 2.1.7 *(Dual Operator) Let $\mathcal{X}$ and $\mathcal{Y}$ be a Banach spaces. For an operator $M \in \mathcal{K}(\mathcal{X}, \mathcal{Y})$ the dual or adjoint operator $M^* \in \mathcal{K}(\mathcal{X}^*, \mathcal{Y}^*)$ is defined via the relation*

$$\langle M^*y, x\rangle_{\mathcal{X}} = \langle y, Mx\rangle_{\mathcal{Y}} \tag{2.4}$$

for all $y \in \mathcal{Y}^*$ and $x \in \mathcal{X}$. Furthemore, it is easy to see that $||M^*||_{\mathcal{Y}^*,\mathcal{X}^*} = ||M||_{\mathcal{X},\mathcal{Y}}$ is satified.

2.2 Hilbert Spaces

Hilbert spaces play a fundamental role in various areas of mathematics. Below we present the properties to define those:

Definition 2.2.1 *(Inner Products) A vector space $\mathcal{H}$ is called inner product space if for every x, $y \in \mathcal{X}$ there exists a complex number $\langle x, y \rangle$, called the inner product of x and y, such that:*

a) $\langle x, x \rangle$ *is real and* $\langle x, x \rangle \geq 0$

b) $\langle x, x \rangle = 0$ *if and only if* $x = 0$

c) $\langle y, x \rangle = \overline{\langle x, y \rangle}$

d) $\langle ax_1 + bx_2, y \rangle = a \langle x_1, y \rangle + b \langle x_2, y \rangle$

Each inner product determines a norm by the formula $||x|| = \langle x, x \rangle^{\frac{1}{2}}$ and every inner product space is a normed linear space. The Cauchy-Schwarz inequality states that $| \langle x, y \rangle | \leq ||x||||y||$ for every x, $y \in \mathcal{H}$. Thus, a Hilbert space is a Banach space equipped with a inner product $\langle \cdot, \cdot \rangle$.

Let H^1, L^2 be Hilbert spaces. We identify L^2 with it is dual L^{-2}. If H^{-1} denotes the dual of H^1 (with norm $|| \quad ||_*$) we have

$$H^1 \hookrightarrow L^2 \hookrightarrow H^{-1} \tag{2.5}$$

each space being dense in the following ($\hookrightarrow$ denotes continuous embedding).

2.3 Ill-posed problems

In *Chapter 4* we present the whole process necessary for the reconstruction of parameters to the problem discussed in *Chapter 3*. There is the use of the concept of inverse problems, which has many applications in various areas, including imaging sciences.

The greatest obstacle in working with inverse problems is that, the mostly are ill-posed problems. Below follows the definition of ill-posed problems [**48**]:

Definition 2.3.1 *Let $\mathcal{L}$ and $\mathcal{M}$ be normed spaces and $\mathcal{D} : \mathcal{L} \to \mathcal{M}$ a operator. The problem of finding a solution f of*

$$\mathcal{D}(f) = g$$

with $g \in \mathcal{M}$ is called well-posed if

i) there exist a solution for all $g \in \mathcal{M}$,

ii) the solution is unique,

iii) the solution f depends continuously on g.

The problem is called ill-posed, if it is not well-posed.

Whenever we seek to solve an inverse problem, one has to overcome obstacles such as instability and ill-posedness. The strategy of regularization is a tool that allows to obtain an approximate solution.

2.4 Variational Calculus

In this section we present a brief summary of Variational Calculus **[36]**, which is the basis for the understanding of the resolution of the optimization problem presented in *Chapter 4*.

Definition 2.4.1 *Let $P : (\mathcal{X}, \tau_1) \to (\mathcal{Y}, \tau_2)$ be a mapping from a Banach spaces $\mathcal{X}$ with topology τ_1 to a Banach space $\mathcal{Y}$ with topology τ_2. Then P is called an operator. If $\mathcal{Y}$ - as a special case of a Banach space - is a field, P is called a functional.*

Definition 2.4.2 *A functional P is called proper, with $P : \mathcal{X} \to \mathcal{R} \cup \{\infty\}$, if the effective domain*

$$dom(P) := \{x \in \mathcal{X} / P(x) < \infty\}$$

is not empty.

Definition 2.4.3 *Let $P : \mathcal{X} \to \mathcal{Y}$ be a functional or operator. The directional derivative(also called first variation) at position $x \in \mathcal{X}$ in direction $y \in \mathcal{Y}$ defined as*

$$d_y P(x) := \lim_{t \downarrow 0} \frac{P(x + ty) - P(x)}{t} \tag{2.6}$$

if that limit exists.

Definition 2.4.4 *Let $P : \mathcal{X} \to \mathcal{Y}$ be a functional or an operator and let $d_y P(x)$ exist. The second* *directional derivative (also called second variation) at position x in direction w is defined as*

$$d^2_{y,w}P(x) := \lim_{t\downarrow 0} \frac{d_yP(x+tw) - d_yP(x)}{t} \tag{2.7}$$

if that limit exists.

Definition 2.4.5 *Let $P : \mathcal{X} \to \mathcal{Y}$ be a functional or an operator. The set*

$$dP(x) = \{d_v P(x) < \infty | y \in \mathcal{U}\} \tag{2.8}$$

is called Gâteaux-derivative. P is called Gâteaux-differentiable, if (2.8) is not empty.

Definition 2.4.6 *Let $P : \mathcal{X} \to \mathcal{Y}$ be a functional or operator, $\mathcal{X}$ and $\mathcal{Y}$ Banach spaces, and suppose $d_yP(x)$ exists for all $y \in \mathcal{X}$. If there exists a continuous linear functional $P'(x) : \mathcal{X} \to \mathcal{Y}$ such that*

$$P'(x)y = d_yP(x) \quad \forall y \in \mathcal{X} \tag{2.9}$$

and

$$\frac{||P(x+y) - P(x) - P'(x)y||_{\mathcal{Y}}}{||y||_{\mathcal{X}}} \longrightarrow 0 \quad \textit{for} \quad ||y||_{\mathcal{X}} \longrightarrow 0 \tag{2.10}$$

holds, then P is called Frechét-differentiable in x and P' is called Fréchet-derivative.

Definition 2.4.7 *Let $\mathcal{U}$ be a Banach space with topology τ. The functional $P : (\mathcal{U}, \tau) \to \mathbb{R} \cup \{+\infty\}$ is called lower semi-continuous at $x \in \mathcal{U}$ if*

$$P(x) \leq \lim_{k\to\infty} \inf P(x_k) \tag{2.11}$$

for all $x_k \to x$ in the topology τ.

Theorem 2.4.8 *(Fundamental Theorem of Optimization) Let $P : (\mathcal{U}, \tau) \to \mathbb{R} \cup \{+\infty\}$ be a functional on a topological space $\mathcal{U}$ (locally convex) in the metric topology τ lower semi-continuous. Furthemore, let the level set*

$$\{x \in \mathcal{U} / P(x) \leq M\} \tag{2.12}$$

be non-empty and compact in the topology τ for some $M \in \mathcal{R}$. Then there exists a global minimum of

$$P(x) \to \min_{x\in\mathcal{U}} \tag{2.13}$$

Proof. Let $\tilde{P} = \inf_{x\in\mathcal{U}} P(x)$. Then a sequence $(x_k)_{k\in\mathbb{N}}$ exists with $P(x_k) \to \tilde{P}$ for $k \to \infty$. For k sufficiently large, $P(x_k) \leq \mathcal{M}$ holds and hence, $(x_k)_{k\in\mathbb{N}}$ is contained in a compact set. As a consequence, a subsequence $(x_k)_{l\in\mathbb{N}}$ exists with $x_{k_1} \to \tilde{x}$, for $l \to \infty$, for some $\tilde{x} \in \mathcal{U}$. From the lower semicontinuity of P we obtain

$$\tilde{P} \leq P(\tilde{x}) \leq \lim_{k\to\infty} \inf P(x_k) \leq \tilde{P}. \tag{2.14}$$

Consequently $\tilde{x}$ is a global minimizer.

Definition 2.4.9 *Let $\mathcal{X}$ be a Banach space, with $\mathcal{X}^*$ denoting its dual space. Then the weak topology is defined as*

$$x_k \rightharpoonup x :\Leftrightarrow \langle y, x_k\rangle_{\mathcal{X}} \to \langle y, x\rangle_{\mathcal{X}} \tag{2.15}$$

for all $y \in \mathcal{X}^*$ and the weak-*topologies are defined as

$$y_k \rightharpoonup^* y :\Leftrightarrow \langle y_k, x\rangle_{\mathcal{X}^*} \to \langle y, x\rangle_{\mathcal{X}^*}, \tag{2.16}$$

for all $x \in \mathcal{X}$.

Theorem 2.4.10 *(Banach-Alaogu) Let $\mathcal{X}$ be a Banach space with dual space $\mathcal{X}^*$. Then the set*

$$\{y \in \mathcal{X}^* \big| ||y||_{\mathcal{X}^*} \leq C\} \tag{2.17}$$

for $C > 0$, is compact in the weak-*topology.

2.5 Lebesgue Measure

In this section we rewiew some of the basic aspects of measure, integration and tools that will be of major interest throughout this work. First we want to recall the fundamental notion of a σ-algebra of sets. All definitions and concepts presented here are based on the introduction of **[51]**.

Definition 2.5.1 *A σ-algebra of subsets of a set X is, by definition, a collection $\mathfrak{B}$ of subsets of X, which satisfies the following requirements:*

(a) $X \in \mathfrak{B}$;

(b) $A \in \mathfrak{B} \to A^c \in \mathfrak{B}$, where $A^c = X - A$ denotes the complement of the set A; and

(c) $\{A_n\}_{n=1}^{\infty} \subset \mathfrak{B} \Rightarrow \bigcup_n A_n \in \mathcal{A}$

A *measurable space* is a pair $(X, \mathfrak{B})$ consisting of a set X and a σ-algebra $\mathfrak{B}$ of subsets of X.

Thus, a σ-algebra is nothing but a collection of sets which contains the whole space and is closed under the formation of complements and countable unions.

Definition 2.5.2 *If* $(X_i, \mathfrak{B}_i)$, $i = 1, 2$, *are measurable spaces, then a function* $f : X_1 \to X_2$ *is said to be measurable if* $f^{-1}(A) \in \mathfrak{B}_1 \forall A \in \mathfrak{B}_2$.

Definition 2.5.3 *Let* $(X, \mathfrak{B})$ *be a measurable space. A measure on* $(X, \mathfrak{B})$ *is a function* $\mu : \mathfrak{B} \to [0, \infty]$ *with the following two properties:*

(i) The empty set has measure zero, $\mu(\emptyset) = 0$*; and*

(ii) μ *is countable additive - i.e., if* $E = \coprod_{n=1}^{\infty} E_n$ *is a sequence of pairwise disjoint sets and a countable "measurable' partition, meaning that* E, $E_n \in \mathfrak{B} \forall n$, *then* $\mu(E) = \sum_{n=1}^{\infty} \mu(E_n)$.

A measure space is a triple $(X, \mathfrak{B}, \mu)$, consisting of a measurable space together with a measure defined on it.

A measure μ is said to be *finite* if $\mu(X) < \infty$ (resp., $\mu(X) = 1$).

Theorem 2.5.4 *There exists the* σ*-algebra* $\mathfrak{B}_n$ *of Lebesgue measurable sets on* $\mathbb{R}^n$ *and the Lebesgue-measure* $\mu : \mathfrak{B}_n \to [0, \infty]$ *with properties:*

(a) $\mathfrak{B}_n$ *contain all open sets (and also, all closed sets),*

(b) μ *is a measure on* $\mathfrak{B}_n$,

(c) if B *is any ball in* $\mathbb{R}^n$, *then we obtain* $\mu(B) = |B|$, *with* $|B|$ *denoting the volume of the ball,*

(d) if $A \subset B$ *is valid, with* $B \in \mathfrak{B}_n$ *and* $\mu(B) = 0$, *then it follows that* $A \in \mathfrak{B}_n$ *and* $\mu(A) = 0$ *hold, which means that* $(\mathbb{R}^n, \mathfrak{B}_n, \mu)$ *is a complete measure space.*

The sets $A \in \mathfrak{B}_n$ *are Lebesgue measurable.*

Definition 2.5.5 *(Lebesgue Measurable Function) The function* $u : \mathbb{R}^n \to [-\infty, \infty]$ *is called Lebesgue measurable if we have*

$$\{x \in \mathbb{R}^n : f(x) > \alpha\} \in \mathfrak{B}, \tag{2.18}$$

for all $\alpha \in \mathbb{R}$. If we furthemore have $A \in \mathfrak{B}_n$, the function $f : A \to [-\infty, \infty]$ is called Lebesgue measurable on A if f_A^1 is Lebesgue measurable, with 1_A denothing the indicator function ($f_A^1 = f$ on A and $f_A^1 = 0$ otherwise).

Lemma 2.5.6 *For any sequence (u_k) of Lebesgue measurable functions*

- $\sup_k u_k$
- $\inf_k u_k$
- $\limsup_{k\to\infty} u_k$
- $\liminf_{k\to\infty} u_k$

are also Lebesgue functions. Furthermore, for any Lebesgue measurable function $u \geq 0$ there exists a monotone increasing sequence $(u_k)_{k\in\mathbb{N}} \subset E_+(\mathbb{R}^n)$ with $u = \sup_k u_k$.

Definition 2.5.7 *(Lebesgue Integral) Let (X, μ) be a measure space. The Lebesgue Integral, over X, of a measurable simple function $\varphi : X \to [0, \infty]$ is defined as*

$$\int\limits_X \varphi d\mu = \int\limits_X \sum_{k=1}^n a_k \prod(E_k) d\mu = \sum_{k=1}^n a_k \mu(E_k) \tag{2.19}$$

we restrict φ to be non-negative, to avoid having to deal with $\infty - \infty$ on the righthand side.

Lemma 2.5.8 *(Linearity of Integral for Simple Functions) The Lebesgue integral for a simple function is linear.*

Definition 2.5.9 *(Integral of non-negative function) Let $f : X \to [0, \infty]$ be a mesurable and non-negative. The Lebesgue integral of f over X is given by*

$$\int\limits_X f d\mu = \sup \left\{ \int\limits_X \varphi d\mu / \varphi simple, 0 \leq \varphi \leq f \right\}, \tag{2.20}$$

and $\int\limits_X \varphi d\mu$ defined in Definition 2.5.7.

Definition 2.5.10 *(Lebesgue Spaces L^p) Let $(X, \mathcal{B}, \mu)$ be a measure space and $1 \leq p \leq \infty$. The space $L^p(X)$ consists of equivalence classes of measurable functions $f : X \to \mathbb{R}$ such that*

$$L^p(\Omega) := \{f : \Omega \to \mathbb{R} \;\; Lebesgue\ measurable \;\; |||f||_{L^p(\Omega)} < \infty\}. \tag{2.21}$$

The L^p-norm of $f \in L^p(X)$ is defined by

$$||f||_{L^p(\Omega)} = \left(\int |f|^p d\mu \right)^{\frac{1}{p}} \tag{2.22}$$

The notation $L^p(X)$ assumes that the measure μ on X is understood. We say that $f_n \to f$ in L^p if $||f - f_n||_{L^p} \to 0$. The reason to regard functions that are equal a.e. as equivalent is so that $||f||_{L^p} = 0$ implies that $f = 0$.

Definition 2.5.11 *Let $L^p_{loc}(\Omega)$ be the locally Lebesgue integrable functions such that*

$$L^p_{loc}(\Omega) := \{f : \Omega \to \mathbb{R} \ \ \textit{Lebesgue measurable} \ \ | f \in L^p(\Psi) \ \ \textit{for all} \ \ \Psi \subset \Omega \ \ \textit{compact}\}. \tag{2.23}$$

2.6 Sobolev Spaces

Taking into account the considerations made above we present here definitions corresponding to the Sobolev Space.

Definition 2.6.1 *(Weak Derivative) Let $\Omega \subset \mathbb{R}^n$ be open and let $f \in L^1_{loc}(\Omega)$ be locally L^1 integrable. If there exists a function $w \in L^1_{loc}$ such that*

$$\int_\Omega w\varphi dx = (-1)^{|\alpha|} \int_\Omega f D^\alpha \varphi dx \tag{2.24}$$

holds, for all $\varphi \in C_0^\infty(\Omega)$, then w is called the α-th weak partial derivative of f.

To easily identify the weak derivative w of f with f we denote w by $D^\alpha f$, for the sake of simplicity.

Definition 2.6.2 *Let $\Omega \subset \mathbb{R}^n$ be open. For $k \in \mathbb{N}_0$ and $p \in [1, \infty]$ the Sobolev space $W^{k,p}(\Omega)$ is defined as*

$$W^{k,p}(\Omega) = \{f \in L^p(\Omega) | \ f \ \ \textit{has weak derivatives} \ \ D^\alpha f \in L^p(\Omega) \ \ \textit{for all} \ \ |\alpha| \leq k\} \tag{2.25}$$

The Sobolev spaces are equipped with the norm

$$||f||_{W^{k,p}(\Omega)} := \left(\sum_{|\alpha| \leq k} ||D^\alpha f||^p_{L^p(\Omega)} \right)^{\frac{1}{p}} \tag{2.26}$$

for $p \in [1, \infty[$, and

$$||f||_{W^{k,\infty}(\Omega)} := \sum_{|\alpha| \leq k} ||D^\alpha f||_{L^\infty(\Omega)} \tag{2.27}$$

3 Compartmental Models

In nuclear medicine and more specifically PET modeling it becomes important to allow quantitative analysis in the interpretation of experimental data, providing information on measurable and not measurable quantities [**24**].

Compartmental models are a classical approach in the estimation of metabolic rates. They are able to describe fairly well a large number of physiological processes such as brain and heart. In a PET image-sequence, fixed spatial compartments are areas defined by the concentration of a radioactive tracer that is a a temporal function. The images obtained by PET are formed by numerous overlapping signals. So we need to use a mathematical model, which includes all possible states of that signal given by a sequence of PET-reconstruction, in order to isolate the desired component. Each of these states is treated as a compartment [**105**].

As a way of describing the interaction between these compartments one associates one constant capable to represent the velocity of absorption, diffusion of the radioactive trace used during the PET scan. Thus data concerning the rate at which radioactive trace is metabolized in the region of interest can be associated with rates of variation in the time of the radioactive tracer concentrations in each compartment [**24**]. The rate of transit of substances between the regions are represented through a dynamic constant that links these compartments.

Thus it becomes possible to describe the kinetics of a radioactive tracer in a physiological system making use of a set of differential equations whose solutions are not linear with respect to parameters of interest. One just has to analyze the variation of the temporal concentration of a radioactive tracer in a specific compartment and thus determine the quantities of interest.

The kinetics of radioactive tracers used with positron emission tomography **[39, 84]** provide examples, which are modelled by compartmental schemes. The kinetics of $[^{18}F]$ -fluorodeoxyglucose (FDG), $[^{13}N]$ -ammonia and $H_2^{15}O$ are typical radioactive tracers used to examine regions of interest, being the last two more used to estimate regional myocardial blood perfusion. In **[80]** a two-compartmental model and in **[67, 66]** a three-compartmental model are applied to the analysis of myocardial PET images.

In the following we want to present the model of parabolic differential equations that describes the kinetic behavior of $H_2^{15}O$ PET tracers during cardiac perfusion, the existence and the uniqueness of the solution of the differential equations problem and the continuity theorem.

3.1 Differential Equations for $H_2^{15}O$ PET Tracers

Let $\Omega \subset \mathbb{R}^d$, for d appropriate, bounded, compact space that denotes the compartmental space, i.e., an element $x \in \Omega$ denotes a compartment. Furthermore $t \in [0, T) \subset R$ lies within a bounded and compact set. Since $V_{\mathcal{A}}, V_{\mathcal{V}}, V_{\mathcal{T}}, D_{\mathcal{A}}, D_{\mathcal{V}}, D_{\mathcal{T}}$ and k_i, $(i = 1, 2, 3)$ are functions in space, depending on a compartment x, we have

$$C_{\mathcal{A}}, C_{\mathcal{V}}, C_{\mathcal{T}} : \mathcal{D}_p(C_{\mathcal{A}}, C_{\mathcal{V}}, C_{\mathcal{T}}) \times L_p([0,T]) \longrightarrow L_p(\Omega \times [0,T])^3, \text{ with}$$

$$\frac{\partial C_{\mathcal{A}}}{\partial t} = -k_0(x)C_{\mathcal{A}}(x,t) - k_1(x)C_{\mathcal{A}}(x,t) + k_3(x)C_{\mathcal{V}}(x,t) + \underbrace{\nabla \cdot (V_{\mathcal{A}}(x)C_{\mathcal{A}}(x,t))}_{Transport} + \underbrace{\nabla \cdot (D_{\mathcal{A}}(x)\nabla C_{\mathcal{A}}(x,t))}_{Diffusion} \tag{3.1}$$

$$\frac{\partial C_{\mathcal{T}}}{\partial t} = -k_0(x)C_{\mathcal{T}}(x,t) + k_1(x)C_{\mathcal{A}}(x,t) - k_2(x)C_{\mathcal{T}}(x,t) + \nabla \cdot (V_{\mathcal{T}}(x)C_{\mathcal{T}}(x,t)) + \nabla \cdot (D_{\mathcal{T}}(x)\nabla C_{\mathcal{T}}(x,t)) \tag{3.2}$$

$$\frac{\partial C_{\mathcal{V}}}{\partial t} = -k_0(x)C_{\mathcal{V}}(x,t) - k_3(x)C_{\mathcal{V}}(x,t) + k_2(x)C_{\mathcal{T}}(x,t) + \nabla \cdot (V_{\mathcal{V}}(x)C_{\mathcal{V}}(x,t)) + \nabla \cdot (D_{\mathcal{V}}(x)\nabla C_{\mathcal{V}}(x,t)) \tag{3.3}$$

and

$$\mathcal{D}_p := \{k_i \in L^2(\Omega), V_{\mathcal{A}/\mathcal{V}/\mathcal{T}} \in L^\infty(\Omega), D_{\mathcal{A}/\mathcal{V}/\mathcal{T}} \in L^\infty(\Omega), k > 0, D > 0\} \tag{3.4}$$

subject to the boundary conditions

$$
\begin{aligned}
&(D\nabla C_{\mathcal{A}/\mathcal{T}/\mathcal{V}} + VC_{\mathcal{A}/\mathcal{T}/\mathcal{V}}) \cdot n = j_{in} \qquad \Gamma \subset \partial\Omega \qquad\qquad j_{in} = const \cdot V \\
&(D\nabla C_{\mathcal{A}/\mathcal{T}/\mathcal{V}} + VC_{\mathcal{A}/\mathcal{T}/\mathcal{V}}) \cdot n = C_{\mathcal{A}/\mathcal{T}/\mathcal{V}} V_{out} \qquad \partial\Omega/\Gamma
\end{aligned}
\tag{3.5}
$$

The blood in an artery, transporting a radioactive tracer is described via a function $C_{\mathcal{A}}(x,t)$. Similarly, the blood containing the radioactive tracer in a tissue and in a vein are described by $C_{\mathcal{T}}(x,t)$ and $C_{\mathcal{V}}(x,t)$ respectively and *const* is a constant.

This model differs from others currently found in the literature because here we also consider the contributions due to diffusion and transport. For these contributions, $D_{\mathcal{A}}$, $D_{\mathcal{T}}$, $D_{\mathcal{V}}$ are the parameters of diffusion and $V_{\mathcal{A}}$, $V_{\mathcal{T}}$, $V_{\mathcal{V}}$ are the velocity parameters in the arteries, tissue and veins respectively. All these parameters are only functions of spatial coordinates, independent of time. The terms $k_0(x)C_{\mathcal{A}}(x,t)$, $k_0(x)C_{\mathcal{T}}(x,t)$ and $k_0(x)C_{\mathcal{V}}(x,t)$ represent the radioactive decay of the compound. And finally the rates k_1, k_2 and k_3 represents the exchange of fluids between the artery, tissue and vein.

The parameters $D_{\mathcal{A}}, D_{\mathcal{V}}, D_{\mathcal{T}}$, k_i and $C_{\mathcal{A}}, C_{\mathcal{V}}, C_{\mathcal{T}}$ are non negative, $C_{\mathcal{A}}, C_{\mathcal{V}}, C_{\mathcal{T}}$ due as a density, k_1, k_2 and k_3 because of physiology and $D_{\mathcal{A}}, D_{\mathcal{V}}, D_{\mathcal{T}}$ because they are diffusion parameters.

3.1.1 Preliminary Considerations

In order to prove the uniqueness of the solution of the problem mentioned above, let $D(A)$ be a subspace of H^1. Thus we have

$$
\begin{pmatrix} \frac{\partial C_{\mathcal{A}}}{\partial t} \\ \frac{\partial C_{\mathcal{V}}}{\partial t} \\ \frac{\partial C_{\mathcal{T}}}{\partial t} \end{pmatrix} = -A \begin{pmatrix} C_{\mathcal{A}} \\ C_V \\ C_{\mathcal{T}} \end{pmatrix} \text{ in } (H^{-1})^3 \tag{3.6}
$$

where

$$
A = \begin{pmatrix} +(k_0+k_1) - \nabla(V_{\mathcal{A}}(\cdot)) - \nabla(D_{\mathcal{A}}\nabla(\cdot)) & -k_3 & 0 \\ 0 & +(k_0+k_3) - \nabla(V_V(\cdot)) - \nabla(D_V\nabla(\cdot)) & -k_2 \\ -k_1 & 0 & +(k_0+k_2) - \nabla(V_{\mathcal{T}}(\cdot)) - \nabla(D_{\mathcal{T}}\nabla(\cdot)) \end{pmatrix}
$$

Definition 3.1.1 *Let $a, b \in \mathbb{R} = \mathbb{R} \cup \{-\infty, +\infty\}$. We denote by $W(a,b;H^1,H^{-1})$ the space*

$$
W(a,b;H^1,H^{-1}) = \{u \in L^2(0,T;H^1)^3 \cap H^1(0,T;H^{-1})^3\} \tag{3.7}
$$

The problem is then to find $u = (C_{\mathcal{A}}(x,t), C_{\mathcal{T}}(x,t), C_{\mathcal{V}}(x,t))$, with

$$
u(t) \in W(a,b;H^1,H^{-1}) \tag{3.8}
$$

and

$$\partial_t u = -Au, \tag{3.9}$$

$$u(0) = u_0 \tag{3.10}$$

A satisfies:

$$< Au, v > \ \leq \ c_1||u||_{(H^1)^3} \cdot ||v||_{(H^1)^3}, \tag{3.11}$$

which is easily verified by Cauchy-Schwarz, and

$$< Au, u > \ \geq \ c_2||u||^2_{(H^1)^3} - c_3||u||^2_{(L^2)^3} \tag{3.12}$$

It follows that, for each $t \in [0, T]$, the bilinear form $a(t; u, v) = Au$ defines a continuous operator A from $H^1 \to H^{-1}$ with

$$\sup_{t\in(0,T)} ||A||_{\mathfrak{L}(H^1,H^{-1})} \leq M \tag{3.13}$$

Definition 3.1.2 *Let $\{H^1_m\}_{m\in\mathbb{N}^*}$ be a family of finite dimensional vector spaces satisfying:*

$$\begin{cases} i)H^1_m \subset H^1 \quad (dim \quad H^1_m < +\infty) \\ ii)H^1_m \to H^1 when \ m \to \infty \ in \ the \ following \ sense: \end{cases} \tag{3.14}$$

there exists $\mathfrak{V}$ a dense subspace of H^1, such that, for all $v \in \mathfrak{V}$, we can find a sequence $\{v_m\}_{m\in\mathbb{N}^*}$ such that, for all $m, v_m \in H^1_m$ and $v_m \to v$ in H^1 as $m \to \infty$. The space H^1_m is called the Galerkin approximation or order m ($m \neq dim \quad H^1_m$) of H^1.

3.1.2 Uniqueness of the Solution of Problem

The proof of uniqueness and the existence of the solution of problem are mainly based on the work of Dautray **[32]**.

Theorem 3.1.3 *(Uniqueness) Suppose that Au satisfies (3.11) and (3.12), $u_0 \in L^2$. Then the solution of problem (3.9), if it exists, is unique.*

Proof. We consider u_1 and u_2 to be two distinct solutions of problem (3.9), then $u = u_1 - u_2$ satisfies $u \in W(a, b; H^1, H^{-1})$ and

$$\begin{cases} \partial_t u - \nabla \cdot (Vu + D\nabla u) + Ku = 0 \\ (D\nabla u + Vu) \cdot n = j_{in} \qquad \Gamma \subset \partial\Omega \\ (D\nabla u + Vu) \cdot n = uv_{out} \qquad \partial\Omega/\Gamma \end{cases} \tag{3.15}$$

with

$$K = \begin{pmatrix} (k_0 + k_1) & -k_3 & 0 \\ 0 & (k_0 + k_3) & -k_2 \\ -k_1 & 0 & (k_0 + k_2) \end{pmatrix}$$

Then by multiplying by the directional derivative and integrating:

$$\int_{\Omega} \partial_t u\varphi \; d\sigma - \int_{\Omega} \nabla \cdot (Vu + D\nabla u)\varphi \; d\sigma + \int_{\Omega} Ku\varphi \; d\sigma = 0$$

$$\int_{\Omega} \partial_t u\varphi \; d\sigma - \left(- \int_{\Omega} (Vu + D\nabla u)\nabla\varphi \; d\sigma + \int_{\partial\Omega} (Vu + D\nabla u) \cdot n\varphi \; d\sigma \right) + \int_{\Omega} Ku\varphi \; d\sigma = 0 \tag{3.16}$$

$$\int_{\Omega} \partial_t u\varphi \; d\sigma + \int_{\Omega} (Vu + D\nabla u)\nabla\varphi \; d\sigma - \left(\int_{\Gamma} j_{in}\varphi \; d\sigma + \int_{\partial\Omega/\Gamma} uv_{out}\varphi \; d\sigma \right) + \int_{\Omega} Ku\varphi \; d\sigma = 0$$

Let

$$-\Theta(u,\varphi) = \int_{\Omega} D\nabla u\nabla\varphi \; d\sigma + \int_{\Omega} Vu \cdot \nabla\varphi \; d\sigma + \int_{\Omega} Ku\varphi \; d\sigma - \int_{\partial\Omega/\Gamma} uv_{out}\varphi \; d\sigma \tag{3.17}$$

Thus

$$\frac{1}{2}\frac{d}{dt}|u(t)|^2 - \Theta(u,\varphi) = \int_{\Gamma} j_{in}\varphi \; d\sigma \tag{3.18}$$

For uniqueness, it satisfies to consider $j_{in} = 0$

$$(\varphi, v) = \int_{\Gamma} j_{in}\varphi \; d\sigma = 0 \tag{3.19}$$

and by Gronwall's Lemma and $\varphi = u$ we have

$$\begin{aligned} \frac{1}{2}\frac{d}{dt}|u(t)|^2 &= \Theta(u,\varphi) \\ &\leq c_3|u|^2_{(L^2)^3} - c_2|u|^2_{(H^1)^3} \leq c_3|u|^2_{(L^2)^3} \end{aligned} \tag{3.20}$$

And we have uniqueness in problem (3.9).

3.1.3 Existence of a Solution of Problem

Theorem 3.1.4 *Under the hypothesis of Theorem (3.1.3), there exists a solution of problem (3.9) and*

$$u \in W(0,T; H^1, H^{-1})$$

Approximate Problem

Let $\{H^1_m\}_{m\in N^*}$ be a family of finite dimensional vector subspaces satisfiying (3.14), H^1 being dense in L^2, for $u_0 \in L^2$, there exists a sequence $\{u_{0m}\}_{m\in N^*}$ such that

$$\forall m, u_{0m} \in (H^1_m)^3 \quad \text{and} \quad u_{0m} \to u_0 \quad \text{in} \quad (L^2)^3 \tag{3.21}$$

Let be

$$d_m = dim \;\; H^1_m, \{W_{jm}\} \quad j = 1, ..., d_m \quad \text{a basis of } H^1_m \tag{3.22}$$

Thus, our problem is to find

$$u_m(t) = \sum_{j=1}^{d_m} g_{jm}(t) W_{jm} \tag{3.23}$$

satisfying

$$\begin{cases} \int_0^T \int_\Omega \partial_t u_m(t) W_{jm} d\sigma dt - \int_0^T \int_\Omega \nabla \cdot (V u_m(t) + D\nabla u_m(t)) W_{jm} d\sigma dt \\ + \int_0^T \int_\Omega K u_m(t) W_{jm} d\sigma dt = 0 \quad 1 \leq j \leq d_m \\ u_m(0) = u_{0m} \end{cases} \tag{3.24}$$

Lemma 3.1.5 *There exists a unique solution u_m to problem (3.24) satisfying:*

$$u_m \in L^2(0,T;H^1)^3 \cap H^1(0,T;H_m^{-1})^3 \tag{3.25}$$

A priori estimates

We multiply equation (3.24) by $g_{jm}(t)$ and we sum from 1 to d_m; it becomes

$$\begin{aligned} &\frac{1}{2}\frac{d}{dt}\int_0^T \int_\Omega |u_m(t)|^2 d\sigma dt - \int_0^T \int_\Omega \nabla \cdot (V u_m(t) + D\nabla u_m(t)) u_m(t) d\sigma dt \\ &+ \int_0^T \int_\Omega K u_m(t) u_m(t) d\sigma dt = 0 \end{aligned} \tag{3.26}$$

and, by integration over $]0,T[$:

$$\begin{aligned} &\int_0^T \int_\Omega \partial_t u_m(t) u_m(t) d\sigma dt + \int_0^T \int_\Omega (V u_m(t) + D\nabla u_m(t)) \nabla u_m(t) d\sigma dt \\ &- \left(\int_0^T \int_\Gamma j_{in} u_m(t) d\sigma dt + \int_0^T \int_{\partial\Omega/\Gamma} u_m(t) v_{out} u_m(t) d\sigma dt \right) + \int_0^T \int_\Omega K u_m(t) u_m(t) d\sigma dt = 0 \end{aligned} \tag{3.27}$$

by (3.12), we have

$$\frac{1}{2}|u_m(t)|^2 - \Theta(u_m, u_m) = + \left(\int_0^T \int_\Gamma j_{in} u_m(t) d\sigma dt \right) + \frac{1}{2}|u_{0m}|^2 \tag{3.28}$$

$$\begin{aligned} \frac{1}{2}|u_m(t)|^2 &= \Theta(u_m, u_m) + \frac{1}{2}|u_{0m}|^2 \\ &\leq -c_2 ||u_m||^2_{(H^1)^3} + c_3 ||u_m||^2_{(L^2)^3} + C|u_0|^2 \end{aligned} \tag{3.29}$$

with $t \in [0,T]$, C a suitable constant, independent of t, m. From which we have

Lemma 3.1.6 *The functions u_m solutions of our problem (3.9) belong to a bounded set of $L^\infty(L^2)^3$ and of $L^2(H^1)^3$.*

Passage to the limit for $m \to \infty$

From Lemma (3.1.6) and from (3.13), we can deduce that

$$A(\cdot)u_m \in \text{a bounded set of} \quad L^2(H^{-1})^3 \tag{3.30}$$

By using the properties of weak (or weak star) compactness of unit balls of the spaces $L^2(H^1), L^\infty(L^2), L^2(H^{-1})$ we deduce

Lemma 3.1.7 *We can extract from the sequence $\{u_m\}_{m\in\mathbb{N}^*}$ a subsequence $\{u_m^{'}\}$ having the following properties:*

$$\begin{cases} i) \;\; u_{m'} \to u \quad \textit{weakly in} \quad L^2(H^1)^3 \\ ii) \;\; u_{m'} \to u \quad \textit{weakly * in} \quad L^\infty(L^2)^3 \\ iii) \;\; A(\cdot)u_m \to A(\cdot)u \quad \textit{weakly in} \quad L^2(H^{-1})^3 \end{cases}$$

Let then $\varphi \in \mathfrak{D}(]0,T[)$ and $v \in \mathfrak{V}$.

From (3.14)(ii), there exists $\{v_m\}_{m\in\mathbb{N}^*}$, $v_m \in H^1_m$, such that $v_m \to v$ strongly in H^1. Therefore, let be

$$\begin{cases} \psi_m = \varphi \otimes v_m \quad \text{i.e } \psi_m(t) = \varphi(t)v_m \\ \psi = \varphi \otimes v \end{cases} \tag{3.31}$$

and, particularly,

$$\begin{cases} i) \;\; \psi_m \to \psi \quad \text{in} \quad L^2(0,T;H^1)^3, \quad \text{strongly}, \;\; m^{'} \to \infty \\ ii) \;\; \psi_{m'} \to \dfrac{d\psi_{m'}}{dt} \to \psi' \;\; \text{in} \quad L^2(0,T;L^2)^3 \quad \text{strongly}, \;\; m' \to +\infty \end{cases} \tag{3.32}$$

From (3.24), we have

$$\begin{cases} \int_0^T \int_\Omega \partial_t u_{m'}(t)\psi'_{m'}(t)d\sigma dt + \int_0^T \int_\Omega (Vu_{m'}(t) + D\nabla u_{m'}(t))\nabla\psi_{m'}(t)d\sigma dt \\ -\left(\int_0^T \int_\Gamma j_{in}\psi_{m'}(t)d\sigma dt + \int_0^T \int_{\partial\Omega/\Gamma} u_{m'}(t)v_{out}\psi_{m'}(t)d\sigma dt \right) + \int_0^T \int_\Omega Ku_{m'}(t)\psi_{m'}(t)d\sigma dt = 0 \\ \psi_m = \varphi \otimes v_m, \quad \forall\varphi \in \mathfrak{D}(]0,T[) \end{cases} \tag{3.33}$$

from (ii) of Lemma (3.1.7) and (3.32) (i)

$$\int_0^T \int_\Omega \partial_t u_{m'}(t)\psi'_{m'}(t)d\sigma dt = \int_0^T \int_\Omega \partial_t u(t)\psi'(t)d\sigma dt \quad \text{as } m' \to \infty \tag{3.34}$$

And, from (iii) of Lemma (3.1.7) and (3.32)(i)

$$\begin{cases} +\int_0^T\int_\Omega \nabla\cdot(Vu_{m'}(t)+D\nabla u_{m'}(t))\psi_{m'}(t)d\sigma dt \\ -\left(\int_0^T\int_\Gamma j_{in}\psi_{m'}(t)d\sigma dt+\int_0^T\int_\Omega u_{m'}(t)v_{out}\psi_{m'}(t)d\sigma dt\right)+\int_0^T\int_\Omega Ku_{m'}(t)\psi_{m'}(t)d\sigma dt \\ =\int_0^T\int_\Gamma -Au_{m'}(t),\psi_{m'}dt \\ \to +\int_0^T\int_\Omega \nabla\cdot(Vu(t)+D\nabla u(t))\psi(t)d\sigma dt \\ -\left(\int_0^T\int_\Gamma j_{in}\psi(t)d\sigma dt+\int_0^T\int_\Omega u(t)v_{out}\psi(t)d\sigma dt\right)+\int_0^T\int_\Omega Ku(t)\psi(t)d\sigma dt \\ \text{as } m'\to\infty \end{cases} \tag{3.35}$$

Thus we can pass to the limit in (3.33) and then we have

$$\begin{cases} \int_0^T\int_\Omega (u(t),v)\varphi'(t)d\sigma dt+\int_0^T\int_\Omega \nabla\cdot(V(u(t),v)+D\nabla(u(t),v))\varphi(t)d\sigma dt \\ -\left(\int_0^T\int_\Gamma j_{in}(u(t),v)\varphi(t)d\sigma dt+\int_0^T\int_{\partial\Omega/\Gamma}(u(t),v)v_{out}\varphi(t)d\sigma dt\right) \\ +\int_0^T\int_\Omega K(u(t),v)\varphi(t)d\sigma dt=0\quad \forall v\in\mathfrak{V}\quad\text{and}\quad\forall\varphi\in\mathfrak{D}(]0,T[). \end{cases} \tag{3.36}$$

Since $\mathfrak{V}$ is dense in H^1, (3.36) remains true for all $v\in H^1$ if we shown that u satisfies (3.9).

u is the solution of (3.9)

First we have to show that u is the solution of problem (3.9), it remains to show that (3.8) and (3.10) are satisfied. *For equation (3.8)*: Considering the equation (3.36), we have

$$\begin{cases} \int_0^T\int_\Omega (u(t),v)\varphi'(t)d\sigma dt=-\int_0^T\int_\Omega \nabla\cdot(V(u(t),v)+D\nabla(u(t),v))\varphi(t)d\sigma dt \\ \qquad +\left(\int_0^T\int_\Gamma j_{in}(u(t),v)\varphi(t)d\sigma dt+\int_0^T\int_{\partial\Omega/\Gamma}(u(t),v)v_{out}\varphi(t)d\sigma dt\right) \\ \qquad -\int_0^T\int_\Omega K(u(t),v)\varphi(t)d\sigma dt \\ \qquad =\int_0^T\int_\Omega -A(u(t),v)\varphi(t)d\sigma dt \end{cases} \tag{3.37}$$

Since $A(\cdot)u(\cdot) \in L^2(0,T;H^{-1})^3 \cap H^1(0,T;H^{-1})^3$,

$$\begin{cases} g = A(\cdot)u \in L^2(0,T;H^{-1}) \cap H^1(0,T;H^{-1})^3 \\ \int_0^T \int_\Omega (u(t),v)\varphi'(t)d\sigma dt = \int_0^T \int_\Omega (g(t),v)\varphi(t)d\sigma dt \quad \forall v \in H^1, \quad \forall \varphi \in \mathfrak{D}(]0,T[) \end{cases} \tag{3.38}$$

and, as seen in **[32]**,

$$u' = \frac{du}{dt} \in L^2(0,T;H^{-1})^3 \cap H^1(0,T;H^{-1})^3 \tag{3.39}$$

and $u(t) \in W(H^1)$ is a continuous function from $[0,T] \to L^2$.

For equation (3.10): Let φ be a function of class $\mathfrak{C}^\infty$ over [0,T], zero in a neighbourhood of T, with $\varphi(0) \neq 0$, with values in $\mathbb{R}$.

Then $\psi = \varphi \otimes v$, $v \in H^1$ is in $W(H^1)$ and by parts formula:

$$\int_0^T \int_\Omega (u'(t),\varphi(t)v)d\sigma dt = -\int_0^T \int_\Omega (u(t),v)\varphi'(t)d\sigma dt - (u(0),v)\varphi(0) \tag{3.40}$$

From (3.9) and (3.39) we have

$$\begin{aligned} \int_0^T \int_\Omega (u'(t),\varphi(t)v)d\sigma dt &= -\int_0^T \int_\Omega \nabla \cdot (V(u(t),v) + D\nabla(u(t),v))\varphi(t)d\sigma dt \\ &+ \left(\int_0^T \int_\Gamma j_{in}(u(t),v)\varphi d\sigma dt + \int_0^T \int_{\partial\Omega/\Gamma} (u(t),v)v_{out}\varphi d\sigma dt \right) \\ &- \int_0^T \int_\Omega K(u(t),v)\varphi(t)d\sigma dt \end{aligned} \tag{3.41}$$

And from (3.24), we deduce

$$\begin{aligned} \int_0^T \int_\Omega (u'_{m'}(t),v_{m'})\varphi(t)d\sigma dt &= -\int_0^T \int_\Omega \nabla \cdot (V(u_{m'}(t),v_{m'}) + D\nabla(u_{m'}(t),v_{m'}))\varphi(t)d\sigma dt \\ &+ \left(\int_0^T \int_\Gamma j_{in}(u_{m'}(t),v_{m'})\varphi(t)d\sigma dt + \int_0^T \int_{\partial\Omega/\Gamma} (u_{m'}(t),v_{m'})v_{out}\varphi(t)d\sigma dt \right) \\ &- \int_0^T \int_\Omega K(u_{m'}(t),v_{m'})\varphi(t)d\sigma dt \end{aligned} \tag{3.42}$$

and also

$$\int_0^T \int_\Omega (u'_{m'}(t),v_{m'})\varphi(t)d\sigma dt = \int_0^T \int_\Omega (u_{m'}(t),v_{m'})\varphi'(t)d\sigma dt - (u_{0m'},v_{m'})\varphi(0) \tag{3.43}$$

If we pass to the limit in (3.42) and (3.43) as $m' \to \infty$ we obtain

$$\begin{aligned}\lim_{m'\to\infty}\int_0^T\int_\Omega (u'_{m'}(t),v_{m'})\varphi(t)d\sigma dt &= -\int_0^T\int_\Omega \nabla\cdot(V(u(t),v)+D\nabla(u(t),v))\varphi(t)d\sigma dt\\ &+\left(\int_0^T\int_\Gamma j_{in}(u(t),v)\varphi(t)d\sigma dt+\int_0^T\int_{\partial\Omega/\Gamma}(u(t),v)v_{out}\varphi(t)d\sigma dt\right)\\ &-\int_0^T\int_\Omega K(u(t),v)\varphi(t)d\sigma dt\\ &=\int_0^T\int_\Omega (u'(t),\varphi(t)v)d\sigma dt\end{aligned} \tag{3.44}$$

$$\lim_{m'\to\infty}\int_0^T\int_\Omega (u'_{m'}(t),v_{m'})\varphi(t)d\sigma dt = -\int_0^T\int_\Omega (u(t),v)\varphi'(t)d\sigma dt-(u_0,v)\varphi(0) \tag{3.45}$$

From (3.40), (3.45) and (3.44):

$$(u(0),v)=(u_0,v)\quad \forall v\in H^1 \tag{3.46}$$

and H^1 being dense in L^2, $\forall v\in L^2$, we have

$$u(0)=u_0 \tag{3.47}$$

Thus

Lemma 3.1.8 *The function u is the solution of problem (3.9).*

Now we need to write in the vector form of (3.24) in the approximate problem relative to the space $L^2(0,T;H^{-1})^3$.

Let H_m^{-1} be the set of $u\in H^{-1}$ such that $(u,v)=0$ for all $v\in H_m^1$ and $P_m^{H^{-1}}$ the projection in H^{-1} over H_m^1, following H_m^{-1}: if $\{\tilde{w}_{j,m}\}_{j=1\ to\ d_m}$ is an orthonormal basis in L^2 of H_m^1, $P_m^{H^{-1}}$ is given by:

$$P_m^{H^{-1}}(u)=\sum_{j=1}^{d_m}(u,\tilde{w}_{j,m})\tilde{w}_{j,m}$$

Then (3.24) ist in the form:

$$\frac{du_m}{dt}+P_m^{H^{-1}}A(\cdot)u_m(\cdot)=0 \tag{3.48}$$

Let be the Galerkin approximation such that: (C) the family $(P_m^{H^{-1}})_{m\in\mathbb{N}}$ is bounded in $\mathfrak{L}(H^{-1})$. If the Galerkin approximation is constructed starting from a ortonormal basis in $\mathfrak{H}$ of elements in H^1, then this condition above is always satisfied and (C) implies that such a basis is also a basis in H^1 and in H^{-1}. And the equation (3.30) implies:

$$P_m^{H^{-1}} A(\cdot) u_m \in \text{a bounded set of} \quad L^2(H^{-1})^3 \tag{3.49}$$

And we deduce from (3.48) that the family $\dfrac{du_m}{dt}$ is in a bounded set of $L^2(H^{-1})^3$

Lemma 3.1.9 *The solution u_m of (3.48) remains in a bounded set of $L^\infty(L^2)^3$ and $W(0,T;H^1,H^{-1})$.*

We can extract a weakly convergent (to u) subsequence in $W(H^1)$ from the preceding sequence (and in L^∞ weakly *), as a consequence of the weak compactness of the unit ball of $W(H^1)$.

From Theorem (3.1.3), the mapping $u \in W(H^1) \to u(0) \in (L^2)^3$ is continuous, we can to deduce that $u_m(0)$ tend towards $u(0)$ weakly in $(L^2)^3$, therefore that the initial condition $u(0) = u_0$ is satisfied.

Strong Convergence

One does not need here to extract a subsequence of u_m, because due to uniqueness of the solution we have

$$u_m \to u \quad \text{in} \quad L^2(H^1)^3 \quad \text{weakly and} \quad u_m \to^* u \quad \text{in} \quad L^\infty(L^2)^3 \quad \text{weakly } * \tag{3.50}$$

We now introduce

$$\begin{aligned} X_m(T) = {} & \frac{1}{2}|u_m(T) - u(T)|^2 + \int_0^T \int_\Omega \nabla \cdot (V(u_m(t) - u(t)) + D\nabla(u_m(t) - u(t)))(u_m(t) - u(t)) d\sigma dt \\ & - \left(\int_0^T \int_\Gamma j_{in}(u_m(t) - u(t))(u_m(t) - u(t)) d\sigma dt + \int_0^T \int_{\partial\Omega/\Gamma} (u_m(t) - u(t)) v_{out}(u_m(t) - u(t)) d\sigma dt \right) \\ & + \int_0^T \int_\Omega K(u_m(t) - u(t))(u_m(t) - u(t)) d\sigma dt \end{aligned} \tag{3.51}$$

From (3.29), $u_m(T)$ remains bounded in $(L^2)^3$ and we can extract $\{u_{m'}\}$ in Lemma (3.1.7) with

$$u_{m'}(T) \to X_1 \quad \text{weakly in} \quad (L^2)^3 \tag{3.52}$$

If we take $\varphi \in \mathfrak{D}([0,T])$ null in a neighbourhood of 0, with $\varphi(T) \neq 0$ and doing the same way as in $u(0) = u_0$, we obtain

$$(u(T), v) = (X_1, v), \quad \forall v \in (H^1)^3$$

from which we deduce

$$u(T) = X_1 \tag{3.53}$$

Taking (3.50), we have

$$u_m(T) \to u(T) \quad \text{weakly in} \quad (L^2)^3 \tag{3.54}$$

This set, $X_m(T)$ can be written:

$$X_m(T) = \frac{1}{2}|u_m(T)|^2 + \int_0^T \int_\Omega \nabla \cdot (Vu_m(t) + D\nabla u_m(t))u_m(t)d\sigma dt - \left(\int_0^T \int_\Gamma j_{in}u_m(t)u_m(t)d\sigma dt + \int_0^T \int_{\partial\Omega/\Gamma} u_m(t)v_{out}u_m(t)d\sigma dt \right) + \int_0^T \int_\Omega Ku_m(t)u_m(t)d\sigma dt + Y_m(T)$$

Thanks to Lemma (3.1.7) and to (3.54), we have

$$\lim_{n\to\infty} Y_m(T) = -\frac{1}{2}|u(T)|^2 - \int_0^T \int_\Omega \nabla \cdot (Vu(t) + D\nabla u(t))u(t)d\sigma dt + \left(\int_0^T \int_\Gamma j_{in}u(t)u(t)d\sigma dt + \int_0^T \int_{\partial\Omega/\Gamma} u(t)v_{out}u(t)d\sigma dt \right) - \int_0^T \int_\Omega Ku(t)u(t)d\sigma dt \quad (3.55)$$

From (3.26), we deduce by integration from 0 to T:

$$\frac{1}{2}|u_m(T)|^2 + \int_0^T \int_\Omega \nabla \cdot (Vu_m(t) + D\nabla u_m(t))u_m(t)d\sigma dt - \left(\int_0^T \int_\Gamma j_{in}u_m(t)u_m(t)d\sigma dt + \int_0^T \int_{\partial\Omega/\Gamma} u_m(t)v_{out}u_m(t)d\sigma dt \right) + \int_0^T \int_\Omega Ku_m(t)u_m(t)d\sigma dt = \frac{1}{2}|u_{0m}|^2$$

from which

$$\lim_{m\to\infty} \frac{1}{2}|u_m(T)|^2 + \int_0^T \int_\Omega \nabla \cdot (Vu_m(t) + D\nabla u_m(t))u_m(t)d\sigma dt - \left(\int_0^T \int_\Gamma j_{in}u_m(t)u_m(t)d\sigma dt + \int_0^T \int_{\partial\Omega/\Gamma} u_m(t)v_{out}u_m(t)d\sigma dt \right) + \int_0^T \int_\Omega Ku_m(t)u_m(t)d\sigma dt = \frac{1}{2}|u_0|^2 \quad (3.56)$$

But from equation (3.9)

$$\begin{aligned}\frac{1}{2}|u_0|^2 = \frac{1}{2}|u(T)|^2 &+ \int_0^T \int_\Omega \nabla \cdot (Vu(t) + D\nabla u(t))u(t)d\sigma dt \\ &- \left(\int_0^T \int_\Gamma j_{in} u(t)u(t)d\sigma dt + \int_0^T \int_{\partial\Omega/\Gamma} u(t)v_{out}u(t)d\sigma dt \right) \\ &+ \int_0^T \int_\Omega Ku(t)u(t)d\sigma dt\end{aligned} \tag{3.57}$$

Thus (3.55), (3.56) and (3.57) imply

$$\lim_{m\to\infty} X_m(T) = 0 \tag{3.58}$$

Since from (3.12), we have

$$0 \le \alpha \int_0^T \int_\Omega ||u_m(t) - u(t)||^2 d\sigma dt \le X_m(T) \tag{3.59}$$

we deduce from (3.58) and (3.59).

Proposition 3.1.10 *When $m \to \infty$, we have $u_m \to u$ strongly in $L^2(H^1)^3$.*

The equation (3.58) implies that $u_m(T) \to u(T)$ strongly in $(L^2)^3$. More generally

$$\forall t \in [0,T], \quad u_m(t) \to u(t) \quad \text{strongly in } (L^2)^3. \tag{3.60}$$

For this, it is sufficient to remark that for $t_0 \in]0,T[$ fixed, $L^2(0,t_0;H^1)^3$ identifies with a subspace of $L^2(H^1)^3$. Then all $v \in L^2(H^1)^3$ define, by restriction to $]0,t_0[$, an element of $L^2(0,t_0,H^1)^3$ and (3.60) results from:

$$\begin{aligned}X_m(t_0) = &\frac{1}{2}|u_m(t_0) - u(t_0)|^2 \\ &+ \int_0^T \int_\Omega \nabla \cdot (V(u_m(\sigma) - u(\sigma)) + D\nabla(u_m(\sigma) - u(\sigma))(u_m(\sigma) - u(\sigma))d\sigma dt \\ &- \left(\int_0^T \int_\Gamma j_{in}(u_m(\sigma) - u(\sigma))(u_m(\sigma) - u(\sigma))d\sigma dt \right. \\ &\left. + \int_0^T \int_{\partial\Omega/\Gamma} (u_m(\sigma) - u(\sigma))v_{out}(u_m(\sigma) - u(\sigma))d\sigma dt \right) \\ &+ \int_0^T \int_\Omega K(u_m(\sigma) - u(\sigma))(u_m(\sigma) - u(\sigma))d\sigma dt\end{aligned} \tag{3.61}$$

3.1.4 Continuity Theorem

Considering the variational formulation of the problem, the uniqueness of the solution and the existence of the solution previously presented, we want to enunciate the following theorem in order to evaluate the continuity of the solution with respect to the data.

Suppose that the equation (3.12) holds.

Theorem 3.1.11 *Let u_0 and $u_0^* \in L^2(0,T;H^{-1})^3 \cap H^1(0,T;H^{-1})^3$ and let u and u^* be the corresponding solutions of problem (3.9), then*

$$||u - u^*||_{L^\infty(L^2)} \leq c_3|u_0 - u_0^*| \tag{3.62}$$

$$||u - u^*||_{L^2(H^1)} \leq \frac{1}{\sqrt{c_2}}|u_0 - u_0^*| \tag{3.63}$$

Proof. Set $w = u - u^*$, $w(0) = u_0 - u_0^*$. Then w satisfies

$$\begin{cases} w \in W(0,T;H^1,H^{-1}) \\ \int_0^T \int_\Omega \partial_t(w(t),v)d\sigma dt = \int_0^T \int_\Omega \nabla \cdot (Vw(t) + D\nabla w(t))vd\sigma dt - \int_0^T \int_\Omega (Kw(t))vd\sigma dt \in \mathfrak{D}(]0,T[) \\ w(0) = u_0 - u_0^* \end{cases} \tag{3.64}$$

and we have

$$\frac{1}{2}|w(t)|^2 - \int_0^t \int_\Omega \nabla \cdot (Vw(\sigma) + D\nabla w(\sigma))w(\sigma)d\sigma dt + \int_0^t \int_\Omega (Kw(\sigma))w(\sigma)d\sigma dt = \frac{1}{2}|w(0)|^2 \tag{3.65}$$

As for the a priori estimates, we obtain:

$$\frac{1}{2}|w(t)|^2 \leq -c_2||w||^2_{(H^1)^3} + c_3||w||^2_{(L^2)^3} + \frac{1}{2}|w(0)|^2 \tag{3.66}$$

and we have (3.62) and (3.63).

4

Parameter Identification Problem

Parameter identification problems are often used in research in applied sciences. For example, the identification of parameters in mathematical models is the key to describe biological systems. Some works take into account a special type of a non-linear function estimator, called sigmoidal networks for estimation of the parameters of compartmental models for neural network analysis [**43, 99**]. An adjoint method for performing automatic parameter identification on differential equation based models with application to protein regulatory networks can be find in [**86**].

The identification of parameters in tracer kinetic models has also increasing importance in medical areas. Our emphasis in this work is into one of the most important applications in clinical and research PET: myocardial perfusion imaging. The radioactive tracer measured with PET can be put in relation with the physiological process by identifying a model describing the kinetics of the tracer in the system [**84**]. The tracers most commonly used to examine the myocardial region in examinations PET are ^{13}N-ammonia [**26, 41, 98**] and $H_2^{15}O$ [**2, 10, 53, 62, 68**]. A general literature on parameter identification can be found in [**5, 54, 55, 30, 38**].

Even after the parameters are identified, it is important to make an analysis of the results, since there are several factors that can influence their quality. As sources of uncertainty we can find the low sensitivity of parameters and measured values, the model adopted to represent the object of study (since the parameters are valid only for the model adopted) and the imprecision of the measured values, either read errors or imprecision of the instrument used.

It is therefore required an evaluation of the model by synthesizing data, which by Ljung [**72**], depends on the following aspects:

- degree of agreement between the values of experimentally obtained data and the values obtained with the utilization of the model in question;
- usefulness of the intended purpose of the model in real cases;
- capacity of the model in describing the real system.

The second point above is the interesting from a practical viewpoint. The usefulness of the proposed model is verified if, using a particular model, the estimated physiological parameters help the medical diagnose a satisfactory manner. The evaluation of the parameters estimated for the problem addressed here is done in *Chapter 7*.

In this chapter we present the parameter identification problem associated with the model proposed here but first we will make a short introduction involving the definition of inverse problems.

4.1 Inverse Problems

Inverse problems constitute a very interesting class of problems involving knowledge in various areas of mathematics and has many applications in many other sciences, including the reconstruction of images using PET.

For our case, in particular, given PET-sinogram data the inverse problem of generating an image $u(x)$ from this data is to compute u from

$$\xi(Ku) = f \tag{4.1}$$

where ξ represents Poisson statistics of the data and K denotes the Radon Transform, defined by

$$(Ku)(\theta, s) = \int_{x\cdot\theta} u(x)dx. \tag{4.2}$$

The maximum likelihood estimate is given by

$$u \in \arg\min_{u\in\Omega}\left\{\int_{\Omega} Ku - flog(Ku)d\sigma(\theta, y)\right\} \Rightarrow u \in \arg\min_{u\in\Omega}\left\{\int_{\Omega} flog\left(\frac{f}{Ku}\right) + Ku - fd\sigma(\theta, y)d\sigma(\theta, y)\right\} \tag{4.3}$$

Thus calculating the partial Fréchet-derivative of the associated Lagrange functional and setting then to zero, yields the optimality condition

$$K^*1 - K^*\left(\frac{f}{Ku}\right) = 0, \tag{4.4}$$

where 1 denotes the constant function taking only the value one and K^* is the adjoint operator of K. Therefore the solution to the above equation can be obtained by the EM-algorithm presented in the next section.

$$u_{k+1} = \frac{u_k}{K^*1}K^*\left(\frac{f}{Ku_k}\right). \tag{4.5}$$

But instead of solving an inverse problem and calculating the parameters directly to u, we will compute the parameters as an inverse problem involving the inversion of a non-linear operator G (which produces a sequence of images $u(x,t)$) for physiological parameters p as follows with more explanations in the next section.

Thus, we want to reconstruct the image u subject to $u(x,t) = G(p(x))$ such that

$$u(x,t) = C_{\mathcal{T}}(x,t) + C_{\mathcal{V}}(x,t) + C_{\mathcal{A}}(x,t) \tag{4.6}$$

where the vector p contain all non-negative parameters

$$p = (k_1(x), k_2(x), k_3(x), D_{\mathcal{T}}(x), D_{\mathcal{A}}(x), D_{\mathcal{V}}(x), V_{\mathcal{T}}(x), V_{\mathcal{A}}(x), V_{\mathcal{V}}(x)) \tag{4.7}$$

4.2 Variational Model

Let G correspond to the conditions cited above. The variational problem for the calculation of the parameters can be written as an optimization problem with appropriate added regularization ($\mathcal{R}(p)$) as follows

$$IM(u) + \mathcal{R}(p) \to \min_p \quad \text{subject to} \quad u(x,t) = G(p) \tag{4.8}$$

with IM representing the image reconstruction process.

Considering the EM-functional (presented in the next Section) and writing the problem as time-dependent data, we have

$$\int_0^T \int_\Omega (Ku - f log(Ku)) + \mathcal{R}(p) \to \min_p, \quad \text{subject to} \quad u = G(p). \tag{4.9}$$

Making the calculation of the partial Fréchet-derivatives of the associate Lagrange functional and setting them to zero **[6]**, we obtain

$$0 = \frac{\partial}{\partial u}\mathcal{L}(u,p;q) = K^*1 - K^*\left(\frac{f}{Ku}\right) - q \tag{4.10}$$

$$0 = \frac{\partial}{\partial p}\mathcal{L}(u,p;q) = \mathcal{R}'(p) + G'(p)^* q \tag{4.11}$$

$$0 = \frac{\partial}{\partial q}\mathcal{L}(u,p;q) = G(p) - u \tag{4.12}$$

with $G(p)$ being positive. Multiplying the first equation with u, we have

$$0 = us - uK^*\left(\frac{f}{Ku}\right) - uq \tag{4.13}$$

$$G'(p)^* q = -\mathcal{R}'(p) \tag{4.14}$$

with $u = G(p)$ and $s := K^*1$.

As seen in **[90]** we can write the minimization problem (with a convex function) as follows

$$\begin{aligned} &\min_{u,p}\{I = KL(f,Ku) + \mathcal{R}(p) | G(p) = u\} \\ &= \min_{p\in\Omega}\{KL(f,F(p)) + \mathcal{R}(p)\} \end{aligned} \tag{4.15}$$

where $KL(f,Ku)$ denotes the Kullback-Leibler (KL) functional defined below.

Definition 4.2.1 *(Kullback-Leibler Functional) The Kullback-Leibler functional is a function* $KL : L^2(\Omega) \times L^2(\Omega) \to \mathbb{R}_{\geq 0} \bigcup \{+\infty\}$ *with* $\Omega \subset \mathbb{R}^m$ *bounded and measurable, given by*

$$KL(\varphi,\psi) = \int_\Omega \left(\varphi \log\left(\frac{\varphi}{\psi}\right) - \varphi + \psi\right)\vartheta \quad \forall \quad \varphi,\psi \geq 0 a.e. \tag{4.16}$$

where ϑ *is a measure. Note that, using the convention* $0 \log 0 = 0$*. the integrand in (4.16) is* *nonnegative and vanishes if only if $\varphi = \psi$.*

Lemma 4.2.2 *(Properties of KL Functional) Let K satisfy Assumption (4.2.5) (i) and (ii). Then the following statements hold:*

(i) The function $(\varphi, \psi) \longmapsto KL(\varphi, \psi)$ is convex and thus, due to the linearity of the operator K, the function $(\varphi, u) \longmapsto KL(\varphi, Ku)$ is also convex.

(ii) For any fixed nonnegative $\varphi \in L^2(\Omega)$, the function $u \longmapsto KL(\varphi, Ku)$ is lower semicontinuous with respect to the topology τ_{L^2}.

(iii) For any nonnegative functions φ and ψ in $L^2(\Omega)$, one has

$$||\varphi - \psi||^2_{L^2(\Omega)} \leq \left(\frac{2}{3}||\varphi||_{L^2(\Omega)} + \frac{4}{3}||\psi||_{L^2(\Omega)}\right) KL(\varphi, \psi) \tag{4.17}$$

Proof. *(i)* See **[90], Lemma 3.4**.

(ii) For the proof we consider **[90], Lemma 3.4 (iii)**. Let be the a nonnegative function ($\varphi \in L^2(\Omega)$) and consider u_n converging in the topology τ_{L^2} to some $u \in \{w \in L^2 : w \geq a.e.\}$; being u_n a sequence in the domain of the function $w \longmapsto KL(\varphi, Kw)$. As the operator K is sequentially continuous with respect to the topologies τ_{L^2} and τ_V we have the convergence of the sequence (Ku_n) to Ku in the norm topology $L^2(\Omega)$. Thus, the sequence $\left(\varphi \log\left(\frac{\varphi}{Ku_n}\right) - \varphi + Ku_n\right)$ converges almost everywhere to $\varphi \log\left(\frac{\varphi}{Ku}\right) - \varphi + Ku$ and we obtain by Fatou's Lemma

$$\int_\Omega \left(\varphi \log\left(\frac{\varphi}{Ku}\right) - \varphi + Ku\right) d\sigma \leq \liminf_{n\to\infty} \int_\Omega \left(\varphi \log\left(\frac{\varphi}{Ku_n}\right) - \varphi + Ku_n\right) d\sigma \tag{4.18}$$

And (4.18) means that the function $w \longmapsto KL(\varphi, Kw)$ is lower semicontinuous with respect to the topology τ_{L^2}.

(iii) See **[90], Lemma 3.3** and **[13], Lemma 2.2**.

Corollary 4.2.3 *If $\{\varphi_n\}$ and $\{\psi_n\}$ are bounded sequences in $L^2(\Omega)$, then*

$$\lim_{n\to\infty} KL(\varphi_n, \psi_n) = 0 \Rightarrow \lim_{n\to\infty} ||\varphi_n - \psi_n||_{L^2(\Omega)} = 0 \tag{4.19}$$

Proof. The statements follows directly from *Lemma 4.2.2 - (iii)*

We make now some considerations involving the functional K and the regularization functional $\mathcal{R}$.

Assumption 4.2.4 *We assume here that the regularization functional $\mathcal{R}(p) : \mathcal{D}_p \to \mathbb{R}_{\geq 0} \cup \{\infty\}$ is convex on a Banach space $\mathcal{D}_p \subset L^2(\Omega)^n$.*

For the next considerations, it is necessary the assumptions below

Assumption 4.2.5 *We assume also that*

(i) The operator $K : L^2(\Omega) \to L^2(\Omega)$ is linear and bounded,

(ii) *The operator K preserves positivity, $(Ku \geq 0)$ a.e. for any $u \geq 0$ a.e. and the equality is fulfilled if and only if $u = 0$.*

(iii) *If $u \in L^2(\Omega)$ satisfies $c_1 \leq u \leq c_2$ a.e. for some positive constants c_1,$c_2 > 0$ then there exist c_3, $c_4 > 0$ such that $c_3 < Ku < c_4$ a.e. on Ω.*

(iv) *The functional $G(p) : (\mathcal{D}_p, \tau) \rightarrow L^2$ is continuous and $G(p) > 0$.*

(v) *The functional $KL(f, KG(p))$ is lower semicontinuous with the topologie τ.*

(vi) *For every $a > 0$, the sub-level sets $\mathcal{S}_\mathcal{R}(a)$ of the functional $\mathcal{R}(p)$, defined by*

$$\mathcal{S}_\mathcal{R}(a) := \{p \in\subset \mathcal{D}_p : \mathcal{R} \leq a\} \tag{4.20}$$

are sequentially precompact in metric topology τ.

(viii) *The functional $\mathcal{R} : \mathcal{D}_p \longrightarrow \mathcal{R}_{\geq 0} \cup \{+\infty\}$ is convex, lower semicontinuous with respect to the topology τ (see Definition 4.2.6 below) and can also be singular, i.e. it is not differentiable in the classical sense.*

(iv) *We consider $\mathcal{D}_p$ compact embedded in $(L^\infty)^3 \times (L^\infty)^{d\times 3} \times (L^2)^3$.*

Definition 4.2.6 *(Lower Semicontinuous Functional) Let U be a linear locally convex space and $I : U \rightarrow \mathbb{R} \cup \{+\infty\}$ a functional (not necessarily convex). Then I is lower semicontinuous, if it satisfies the following equivalent conditions:*

(i) *The sub-level sets*

$$\{p \in U : I(p) \leq a\} \tag{4.21}$$

are closed for every $a \in \mathcal{R}$.

(ii) *For any $u \in U$ and for every converging sequence (p_n) with limit u it holds*

$$I(p) \leq \lim \inf_{n\rightarrow\infty} I(p_n) \tag{4.22}$$

4.3 Existence of a Minimum

Theorem 4.3.1 *Let K, $\mathcal{R}$ and I satisfy Assumption (4.2.5). Moreover assume that $\alpha > 0$, $f \in V_\mu(\Omega)$ is nonnegative and that the operator K satisfies $K\mathbf{1} \neq 0$, where $\mathbf{1}$ denotes the characteristic function on Ω. Then, the functional I defined in (4.15) has a minimizer.*

Proof. To prove the above theorem, we use the method of calculus of variations proposed in **[4]**.

Let $\mathcal{D}(I) \neq \emptyset$, i.e., there exists at least one $v \in L^2(\Omega)$ such that $I(v) < \infty$. Thus, consider $(p_n) \subset \mathcal{D}(I)$, $p_n \geq 0$ a.e., be a minimizing sequence of the functional I, i.e.

$$\lim_{n\rightarrow\infty} I(p_n) = \inf_{p\in\mathcal{D}(I)} I(p) =: I_{min} < \infty \tag{4.23}$$

Thus, for all $\epsilon > 0$ there exists $n_0 \in \mathbb{N}$ such that for all $n \geq n_0$

$$\begin{aligned} a := I_{min} + \epsilon \geq I(p_n) &\overset{4.15}{=} KL(f, KG(p_n)) + \alpha\mathcal{R}(p_n) \\ &\geq \mathcal{R}(p_n) \end{aligned} \tag{4.24}$$

due to the positivity of the KL functional and $\alpha > 0$. Thus $(p_n)_{n \geq n_0} \subset \mathcal{S}_{\mathcal{R}}(a)$ and it follows from *Assumption 4.2.5 - (v)* that (p_n) has a τ_{L^2}-convergent subsequence (p_{n_j}), which converges to some $\tilde{p} \in L^2(\Omega)$. As $\mathcal{R}$ is lower semicontinuous with respect to topology τ_{L^2}, we have

$$\mathcal{R}(\tilde{p}) \overset{\text{Definition 4.2.6}}{\leq} \liminf_{j\to\infty} \mathcal{R}(p_{n_j}) \overset{4.24}{\leq} a \tag{4.25}$$

and with it that $\tilde{p} \in \mathcal{S}_{\mathcal{R}}(a)$. Simultaneously, caused by *Lemma 4.2.2*, the functional I in (4.15) is lower semicontinuous with respect to the topology τ_{L^2} and implies

$$I(\tilde{p}) \overset{\text{Definition 4.2.6}}{\leq} \liminf_{j\to\infty} I(p_{n_j}) \overset{4.23}{=} I_{min} \tag{4.26}$$

which means that $\tilde{p}$ is a minimizer of I.

4.4 Properties of $G(p)$

Theorem 4.4.1 *Let* $(k_1, k_2, k_3, V_{\mathcal{A}}, V_{\mathcal{T}}, V_{\mathcal{V}}, D_{\mathcal{A}}, D_{\mathcal{T}}, D_{\mathcal{V}}) \in \mathcal{D}_p(G(p))$*;* $G(p)$ *being defined as in (4.9) and the vector* p *containing all nonnegative parameters (4.7). Then,* $u = G(p)$ *is non-negative.*

Proof. By the equation (4.9) we have

$$G(p) = u(x,t) = C_{\mathcal{A}}(x,t) + C_{\mathcal{T}}(x,t) + C_{\mathcal{V}}(x,t) \tag{4.27}$$

Then we need to show that the radioactive concentration in artery, tissue and vein are nonnegative. First consider $C_{\mathcal{A}}(x,t)$ as in the equation (3.1). We can write

$$L(p)C_{\mathcal{A}}(x,t) = D_{\mathcal{A}}\Delta C_{\mathcal{A}}(x,t) + V_{\mathcal{A}}\nabla C_{\mathcal{A}}(x,t) + (k_0 + k_1)C_{\mathcal{A}}(x,t) = f(x), \quad x \in \Omega \tag{4.28}$$

This type of differential equations satisfy the so-called maximum principle implying that the maximum/ minimum of a function in a domain is to be found on the boundary of that domain **[40]**. Consider the following proposition:

Proposition 4.4.2 *(Strong Maximum Principle) Let* $C_{\mathcal{A}}(x,t)$ *and* $L(p)$ *as in the equation (4.28) with* $LC_{\mathcal{A}} > 0$*. Then* $C_{\mathcal{A}} \geq 0$ *or* $C_{\mathcal{A}}$ *has no local minimum in the interior of* Ω *on* $t > 0$*.*

In addition, we want apply the maximum principle for the case $LC_{\mathcal{A}} \geq 0$.

Proposition 4.4.3 *(Weak Maximum Principle) Let* $C_{\mathcal{A}}(x,t)$ *and* $L(p)$ *as in the equation (4.28) with* $LC_{\mathcal{A}} \geq 0$*. Then if* $C_{\mathcal{A}}$ *has the global minimum, it is on at* $t = 0$*.*

Proof. Let $C_{\mathcal{A}}$ such that the global minimum at an interior point $\overline{x} \in \Omega$ and $C_{\mathcal{A}}(\overline{x}) > 0$. Consider then the function $C^{\epsilon}_{\mathcal{A}} = C_{\mathcal{A}} + \varepsilon t$ and $C_{\mathcal{V}} = 0$. Then holds

$$\partial_t C^{\varepsilon}_{\mathcal{A}} = \partial_t C_{\mathcal{A}} + \varepsilon$$
$$\partial_t C^{\varepsilon}_{\mathcal{A}} = D_{\mathcal{A}} \Delta C_{\mathcal{A}} + V_{\mathcal{A}} \nabla C_{\mathcal{A}} - (k_0 + k_1) C_{\mathcal{A}} + \varepsilon$$

First consider the case $C^{\varepsilon}_{\mathcal{A}} \geq 0$ in (x,t) and assume the minimum of $C_{\mathcal{A}}$ in $C_{\mathcal{A}} = 0$, we have then $\partial_t C^{\varepsilon}_{\mathcal{A}} = 0$, $(k_0 + k_1) C_{\mathcal{A}} = 0$, $\nabla C_{\mathcal{A}} = 0$ and $D_{\mathcal{A}} \Delta C_{\mathcal{A}} \geq 0$, which implies

$$-\varepsilon + \partial_t C^{\varepsilon}_{\mathcal{A}} = D_{\mathcal{A}} \Delta C_{\mathcal{A}} + V_{\mathcal{A}} \nabla C_{\mathcal{A}} - (k_0 + k_1) C_{\mathcal{A}}$$
$$0 > -\varepsilon = D_{\mathcal{A}} \Delta C_{\mathcal{A}} \geq 0$$

And as $C^{\varepsilon}_{\mathcal{A}} \geq 0$, we have

$$C^{\varepsilon}_{\mathcal{A}} = C_{\mathcal{A}} + \varepsilon t \geq 0 \Longrightarrow C_{\mathcal{A}} \geq -\varepsilon t \quad \forall \varepsilon$$

And thus $C_{\mathcal{A}} \geq 0$ when $\varepsilon \to 0$ (considering α sufficiently small) which is a contradiction to a Strong Maximum Principle. In the same way, the proof holds for $C_{\mathcal{T}}$ and $C_{\mathcal{V}}$, considering the functions $C^{\epsilon}_{\mathcal{T}} = C_{\mathcal{T}} + \varepsilon t$ and $C^{\epsilon}_{\mathcal{V}} = C_{\mathcal{V}} + \varepsilon t$. For more examples see **[40]**.

We know then that in $t = 0$, $C^{\varepsilon}_{\mathcal{A}}(x,0) > 0$, $C^{\varepsilon}_{\mathcal{T}}(x,0) > 0$ and $C^{\varepsilon}_{\mathcal{V}}(x,0) > 0$. Consider then the case where $C^{\varepsilon}_{i}(x,t) < 0$ and exists $C_{\mathcal{A}_i}(\overline{x},\overline{t})$ so that the minimum is found when $C^{\varepsilon}_{\mathcal{A}}(\overline{x},\overline{t}) = 0$ for $t \leq \overline{t}$ without loss of generality and

$$C^{\varepsilon}_{\mathcal{A}}(x,t) \geq 0 \quad C^{\varepsilon}_{\mathcal{T}}(x,t) \geq 0 \quad C^{\varepsilon}_{\mathcal{V}}(x,t) \geq 0$$

and, therefore

$$-\varepsilon \underbrace{\frac{\partial C_{\mathcal{A}}}{\partial t}}_{=0} = \underbrace{D_{\mathcal{A}} \Delta C_{\mathcal{A}}}_{\geq 0} + \underbrace{V_{\mathcal{A}} \nabla C_{\mathcal{A}}}_{=0} + \underbrace{(k_0 + k_1) C_{\mathcal{A}}}_{=0} + \underbrace{k_3}_{\geq 0} \underbrace{C_{\mathcal{V}}}_{\geq 0}$$
$$\Longrightarrow 0 = -\varepsilon \geq 0$$

and the same is true for the equations (3.2) and (3.3).

Theorem 4.4.4 *(Continuity) Let $(k_1, k_2, k_3, V_{\mathcal{A}}, V_{\mathcal{T}}, V_{\mathcal{V}}, D_{\mathcal{A}}, D_{\mathcal{T}}, D_{\mathcal{V}}) \in \mathcal{D}_p(G(p))$ and let $\alpha \in \mathbb{R}_+$ be positive. Then $u = G(p)$, $G : \mathcal{D}_p \to W(0,T; H^1, H^{-1})$ is continuous.*

Proof. To prove the continuity, let $u = G(p) = \begin{pmatrix} \frac{\partial C_{\mathcal{A}}}{\partial t} \\ \frac{\partial C_{\mathcal{V}}}{\partial t} \\ \frac{\partial C_{\mathcal{T}}}{\partial t} \end{pmatrix}$ and let for this case $\partial_t u = L(p)u$, according to the equation (3.6).

Consider $u_1 = \begin{pmatrix} \frac{\partial C_{\mathcal{A}_1}}{\partial t} \\ \frac{\partial C_{\mathcal{V}_1}}{\partial t} \\ \frac{\partial C_{\mathcal{T}_1}}{\partial t} \end{pmatrix}$ and $u_2 = \begin{pmatrix} \frac{\partial C_{\mathcal{A}_2}}{\partial t} \\ \frac{\partial C_{\mathcal{V}_2}}{\partial t} \\ \frac{\partial C_{\mathcal{T}_2}}{\partial t} \end{pmatrix}$ associated respectively to the vectors of parameters p_1 and p_2. Writing

$$\partial_t u_i = L(p_i) u_i \tag{4.29}$$

Applying above the difference $\tilde{u} = u_1 - u_2$, we have

$$\begin{aligned} \partial_t (u_1 - u_2) &= L(p_1) u_1 - L(p_2) u_2 \\ &= L(p_1)(u_1 - u_2) + (L(p_1) - L(p_2)) u_2 \end{aligned} \tag{4.30}$$

$$\begin{aligned} \Longrightarrow \partial_t \tilde{u} - L(p_1)\tilde{u} &= f \\ &= (L(p_1) - L(p_2))u_2 \end{aligned} \tag{4.31}$$

Finally the continuity in u can be shown by a Lipschitz-argument:

$$\begin{aligned} \Longrightarrow ||\tilde{u}||_{W(0,T;H^1,H^{-1})} &\leq c||f||_{L^2(0,T;H^{-1})} \\ &\leq \tilde{c}||L(p_1) - L(p_2)||_{L^2(0,T;H^{-1})} \end{aligned} \tag{4.32}$$

Then since L is linear, we have

$$||(L(p_1) - L(p_2))v||_{L^2(0,T;H^{-1})} \leq c||p_1 - p_2||_{\mathcal{D}_p}||v||_{W(0,T;H^1,H^{-1})} \tag{4.33}$$

Lemma 4.4.5 *Let $L(p)$ satisfy the conditions above then*

$$||L(p)v||_{L^2(0,T;H^{-1})} \leq c||p||_{\mathcal{D}_p}||v||_{L^2(0,T;H^1)} \tag{4.34}$$

Proof. First we consider only the portion that represent the diffusion. Calculating the norm for this portion, we have:

$$||\nabla \cdot (\varphi \nabla v)||_{L^2(0,T;H^{-1})} \leq c||\varphi \nabla v||_{L^2} \tag{4.35}$$

And considering $\varphi(x) \in \mathcal{D}_p$, we can calculate

$$\begin{aligned} \int_0^T \int_\Omega \varphi^2 |\nabla v|^2 dx dt &\leq ||\varphi||_\infty^2 \left|\left| \int_0^T \int_\Omega |\nabla v|^2 dx dt \right|\right| \\ &\leq ||\varphi||_\infty ||\nabla v||_{L^2} \\ &\leq ||\varphi||_\infty ||v||_{L^2(0,T;H^1)} \end{aligned} \tag{4.36}$$

Analyzing now only the portion that represents the transport we have

$$\begin{aligned} ||\nabla \cdot (\varphi v)||_{L^2(0,T;H^{-1})} &\leq \bar{c}||\varphi v||_{L^2} \\ &\leq \bar{c}||\varphi v||_{L^2(0,T;L^q)} \end{aligned} \tag{4.37}$$

with $q < 2$ optimal so that

$$L^q \hookrightarrow H^{-1}.$$

Considering the regularization functional cited previously, remembering that $\Omega \subset \mathbb{R}^d$, the following embedding of H^1 holds by **[95] Lemma 4**:

$$H^1 \hookrightarrow L^\Upsilon$$

$$\text{for } 2 \leq \Upsilon \begin{cases} \leq \infty, & \text{if } d = 1, \\ < \infty, & \text{if } d = 2, \\ < \dfrac{2d}{d-2}, & \text{if } d = 3 \end{cases} \tag{4.38}$$

and thus, employing the Hölder's inequality

$$||\varphi v||_{L^2(0,T;L^q)} \leq ||\varphi||_{L^2(0,T;L^q)}||v||_{L^2(0,T;L^\Upsilon)} \tag{4.39}$$

And finally, considering the portion that represents the exchange of materials and using again the Hölder's inequality we have

$$||\varphi v||_{L^2(0,T;H^{-1})} \leq \widetilde{c}||\varphi||_{L^2} \tag{4.40}$$

Theorem 4.4.6 *Under the condition of Theorem 4.4.4, the operator $G(p)$ for $G(p)$ defined as in the equation (4.9) is Fréchet-differentiable.*

Proof. Let $\partial_t u = L(p)u$, $u = G(p)$ and consider $v = G'(p)\varphi$ being the derivative in the direction φ. Therefore

$$\begin{aligned} \frac{\partial}{\partial t}(G'(p)\varphi) = \partial_t v &= L(p)(G'(p)\varphi) + (L'(p)\varphi)G(p) \\ &= L(p)v + \underbrace{K(\varphi)G(p)}_{f} \end{aligned} \tag{4.41}$$

$$\Longrightarrow \frac{\partial v}{\partial t} = L(p)v + f \tag{4.42}$$

Where

$$\begin{aligned} G'(p)\varphi &= \lim_{\varepsilon \to 0} \frac{G(p+\varepsilon\varphi) - G(p)}{\varepsilon} \\ \varepsilon G'(p)\varphi &\approx G(p+\varepsilon\varphi) - G(p) \end{aligned}$$

Thus,

$$\begin{aligned} ||G(p+\varepsilon\varphi) - G(p) - \varepsilon G'(p)\varphi|| &= \theta(\varepsilon) \\ \Longrightarrow ||G^\varepsilon - G - \varepsilon v|| &= \theta(\varepsilon) \underset{\varepsilon \to 0}{\Longrightarrow} 0 \end{aligned} \tag{4.43}$$

and hence, the equation (2.10) is satisfied for all $\varphi \in L^\infty$.

Consider now that $\dfrac{\partial G^\varepsilon}{\partial t} = L(p+\varepsilon\varphi)G^\varepsilon, G^\varepsilon = G(p+\varepsilon\varphi)$, $\dfrac{\partial G}{\partial t} = L(p)G(p)$, $\dfrac{\partial v}{\partial t} = L(p) + f$ and $w = G^\varepsilon - G - \varepsilon v$, then

$$\begin{aligned} \frac{\partial(G^\varepsilon - G - \varepsilon v)}{\partial t} = \frac{\partial w}{\partial t} &= L(p+\varepsilon\varphi)G(p+\varepsilon\varphi) - L(p)G(p) - \varepsilon(L(p) + f) \\ &= L^\varepsilon \underbrace{(G^\varepsilon - G - \varepsilon v)}_{w} + \underbrace{L^\varepsilon(G+\varepsilon v) - L(G+\varepsilon v) - \varepsilon f}_{g} \end{aligned} \tag{4.44}$$

and thus,

$$\begin{aligned} \frac{\partial w}{\partial t} &= L(p)w + g \\ \Longrightarrow ||w||_{W(0,T;H^1,H^{-1})} &\leq c||g||_{L^2(0,T;H^{-1})} \end{aligned} \tag{4.45}$$

Since $L^\varepsilon = L(p+\varepsilon\varphi)$, L is linear i.e. $L(p_1) + L(p_2) = L(p_1 + p_2)$ and $L'(p)\varphi = L(\varphi)$, we have

$$\begin{aligned} g &= L^\varepsilon(G+\varepsilon v) - L(G+\varepsilon v) - \varepsilon f \\ &= L(p+\varepsilon\varphi)(G+\varepsilon v) - L(p)(G+\varepsilon v) - \varepsilon L(\varphi)G \\ &= \underbrace{(L(p+\varepsilon v) - L(p) - \varepsilon L(\varphi))}_{=0(\varepsilon\to 0)} G + \underbrace{(L(p+\varepsilon\varphi) - L(\varphi))}_{\varepsilon L(\varphi)} \varepsilon v \\ &= \varepsilon^2 L(\varphi)v. \end{aligned} \tag{4.46}$$

And we have to verify

$$||L(\varphi)v|| \leq c||\varphi||^2 \tag{4.47}$$

where the physiological parameters $D_{\mathcal{A}/\mathcal{T}/\mathcal{V}} \in (L^\infty)^3$, $V_{\mathcal{A}/\mathcal{T}/\mathcal{V}} \in (L^\infty)^{d\times 3}$ and $k_i \in (L^2)^3$, for $i = 1, 2, 3$.

First we consider only the portion that represent the diffusion. Calculating the norm for this portion, we have:

$$||\nabla \cdot (\varphi \nabla v)||_{L^2(0,T;H^{-1})} \leq c||\varphi \nabla v||_{L^2} \tag{4.48}$$

And considering $\varphi(x) \in \mathcal{D}_p$, we can calculate

$$\begin{aligned} \int_0^T \int_\Omega \varphi^2 |\nabla v|^2 dx dt &\leq ||\varphi||_\infty^2 \left|\left| \int_0^T \int_\Omega |\nabla v|^2 dx dt \right|\right| \\ &\leq ||\varphi||_\infty \underbrace{||\nabla v||_{L^2}}_{\leq ||v||_{L^2(0,T;H^1)}} \end{aligned} \tag{4.49}$$

As we know that $\dfrac{\partial v}{\partial t} = L(p)v + L(\varphi)G(p)$ and it implies

$$||v||_{W(0,T;H^1,H^{-1})} \leq c||f||_{L^2(0,T;H^1)}, \tag{4.50}$$

calculating $||f||$ we have

$$\begin{aligned} ||f||_{W(0,T;H^1,H^{-1})} &= ||\nabla \cdot (\varphi \nabla G(p))|| \\ &\leq ||\varphi||_\infty \cdot ||G(p)||_{L^2(0,T;H^1)} \\ &\leq \tilde{c}||\varphi||_\infty \cdot ||G(p)||_{L^2(0,T;H^1)} \end{aligned} \tag{4.51}$$

And thus,

$$\begin{aligned} ||\nabla(\varphi \nabla v)||_{W(0,T;H^1,H^{-1})} &\leq c||\varphi \nabla v||_{L^2} \\ &\leq ||\varphi||_\infty ||v||_{L^2} \\ &\leq ||\varphi||_\infty \left(c||f||_{L^2}\right) \\ &\leq ||\varphi||_\infty \tilde{c}||\varphi||_\infty ||G(p)||_{L^2(0,T;H^1)} \\ &\leq \tilde{c}||\varphi||_\infty^2 ||G(p)||_{L^2} \end{aligned} \tag{4.52}$$

Analyzing now only the portion that represents the transport we have

$$\begin{aligned} ||\nabla \cdot (\varphi v)||_{L^2(0,T;H^{-1})} &\leq \bar{c}||\varphi v||_{L^2} \\ &\leq \bar{c}||\varphi v||_{L^2(0,T;L^q)} \end{aligned} \tag{4.53}$$

with $q < 2$ optimal so that

$$L^q \hookrightarrow H^{-1}.$$

Considering the regularization functional cited previously, remembering that $\Omega \subset \mathbb{R}^d$, the following embedding of H^1 holds by **[95] Lemma 4**:

$$H^1 \hookrightarrow L^\Upsilon$$

$$\text{for } 2 \leq \Upsilon \begin{cases} \leq \infty, & \text{if } d = 1, \\ < \infty, & \text{if } d = 2, \\ < \dfrac{2d}{d-2}, & \text{if } d = 3 \end{cases} \tag{4.54}$$

and thus, employing the Hölder's inequality

$$||\varphi v||_{L^2(0,T;L^q)} \leq ||\varphi||_{L^2(0,T;L^q)}||v||_{L^2(0,T;L^\Upsilon)} \tag{4.55}$$

and, as seen previously, we need to calculate $||f||$:

$$\begin{aligned} ||f||_{L^2(0,T;H^{-1})} &= c||(\varphi\nabla G(p))||_{L^2(0,T;H^1)} \\ &\leq ||\varphi||_{L^2(0,T;L^q)} \cdot ||G(p)||_{L^2(0,T;H^1)} \end{aligned} \tag{4.56}$$

that implies

$$\begin{aligned} ||(\varphi\nabla v)||_{L^2(0,T;H^{-1})} &\leq \overline{c}||\varphi\nabla v||_{L^2(0,T;H^{-1})} \\ &\leq \overline{\overline{c}}||\varphi||_{L^2(0,T;L^q)}||v||_{L^2(0,T;H^1)} \\ &\underset{(4.42)}{\leq} \overline{\overline{c}}||\varphi||^2_{L^q}||G(p)||_{L^2(0,T;H^1)} \end{aligned} \tag{4.57}$$

for appropriated Υ and q. And finally, considering the portion that represents the exchange of materials and using again the Hölder's inequality we have

$$||\varphi v||_{L^2(0,T;H^{-1})} \leq \widetilde{c}||\varphi||_{L^2} \tag{4.58}$$

Thus, with all the considerations made above, we have that $G(p)$ is Fréchet-differentiable.

4.5 Stability of the regularized Poisson estimation problem

The stability results guarantee that the regularized approximations converge to a solution p, if the approximated data converge to a smooth function f.

Theorem 4.5.1 *Let K, $\mathcal{R}$, I and $V_\mu(\Omega)$ satisfy Assumption 4.2.5. Let also $\alpha > 0$ be fixed and assume that the functions $f_n \in V_\mu(\Omega)$, $n \in \mathbb{N}$, are nonnegative approximations of a data function $f \in V_\mu(\Omega)$ such that*

$$\lim_{n\to\infty} KL(f_n, f) = 0 \tag{4.59}$$

Also let

$$p_n \in \arg \min_{\substack{p\in L^2(\Omega) \\ p\geq 0 a.e.}} \{I_n(p) := KL(f_n, F(p)) + \mathcal{R}(p)\}, \quad n \in \mathbb{N} \tag{4.60}$$

with $F(p) = KG(p)$ and p a solution of the regularized problem (4.15) corresponding to the data function f. Additionally, we assume that $\log f$ and $\log(KG(p))$ belong to the function space $L^\infty_\mu(\Omega)$ and there exists positive constants $c_1, ..., c_4$ such that

$$0 < c_1 \leq f \leq c_2 \quad \textit{and} \quad 0 < c_3 \leq KG(p) \leq c_4 \quad \textit{a.e. on } \Omega \tag{4.61}$$

We supose now that the sequence (f_n) is uniformly bounded in the V_μ-norm, i.e, there exists a *positive constant* c_5 *such that*

$$||f_n||_{V_\mu} \leq c_5, \quad \forall \; n \; in \; \mathbb{N} \tag{4.62}$$

Then the problem (4.15) is stable with respect to the perturbations in the data, i.e, the sequence (p_n) *has a* τ*-convergent subsequence and every* τ*-convergent subsequence converges to a minimizer of the functional* I *in (4.15).*

Proof. We will use the pre-compactness property of the sublevel sets $\mathcal{S}_\mathcal{R}$ from *Assumption 4.2.5 - (vi)* for the existence of a τ-convergent subsequence of (p_n). We have to show also the uniform boundedness of the sequence $(\mathcal{R}(p_n))$. Consider $\alpha > 0$ a fixed regularization parameter. For any $n \in \mathbb{N}$, the positivity of the KL functional and the definition of p_n as a minimizer of the objective functional I_n in (4.60) implies that

$$\mathcal{R}(p_n) \leq \underbrace{KL(f_n, F(p_n)) + \mathcal{R}(p_n)}_{I_n(p_n)} \leq \underbrace{KL(f_n, F(p)) + \mathcal{R}(p)}_{I_n(p)} \tag{4.63}$$

Hence, the sequence $\mathcal{R}(p_n)$ is bounded if the sequence $KL(f_n, F(p))$ on the right-hand side of (4.63) is bounded. To show this, we use the condition (4.62) and obtain the uniform boundedness of sequence (f_n) in the $L^2(\Omega)$-norm, due to continuous embedding of V_μ in *Assumption 4.2.5 - (vii)*. Therefore, condition (4.59) and the result in *Corollary 4.2.3* yield the strong convergence of (f_n) to f in $L^2(\Omega)$, i.e, we have

$$\lim_{n \to \infty} ||f - f_n||_{L^2(\Omega)} = 0 \tag{4.64}$$

Thus the condition (4.61) implies together with the inequality

$$\begin{aligned} |KL(f_n, F(p)) - KL(f, F(p)) - KL(f_n, f)| &= \left| \int_\Omega (\log KF(p) - \log f)(f - f_n) d\mu \right| \\ &\leq \underbrace{|| \log KF(p) - \log f||_{L^\infty(\Omega)}}_{<\infty} \; \underbrace{||f - f_n||_{L^2_\Omega}}_{\overset{(4.64)}{\longrightarrow} 0} \end{aligned}$$

the following convergence:

$$\lim_{n \to \infty} KL(f_n, KF(p)) = KL(f, KF(p)) \tag{4.65}$$

The expressions $KL(f, F(p))$ and $\mathcal{R}(p)$ are bounded because p is a minimizer of the regularized problem (4.15) corresponding to the data function f and thus also the sequence $(KL(f_n, F(p)))$ is bounded, since convergent to $KL(f, F(p))$. This means, together with the boundedness of $\mathcal{R}(p)$ and the property (4.63), the uniform boundedness of the sequence $(\mathcal{R}(p_n))$.

The uniform boundedness of the sequence $(\mathcal{R}(p_n))$ means that exists $a \in \mathbb{R}_{\geq 0}$ such that $(\mathcal{R}(p_n))$ is contained in the sub-level set $\mathcal{S}_\mathcal{R}(a)$. Thus, the precompactness *Assumption 4.2.5 - (vi)* ensures the existence of a τ-convergent subsequence (p_{n_j}), which converges to some $\tilde{p} \in \mathcal{D}_p$. Actually $\tilde{p}$ lies in $\mathcal{S}_\mathcal{R}(a)$, since $\mathcal{R}$ is lower semi-continuous with respect to the topology τ and therefore $\mathcal{S}_\mathcal{R}(a)$ is τ-closed. (see *Definition 4.2.6*).

Consider now an arbitrary subsequence (p_{n_j}) of (p_n), which converges to some $\tilde{p} \in \mathcal{D}_p$ with respect to the topology τ. Due to the sequential continuity of the operator K we have also the convergence of $(KF(p_{n_j}))$ to $KF(\tilde{p})$ in the strong norm topology on $L^2(\Omega)$, as well as the pointwise convergence almost everywhere on Ω. Similarly, it holds also for the sequence (f_n), which converges strongly to f in $L^2(\Omega)$ (4.64). Thus, since the functions f_n and p_n are nonnegative for all $n \in \mathbb{N}$ and K is an operator that preserves positivity (see Assumption 4.2.5 - (ii)), we can apply Fatou's Lemma to the sequence $(f_{n_j} \log(f_{n_j}/KF(p_{n_j})) - f_{n_j} + KF(p_{n_j}))$ and we have

$$KL(f, KF(\tilde{p})) \leq \lim_{j\to\infty}\inf KL(f_{n_j}, KF(p_{n_j})) \tag{4.66}$$

Due the lower semicontinuity of the regularization energy $\mathcal{R}$ (see *Assumption 4.2.5 - (viii)*) and due to (4.63), (4.65) and (4.66), we obtain the inequality

$$\begin{aligned}
KL(f, KF(\tilde{p})) + \mathcal{R}(\tilde{p}) &\overset{4.66}{\leq} \lim_{j\to\infty}\inf KL(f_{n_j}, KF(p_{n_j})) + \lim_{j\to\infty}\inf \mathcal{R}(p_{n_j}) \\
&\leq \lim_{j\to\infty}\inf \Big(KL(f_{n_j}, KF(p_{n_j})) + \mathcal{R}(p_{n_j})\Big) \\
&\leq \lim_{j\to\infty}\sup \Big(KL(f_{n_j}, KF(p_{n_j}) + \mathcal{R}(p_{n_j})\Big) \\
&\overset{4.63}{\leq} \lim_{j\to\infty}\sup \Big(KL(f_{n_j}, KF(p)) + \mathcal{R}(p)\Big) \\
&\overset{4.65}{=} KL(f, KF(p)) + \mathcal{R}(p)
\end{aligned} \tag{4.67}$$

which means that $\tilde{p}$ is a minimizer of the functional I in (4.15).

4.6 EM Algorithm

We present in this section the Expectation Maximization algorithm **[34, 82, 97]**, which was created by Dempster, Laird and Rubin (1977) and is commonly used to solve maximun likehood estimation problems. Such problems appear in several areas e.g. astronomy, microscopy and medical imaging.

We work here with a formulation based on inverse problems with measured data from Poisson statistics associated with the problem (4.9).

Computing the first order optimality condition for (4.9), we have

$$\begin{aligned}
&0 = K * \mathbf{1} - K^*\left(\frac{f}{Ku}\right) - \lambda \\
&0 = \lambda u
\end{aligned} \tag{4.68}$$

where λ represents the Lagrange multiplier ($\lambda \geq 0$) for the Karush-Kuhn-Tucker (KKT) conditions **[52]**, K^* is the adjoint operator of K and $\mathbf{1}$ is the constant function taking only the value one.

If we multiply the equation (4.68) by u we obtain the iterative scheme

$$u_{k+1} = \frac{u_k}{K^*\mathbf{1}} K^*\left(\frac{f}{Ku_k}\right) \tag{4.69}$$

just eliminating the second equation in (4.68) and preserving the positivity of K.

We now consider two cases, the case of noisy data and noise-free data. In the case of noisy data, we must take in consideration if the operator K is discrete or continuous. If K is a matrix and u

a vector (discrete case) it is guaranteed the existence of the minimizer since the smallest singular value is bounded away from zero by a positive value [**93**]. If it is continuous, we can prove the convergence but even a divergence of the EM-algorithm is possible due to underlying ill-posedness of the image reconstruction problems.

Already in the case of noise-free data the convergence proofs of the EM-algorithm can be found in [**56, 82, 91, 102**], even though the speed of convergence of iteration (4.69) is slow.

4.7 Forward-Backward Splitting

The splitting methods are based on the simple idea of dividing the original problem into two subproblems that, when solved iteratively, provide a solution to the original problem [**7**]. A major advantage of using splitting methods is the effort required to solve a simple problem. Here we present a splitting method called Forward-Backward Splitting that in comparison to the Gradient method, gives a significant gain of time in search of minimizers parameters for our optimization problem. Forward-Backward Splitting methods are versatile in offering ways of exploiting the special structure of variational inequality problems [**28**].

We apply the method to the minimization problem following

$$u \in \arg\min_{u\in\Omega}\{K(u) = L(u) + M(u)\} \tag{4.70}$$

where for our case $L(u)$ denotes the Kullback-Leibler functional and $M(u)$ represents the regularization functional $\mathcal{R}(p)$. Thus, we can solve the problem with the aid of a variable stepsize:

$$\begin{aligned} u_{k+\frac{1}{2}} &\in \{u_k - \tau_k \partial_u L(u_k)\} \\ u_{k+1} &\in \{u_{k+\frac{1}{2}} - \tau_k \partial_u M(u_{k+1})\} \end{aligned} \tag{4.71}$$

for τ a positive stepsize sequence.

The first-half step can be realized via the well-known EM iteration to reconstruct the image u by

$$u_{k+\frac{1}{2}} = \frac{u_k}{K^*1} K^* \left(\frac{f}{Ku_k}\right) \tag{4.72}$$

Thus, $u_{k+\frac{1}{2}}$ is obtained with the above equation and (4.13) can be rewritten as

$$q = \frac{u_k - u_{k+\frac{1}{2}}}{u_k} \tag{4.73}$$

Equation (4.73) can be treated as a solution of the minimization problem

$$\frac{1}{2}\int_0^T\int_\Omega \frac{\left(u - u_{k+\frac{1}{2}}\right)^2}{u_k} dxdt - \langle u, q\rangle_{L_2(\Omega)} \to \min_u \,, \tag{4.74}$$

And, if we change u by $G(p)$ we obtain

$$\frac{1}{2}\int_0^T\int_\Omega \frac{\left(G(p)-u_{k+\frac{1}{2}}\right)^2}{u_k}dxdt - \langle G(p),q\rangle_{L_2(\Omega)} \to \min_p \ , \tag{4.75}$$

The Fréchet-derivative of $\langle G(p),q\rangle$ in p is simply $G'(p)^*q$. Using (4.14) we can replace $-\langle G(p),q\rangle$ by $\mathcal{R}(p)$ to obtain the reduced problem

$$\frac{1}{2}\int_0^T\int_\Omega \frac{\left(G(p)-u_{k+\frac{1}{2}}\right)^2}{u_k}dxdt + \mathcal{R}(p) \to \min_p \ , \tag{4.76}$$

The second half-step is a parameter identification problem, formulated as the constrained optimization problem with added regularization, given by the equation (4.76).

Finally the first-order optimality condition for (4.76) is given by

$$0 = G'(p)^*\left(\frac{G(p)-u_{k+\frac{1}{2}}}{u_k}\right) + \mathcal{R}'(p), \tag{4.77}$$

We can not solve the above equation directly, since the parameter p contains several functions that have to be computed each on their own. This problem will be treated as a problem of identification of parameters, discussed in *Section 4.8*.

4.8 Parameter Identification Problem

The purpose of this section is the development of the parameter identification problem to allow the calculation of all the biological parameters that composes the vector p. Unfortunately we can not directly solve the equation (4.77) for p, since p contains several functions and $G'(p)^*$ is also difficult to calculate because it is a vector of functions itself. Thus, minimizing the function below (with the regularization added)) we can find the values that correspond to the desired physiological parameters

$$\frac{1}{2}\int_0^T\int_\Omega \frac{\left(u-u_{k+\frac{1}{2}}\right)^2}{u_k}dxdt + \mathcal{R}(p) + \int_0^T\int_\Omega (G(p)-u)\,q\,dxdt \to \min_p \ , \tag{4.78}$$

with $G(p) = G(p(x,t)) = u(x,t)$, for all $(x,t)\in\Omega\times[0,T]$. With the associated Lagrange functional one has

$$\mathcal{L}(u,p;q) = \frac{1}{2}\int_0^T\int_\Omega \frac{(u-u_{k+\frac{1}{2}})^2}{u_k}dxdt + \mathcal{R}(p) + \int_0^T\int_\Omega (G(p)-u)\ q\ dxdt \tag{4.79}$$

And with all constrains to $C_{\mathcal{A}}, C_{\mathcal{V}}$ and C_T we obtain the follows Lagrange functional:

$$
\begin{aligned}
&\mathcal{L}(u(x,T), C_{\mathcal{A}}(x,t), C_{\mathcal{T}}(x,t), C_{\mathcal{V}}(x,t), D_{\mathcal{T}}(x), D_{\mathcal{A}}(x), D_{\mathcal{V}}(x), V_{\mathcal{T}}(x), V_{\mathcal{A}}(x),\\
&\quad V_{\mathcal{V}}(x), k_1(x), k_2(x), k_3(x); q(x,t), \mu(x,t), \eta(x,t), \gamma(x,t))\\
&= \frac{1}{2}\int_0^T\int_\Omega \frac{(u-u_{k+\frac{1}{2}})^2}{u_k} dxdt + \mathcal{R}_1(\mathcal{D}_{\mathcal{A}}(x)) + \mathcal{R}_2(\mathcal{D}_{\mathcal{V}}(x)) + \mathcal{R}_3(\mathcal{D}_{\mathcal{T}}(x)) + \mathcal{R}_4(\mathcal{V}_{\mathcal{A}}(x))\\
&+ \mathcal{R}_5(\mathcal{V}_{\mathcal{V}}(x)) + \mathcal{R}_6(\mathcal{V}_{\mathcal{T}}(x)) + \mathcal{R}_7(k_1(x)) + \mathcal{R}_8(k_2(x)) + \mathcal{R}_9(k_3(x))\\
&+ \int_0^T\int_\Omega \left(G(C_{\mathcal{A}}(x,t), C_{\mathcal{T}}(x,t), C_{\mathcal{V}}(x,t), D_{\mathcal{T}}(x), D_{\mathcal{A}}(x), D_{\mathcal{V}}(x), V_{\mathcal{T}}(x), V_{\mathcal{A}}(x), V_{\mathcal{V}}(x)) - u\right) q(x,t) dxdt\\
&+ \int_0^T\int_{\mathcal{T}} \Big(\frac{\partial C_{\mathcal{T}}}{\partial t}(x,t) - \nabla(V_{\mathcal{T}}(x)C_{\mathcal{T}}(x,t)) - \nabla\cdot(D_{\mathcal{T}}(x)\nabla C_{\mathcal{T}}(x,t))\\
&-k_1(x)C_{\mathcal{A}}(x,t) + (k_0+k_2)(x)C_{\mathcal{T}}(x,t)\Big)\,\mu(x,t)dxdt\\
&+ \int_0^T\int_{\mathcal{A}} \Big(\frac{\partial C_{\mathcal{A}}}{\partial t}(x,t) - \nabla(V_{\mathcal{A}}(x)C_{\mathcal{A}}(x,t)) - \nabla\cdot(D_{\mathcal{A}}(x)\nabla C_{\mathcal{A}}(x,t))\\
&-k_3(x)C_{\mathcal{V}}(x,t) + (k_0+k_1)(x)C_{\mathcal{A}}(x,t)\Big)\,\eta(x,t)dxdt\\
&+ \int_0^T\int_{\mathcal{V}} \Big(\frac{\partial C_{\mathcal{V}}}{\partial t}(x,t) - \nabla(V_{\mathcal{V}}(x)C_{\mathcal{V}}(x,t)) - \nabla\cdot(D_{\mathcal{V}}(x)\nabla C_{\mathcal{V}}(x,t))\\
&-k_2(x)C_{\mathcal{T}}(x,t) + (k_0+k_3)(x)C_{\mathcal{V}}(x,t)\Big)\,\gamma(x,t)dxdt
\end{aligned}
\tag{4.80}
$$

One must now calculate the optimality conditions to the problem, which means that all the partial Fréchet-derivatives must be zero. Thus, considering the previous equation (4.80) we obtain

$$
\frac{\partial \mathcal{L}}{\partial u} = \frac{u(x,t) - u_{k+\frac{1}{2}}(x,t)}{u_k(x,t)} - q(x,t) = 0 \tag{4.81}
$$

To calculate the derivative in relation to $D_{\mathcal{A}}(x)$, let be $J(D_{\mathcal{A}}(x))$ the equation formed only by the terms of $\mathcal{L}$ (4.80) containing $D_{\mathcal{A}}(x)$

$$
J(D_{\mathcal{A}}(x)) = \int_0^T\int_{\mathcal{A}} D_{\mathcal{A}}(x)\nabla C_{\mathcal{A}}(x,t)\cdot\nabla\eta(x,t)\; dxdt + \mathcal{R}_1(D_{\mathcal{A}}(x))
$$

Take the directional derivative in direction $\varphi(x)$

$$
\begin{aligned}
J(D_{\mathcal{A}}(x) + \tau\varphi(x)) = &\int_0^T\int_{\mathcal{A}} (D_{\mathcal{A}}(x) + \tau\varphi(x))\nabla C_{\mathcal{A}}(x,t)\cdot\nabla\eta(x,t)\; dxdt\\
&+ \mathcal{R}_1(D_{\mathcal{A}}(x) + \tau\varphi(x))
\end{aligned}
$$

Thus

$$\frac{d}{d\tau}J(D_{\mathcal{A}}(x)+\tau\varphi(x)) = \int_0^T\int_{\mathcal{A}} \varphi(x)\nabla C_{\mathcal{A}}(x,t)\cdot\nabla\eta(x,t)\ dxdt + \mathcal{R}'_1(D_{\mathcal{A}}(x))\varphi(x)$$
$$= \int_{\mathcal{A}} \varphi(x)\left[\int_0^T \nabla C_{\mathcal{A}}(x,t)\nabla\eta(x,t)\ dt\right] dx$$
$$= \left\langle \varphi(x), \int_0^T \nabla C_{\mathcal{A}}(x,t)\nabla\eta(x,t)\ dt\right\rangle$$

And the derivative in relation to $D_{\mathcal{A}}(x)$ is

$$\frac{\partial\mathcal{L}}{\partial D_{\mathcal{A}}} = \int_0^T \nabla C_{\mathcal{A}}(x)\cdot\nabla\eta(x,t)\ dt + \mathcal{R}'_1(D_{\mathcal{A}}(x)) \tag{4.82}$$

Then, we obtain additional optimality conditions for $D_{\mathcal{V}}(x)$ and $D_{\mathcal{T}}(x)$

$$\frac{\partial\mathcal{L}}{\partial D_{\mathcal{V}}} = \int_0^T \nabla C_{\mathcal{V}}(x)\cdot\nabla\gamma(x,t)\ dt + \mathcal{R}'_2(D_{\mathcal{V}}(x)) \tag{4.83}$$

$$\frac{\partial\mathcal{L}}{\partial D_{\mathcal{T}}} = \int_0^T \nabla C_{\mathcal{T}}(x)\cdot\nabla\mu(x,t)\ dt + \mathcal{R}'_3(D_{\mathcal{T}}(x)) \tag{4.84}$$

For $V_{\mathcal{A}}(x)$, $V_{\mathcal{V}}(x)$ and $V_{\mathcal{T}}(x)$ one proceeds at the same way. Let the directional derivative in direction $\varphi(x)$

$$J(V_{\mathcal{A}}(x)+\tau\varphi(x)) = \int_0^T\int_{\mathcal{A}} (V_{\mathcal{A}}(x)+\tau\varphi(x))C_{\mathcal{A}}(x,t)\cdot\nabla\eta(x,t)\ dxdt + \mathcal{R}_4(V_{\mathcal{A}}(x)+\tau\varphi(x))$$

Thus

$$\frac{d}{d\tau}J(V_{\mathcal{A}}(x)+\tau\varphi(x)) = \int_0^T\int_{\mathcal{A}} \varphi(x)C_{\mathcal{A}}(x,t)\cdot\nabla\eta(x,t)\ dxdt + \mathcal{R}'_4(V_{\mathcal{A}}(x))\varphi(x)$$
$$= \int_{\mathcal{A}} \varphi(x)\left[\int_0^T C_{\mathcal{A}}(x,t)\nabla\eta(x,t)\ dt\right] dx$$
$$= \left\langle \varphi(x), \int_0^T C_{\mathcal{A}}(x,t)\nabla\eta(x,t)\ dt\right\rangle$$

Thus,

$$\frac{\partial\mathcal{L}}{\partial V_{\mathcal{A}}} = \int_0^T V_{\mathcal{A}}(x)\cdot\nabla\eta(x,t)\ dt + \mathcal{R}'_4(V_{\mathcal{A}}(x)) \tag{4.85}$$

Consequently

$$\frac{\partial \mathcal{L}}{\partial V_{\mathcal{V}}} = \int_0^T V_{\mathcal{V}}(x) \cdot \nabla \gamma(x,t)\, dt + \mathcal{R}'_5(V_{\mathcal{V}}(x)) \tag{4.86}$$

$$\frac{\partial \mathcal{L}}{\partial V_{\mathcal{T}}} = \int_0^T V_{\mathcal{T}}(x) \cdot \nabla \mu(x,t)\, dt + \mathcal{R}'_6(V_{\mathcal{T}}(x)) \tag{4.87}$$

For the derivative in relation to $C_{\mathcal{T}}(x,t)$ consider the directional derivative in the direction $\varphi_{\mathcal{T}}(x,t)$.

$$\begin{aligned}
\frac{\partial \mathcal{L}}{\partial C_{\mathcal{T}}}\varphi_{\mathcal{T}}(x,t) = &\int_0^T \int_\Omega \frac{d}{d\tau}(G(C_{\mathcal{A}}(x,t), C_{\mathcal{V}}(x,t), C_{\mathcal{T}}(x,t) + \tau\varphi_T(x,t), \lambda_{\mathcal{T}}(x), \lambda_{\mathcal{A}}(x), \lambda_{\mathcal{V}}(x), D_{\mathcal{V}}(x),\\
&V_{\mathcal{V}}(x), D_{\mathcal{A}}(x), V_{\mathcal{A}}(x), D_{\mathcal{T}}(x), V_{\mathcal{T}}(x), k_1(x), k_2(x), k_3(x)) - u(x,t))q(x,t)dxdt\\
&+ \int_0^T \int_\Omega \frac{d}{d\tau}\left(\frac{\partial}{\partial t}(C_{\mathcal{T}}(x,t) + \tau\varphi_{\mathcal{T}}(x,t)) + \nabla(V_{\mathcal{T}}(x)(C_{\mathcal{T}}(x,t) + \tau\varphi_{\mathcal{T}}(x,t)))\right.\\
&+ \nabla \cdot (D_{\mathcal{T}}(x)\nabla(C_{\mathcal{T}}(x,t) + \tau\varphi_{\mathcal{T}}(x,t)))\\
&+ (k_0 + k_2)(x)(C_{\mathcal{T}}(x,t) + \tau\varphi_{\mathcal{T}}(x,t))\mu(x,t)\\
&\left.-k_2(x)(C_{\mathcal{T}}(x,t) + \tau\varphi_{\mathcal{T}}(x,t))\gamma(x,t)\right) dxdt\\
&= \int_0^T \int_\Omega \frac{\partial G}{\partial C_{\mathcal{T}}}\varphi_{\mathcal{T}}(x,t)q(x,t)dxdt\\
&+ \int_0^T \int_\Omega \frac{\partial \varphi_{\mathcal{T}}}{\partial t}\mu(x,t) + V_{\mathcal{T}}(x)\varphi_{\mathcal{T}}(x,t)\nabla\mu(x,t) + D_{\mathcal{T}}(x)\nabla\varphi_{\mathcal{T}}(x,t)\nabla\mu(x,t)\\
&+ (k_0 + k_2)(x)\varphi_{\mathcal{T}}(x,t)\mu(x,t) - k_2(x)\varphi_{\mathcal{T}}(x,t)\gamma(x,t)dxdt\\
&= \int_0^T \int_\Omega \left(\frac{\partial G}{\partial C_{\mathcal{T}}}q(x,t) - \frac{\partial \mu}{\partial t}(x,t) + V_{\mathcal{T}}(x)\nabla\mu(x,t) - \nabla \cdot (D_{\mathcal{T}}(x)\nabla\mu(x,t))\right.\\
&\left.+(k_0 + k_2)(x)\mu(x,t) - k_2(x)\gamma(x,t)\right)\varphi_{\mathcal{T}}(x,t)dxdt\\
&+ \int_{\mathcal{T}} \varphi_{\mathcal{T}}(x,t)\mu(x,t)\Big|_0^T + \int_0^T \int_{\partial\Omega} D_{\mathcal{T}}(x)\varphi_{\mathcal{T}}(x,t)\nabla\mu \cdot n dxdt
\end{aligned} \tag{4.88}$$

As the above equation is zero, we have

$$\begin{aligned}
\frac{\partial \mu}{\partial t} &= V_{\mathcal{T}}(x)\nabla\mu(x,t) - \nabla \cdot (D_{\mathcal{T}}(x)\nabla\mu(x,t)) + (k_0 + k_2)(x)\mu(x,t)\\
&\quad - k_2(x)\gamma(x,t) + \frac{\partial G}{\partial C_{\mathcal{T}}}q(x,t)\\
&\quad \text{subject to} \quad \mu(x,T) = 0 \quad \text{for all } x \in \mathcal{T}.
\end{aligned} \tag{4.89}$$

Similarly, one can calculate the derivatives in relation to $C_{\mathcal{A}}(x,t)$ and $C_{\mathcal{V}}(x,t)$:

$$\frac{\partial \mathcal{L}}{\partial C_{\mathcal{A}}}\varphi_{\mathcal{A}}(x,t) = \int_0^T \int_\Omega \left(\frac{\partial G}{\partial C_{\mathcal{A}}} q(x,t) - \frac{\partial \eta}{\partial t}(x,t) + V_{\mathcal{A}}(x)\nabla\eta(x,t) - \nabla\cdot(D_{\mathcal{A}}(x)\nabla\eta(x,t)) \, dxdt \right.$$
$$\left. + (k_0+k_1)(x)\eta(x,t) - k_1(x)\mu(x,t) \right) \varphi_{\mathcal{A}}(x,t)dxdt + \int_{\mathcal{A}} \varphi_{\mathcal{A}}(x,t)\eta(x,t)\Big|_0^T \tag{4.90}$$
$$+ \int_0^T \int_{\partial\Omega} D_{\mathcal{A}}(x)\varphi_{\mathcal{A}}(x,t)\nabla\eta\cdot n dxdt$$

with

$$\frac{\partial \eta}{\partial t} = V_{\mathcal{A}}(x)\nabla\eta(x,t) - \nabla\cdot(D_{\mathcal{A}}(x)\nabla\eta(x,t)) + (k_0+k_1)(x)\eta(x,t) - k_1(x)\mu(x,t) + \frac{\partial G}{\partial C_{\mathcal{A}}}q(x,t)$$
$$\text{subject to} \quad \eta(x,T) = 0 \quad \text{for all } x\in\mathcal{A}. \tag{4.91}$$

and

$$\frac{\partial \mathcal{L}}{\partial C_{\mathcal{V}}}\varphi_{\mathcal{V}}(x,t) = \int_0^T \int_\Omega \left(\frac{\partial G}{\partial C_{\mathcal{V}}} q(x,t) - \frac{\partial \gamma}{\partial t}(x,t) + V_{\mathcal{V}}(x)\nabla\gamma(x,t) - \nabla\cdot(D_{\mathcal{V}}(x)\nabla\gamma(x,t)) \, dxdt \right.$$
$$\left. +(k_0+k_3)(x)\gamma(x,t) - k_3(x)\eta(x,t) \right) \varphi_{\mathcal{V}}(x,t)dxdt \tag{4.92}$$
$$+ \int_{\mathcal{V}} \varphi_{\mathcal{V}}(x,t)\gamma(x,t)\Big|_0^T + \int_0^T \int_{\partial\Omega} D_{\mathcal{V}}(x)\varphi_{\mathcal{V}}(x,t)\nabla\gamma\cdot n dxdt$$

with

$$\frac{\partial \gamma}{\partial t} = V_{\mathcal{V}}(x)\nabla\gamma(x,t) - \nabla\cdot(D_{\mathcal{V}}(x)\nabla\gamma(x,t)) + (k_0+k_3)(x)\gamma(x,t) - k_3(x)\eta(x,t) + \frac{\partial G}{\partial C_{\mathcal{V}}}q(x,t)$$
$$\text{subject to} \quad \gamma(x,T) = 0 \quad \text{for all } x\in\mathcal{V}. \tag{4.93}$$

$$\frac{\partial \mathcal{L}}{\partial q} = G(C_{\mathcal{A}}(x,t), C_{\mathcal{V}}(x,t), C_{\mathcal{T}}(x,t) + \tau\varphi_T(x,t), \lambda_{\mathcal{T}}(x), \lambda_{\mathcal{A}}(x), \lambda_{\mathcal{V}}(x), D_{\mathcal{V}}(x), V_{\mathcal{V}}(x), D_{\mathcal{A}}(x),$$
$$V_{\mathcal{A}}(x), D_{\mathcal{T}}(x), V_{\mathcal{T}}(x), k_1(x), k_2(x), k_3(x)) - u(x,t) \tag{4.94}$$

4.9 Regularization

The regularization consists in the determination of the smoother approximate solution compatible with the data of observation for a certain level of noise. The fact of seeking a smoother solution (regular) transforms the ill-posed problem in a well-posed, but still able to reflect the physical situation to be modeled **[33]**.

We choose the regularization parameter as the lowest value one able to produce a stable solution to the problem, reducing the influence of a-priori information and also the bias. Then we apply the regularization incorporating a-priori knowledge and the gradient regularization as follows in the next sections.

4.9.1 Regularization Incorporating A-priori Knowledge

We will here use a-priori knowledge in the regularization functional for each parameter of the problem. Whereas, for example, the velocity of the radioactive concentration in the artery has a typical value of $V_{\mathcal{A}}^*$, we can regularize $V_{\mathcal{A}}$ by

$$\mathcal{R}(V_{\mathcal{A}}(x)) = \frac{\alpha}{2} \int_{\Omega} (V_{\mathcal{A}} - V_{\mathcal{A}}^*)^2 dx \tag{4.95}$$

where α denotes the regularization parameter, $\alpha \in \mathbb{R}_+$. As seen in **[6]**, such a-priori regularization can also be generalized to all biological parameters of vector p as follows

$$\mathcal{R}_{\alpha,\Psi}(g(\omega), g^*) = \frac{\alpha}{2} \int_{\Psi} (g(\omega) - g^*)^2 d\omega \tag{4.96}$$

for a set $\Psi \subset \Omega$ or $\Psi = [0,T]$ and $\alpha \in \mathbb{R}_+$. In the following, the a-priori knowledge will be incorporated in each parameter of the problem independently. We denote our a-priori knowledge with $k_1, k_2, k_3, V_{\mathcal{A}}, V_{\mathcal{T}}, V_{\mathcal{V}}, D_{\mathcal{A}}, D_{\mathcal{T}}, D_{\mathcal{V}}$ and for the sake of simplicity, we write $\mathcal{R}_{\alpha,\mathcal{A}}(V_{\mathcal{A}}(x))$ instead of $\mathcal{R}_{\alpha,\mathcal{A}}(V_{\mathcal{A}}(x), V_{\mathcal{A}}^*)$.

4.9.2 Gradient Regularization

Like the a-priori regularization we also will apply the Gradient regularization in each parameter independently. The regularization of the gradient is designed to ensure (guarantee) smoothness in space and time, adding a bound to the spatial gradients ($\nabla k_1, \nabla k_2, \nabla k_3, \nabla V_{\mathcal{A}}, \nabla V_{\mathcal{T}}, \nabla V_{\mathcal{V}}, \nabla D_{\mathcal{A}}, \nabla D_{\mathcal{T}}$, $\nabla D_{\mathcal{V}}$). The regularization added to the terms is given by

$$\mathcal{R}_{\xi,\Phi}(g) = \frac{\xi}{2} \int_{\Phi} |\nabla g(x)|^2 dx \tag{4.97}$$

with $\Phi \in \Omega$. Thus, replacing in the equation (4.80) by the a-priori and gradient regularizations, we have

$$\begin{aligned}
&\mathcal{L}(u(x,T),\lambda_{\mathcal{T}}(x),\lambda_{\mathcal{A}}(x),\lambda_{\mathcal{V}}(x),C_{\mathcal{A}}(x,t),C_{\mathcal{T}}(x,t),C_{\mathcal{V}}(x,t),D_{\mathcal{T}}(x),D_{\mathcal{A}}(x),D_{\mathcal{V}}(x),\\
&V_{\mathcal{T}}(x),V_{\mathcal{A}}(x),V_{\mathcal{V}}(x),k_1(x),k_2(x),k_3(x);q(x,t),\mu(x,t),\eta(x,t),\gamma(x,t))\\
&=\frac{1}{2}\int_0^T\int_\Omega \frac{(u-u_{k+\frac{1}{2}})^2}{u_k}dxdt\\
&+\mathcal{R}_{\alpha,\mathcal{T}}(\lambda_{\mathcal{T}}(x))+\mathcal{R}_{\alpha,\mathcal{T}}(\lambda_{\mathcal{A}}(x))+\mathcal{R}_{\alpha,\mathcal{T}}(k_2(x))+\mathcal{R}_{\alpha,\mathcal{T}}(k_1(x))\\
&+\mathcal{R}_{\alpha,\mathcal{T}}(V_{\mathcal{T}}(x))+\mathcal{R}_{\alpha,\mathcal{T}}(D_{\mathcal{T}}(x))+\mathcal{R}_{\alpha,\mathcal{A}}(\lambda_{\mathcal{A}}(x))+\mathcal{R}_{\alpha,\mathcal{A}}(\lambda_{\mathcal{V}}(x))\\
&+\mathcal{R}_{\alpha,\mathcal{A}}(k_1(x))+\mathcal{R}_{\alpha,\mathcal{A}}(k_3(x))+\mathcal{R}_{\alpha,\mathcal{A}}(V_{\mathcal{A}}(x))+\mathcal{R}_{\alpha,\mathcal{A}}(D_{\mathcal{A}}(x))\\
&+\mathcal{R}_{\alpha,\mathcal{V}}(\lambda_{\mathcal{V}}(x))+\mathcal{R}_{\alpha,\mathcal{V}}(\lambda_{\mathcal{T}}(x))+\mathcal{R}_{\alpha,\mathcal{V}}(k_2(x))+\mathcal{R}_{\alpha,\mathcal{V}}(k_3(x))\\
&+\mathcal{R}_{\alpha,\mathcal{V}}(V_{\mathcal{V}}(x))+\mathcal{R}_{\alpha,\mathcal{V}}(D_{\mathcal{V}}(x))+\mathcal{R}_{\xi,\mathcal{T}}(\lambda_{\mathcal{T}}(x))+\mathcal{R}_{\xi,\mathcal{T}}(\lambda_{\mathcal{A}}(x))\\
&+\mathcal{R}_{\xi,\mathcal{T}}(k_2(x))+\mathcal{R}_{\xi,\mathcal{T}}(k_1(x))+\mathcal{R}_{\xi,\mathcal{T}}(V_{\mathcal{T}}(x))+\mathcal{R}_{\xi,\mathcal{T}}(D_{\mathcal{T}}(x))\\
&+\mathcal{R}_{\xi,\mathcal{A}}(\lambda_{\mathcal{A}}(x))+\mathcal{R}_{\xi,\mathcal{A}}(\lambda_{\mathcal{V}}(x))+\mathcal{R}_{\xi,\mathcal{A}}(k_1(x))+\mathcal{R}_{\xi,\mathcal{A}}(k_3(x))\\
&+\mathcal{R}_{\xi,\mathcal{A}}(V_{\mathcal{A}}(x))+\mathcal{R}_{\xi,\mathcal{A}}(D_{\mathcal{A}}(x))+\mathcal{R}_{\xi,\mathcal{V}}(\lambda_{\mathcal{V}}(x))+\mathcal{R}_{\xi,\mathcal{V}}(\lambda_{\mathcal{T}}(x))\\
&+\mathcal{R}_{\xi,\mathcal{V}}(k_2(x))+\mathcal{R}_{\xi,\mathcal{V}}(k_3(x))+\mathcal{R}_{\xi,\mathcal{V}}(V_{\mathcal{V}}(x))+\mathcal{R}_{\xi,\mathcal{V}}(D_{\mathcal{V}}(x))\\
&+\int_0^T\int_\Omega (G(\lambda_{\mathcal{T}}(x),\lambda_{\mathcal{A}}(x),\lambda_{\mathcal{V}}(x),C_{\mathcal{A}}(x,t),C_{\mathcal{T}}(x,t),C_{\mathcal{V}}(x,t),D_{\mathcal{T}}(x),D_{\mathcal{A}}(x),D_{\mathcal{V}}(x),\\
&V_{\mathcal{T}}(x),V_{\mathcal{A}}(x),V_{\mathcal{V}}(x))-u)q\,dxdt\\
&+\int_0^T\int_{\mathcal{T}}\left(\frac{\partial C_{\mathcal{T}}(x,t)}{\partial t}-\nabla(V_{\mathcal{T}}(x)C_{\mathcal{T}}(x,t))-\nabla\cdot(D_{\mathcal{T}}(x)\nabla C_{\mathcal{T}}(x,t))-k_1(x,y)C_{\mathcal{A}}(x,t)\right.\\
&\left.+(k_0+k_2)(x)C_{\mathcal{T}}(x,t)\right)\mu(x,t)dxdt\\
&+\int_0^T\int_{\mathcal{A}}\left(\frac{\partial C_{\mathcal{A}}(x,t)}{\partial t}-\nabla(V_{\mathcal{A}}(x)C_{\mathcal{A}}(x,t))-\nabla\cdot(D_{\mathcal{A}}(x)\nabla C_{\mathcal{A}}(x,t))-k_3(x)C_{\mathcal{V}}(x,t)\right.\\
&\left.+(k_0+k_1)(x)C_{\mathcal{A}}(x,t)\right)\eta(x,t)dxdt\\
&+\int_0^T\int_{\mathcal{V}}\left(\frac{\partial C_{\mathcal{V}}(x,t)}{\partial t}-\nabla(V_{\mathcal{V}}(x)C_{\mathcal{V}}(x,t))-\nabla\cdot(D_{\mathcal{V}}(x)\nabla C_{\mathcal{V}}(x,t))-k_2(x)C_{\mathcal{T}}(x,t)\right.\\
&\left.+(k_0+k_3)(x)C_{\mathcal{V}}(x,t)\right)\gamma(x,t)dxdt
\end{aligned} \tag{4.98}$$

By the gradient regularization we have the guarantee that the reconstructed parameters $k_1, k_2, k_3, V_{\mathcal{A}}$, $V_{\mathcal{T}}$, $V_{\mathcal{V}}, D_{\mathcal{A}}, D_{\mathcal{T}}, D_{\mathcal{V}}$ become parameters in the Hilbert space.

Thus

$$
\begin{aligned}
&\mathcal{L}(u(x,T),\lambda_{\mathcal{T}}(x),\lambda_{\mathcal{A}}(x),\lambda_{\mathcal{V}}(x),C_{\mathcal{A}}(x,t),C_{\mathcal{T}}(x,t),C_{\mathcal{V}}(x,t),D_{\mathcal{T}}(x),D_{\mathcal{A}}(x),D_{\mathcal{V}}(x),\\
&V_{\mathcal{T}}(x),V_{\mathcal{A}}(x),V_{\mathcal{V}}(x),k_1(x),k_2(x),k_3(x);q(x,t),\mu(x,t),\eta(x,t),\gamma(x,t))\\
&=\frac{1}{2}\int_0^T\int_\Omega \frac{(u-u_{k+\frac{1}{2}})^2}{u_k}dxdt\\
&\quad+\frac{\alpha}{2}\Bigg(\int_{\mathcal{T}}(\lambda_{\mathcal{T}}(x)-\lambda_T^*)^2+(\lambda_{\mathcal{A}}(x)-\lambda_A^*)^2+(k_2(x)-k_2^*)^2+(k_1(x)-k_1^*)^2\\
&\quad+(V_{\mathcal{T}}(x)-V_T^*)^2+(D_{\mathcal{T}}(x)-D_T^*)^2dx\\
&\quad+\int_{\mathcal{A}}(\lambda_{\mathcal{A}}(x)-\lambda_A^*)^2+(\lambda_{\mathcal{V}}(x)-\lambda_V^*)^2+(k_1(x)-k_1^*)^2+(k_3(x)-k_3^*)^2\\
&\quad+(V_{\mathcal{A}}(x)-V_A^*)^2+(D_{\mathcal{A}}(x)-D_A^*)^2dx\\
&\quad+\int_{\mathcal{V}}(\lambda_{\mathcal{V}}(x)-\lambda_V^*)^2+(\lambda_{\mathcal{T}}(x)-\lambda_T^*)^2+(k_2(x)-k_2^*)^2+(k_3(x)-k_3^*)^2\\
&\quad+(V_{\mathcal{V}}(x)-V_V^*)^2+(D_{\mathcal{V}}(x)-D_V^*)^2dx\Bigg)\\
&\quad+\frac{\beta}{2}\Bigg(\int_{\mathcal{T}}(\lambda_{\mathcal{T}}(x)+\lambda_A(x)-1)^2dx+\int_{\mathcal{A}}(\lambda_{\mathcal{A}}(x)+\lambda_V(x)-1)^2dx+\int_{\mathcal{V}}(\lambda_{\mathcal{V}}(x)+\lambda_T(x)-1)^2dx\\
&\quad+\int_{\mathcal{S}}(\lambda_{\mathcal{T}}(x)+\lambda_A(x)+\lambda_V(x)-1)^2dx\Bigg)\\
&\quad+\frac{\rho}{2}\Bigg(\int_{\mathcal{T}}(\lambda_{\mathcal{T}}(x)\lambda_A(x))^2dx+\int_{\mathcal{A}}(\lambda_{\mathcal{A}}(x)\lambda_V(x))^2dx+\int_{\mathcal{V}}(\lambda_{\mathcal{V}}(x)\lambda_T(x))^2dx+\int_{\mathcal{S}}(\lambda_{\mathcal{T}}(x)\lambda_A(x)\lambda_V(x))^2dx\Bigg)\\
&\quad+\frac{\xi}{2}\Bigg(\int_{\mathcal{T}}|\nabla\lambda_{\mathcal{T}}(x)|^2+|\nabla\lambda_{\mathcal{A}}(x)|^2+|\nabla k_2(x)|^2+|\nabla k_1(x)|^2+|\nabla V_{\mathcal{T}}(x)|^2+|\nabla D_{\mathcal{T}}(x)|^2\ dx\\
&\quad+\int_{\mathcal{A}}|\nabla\lambda_{\mathcal{A}}(x)|^2+|\nabla\lambda_{\mathcal{V}}(x)|^2+|\nabla k_1(x)|^2+|\nabla k_3(x)|^2+|\nabla V_{\mathcal{A}}(x)|^2+|\nabla D_{\mathcal{A}}(x)|^2dx\\
&\quad+\int_{\mathcal{V}}|\nabla\lambda_{\mathcal{V}}(x)|^2+|\nabla\lambda_{\mathcal{T}}(x)|^2+|\nabla k_2(x)|^2+|\nabla k_3(x)|^2+|\nabla V_{\mathcal{V}}(x)|^2+|\nabla D_{\mathcal{V}}(x)|^2\Bigg)dx\\
&+\int_0^T\int_\Omega(G(\lambda_{\mathcal{T}}(x),\lambda_{\mathcal{A}}(x),\lambda_{\mathcal{V}}(x),C_{\mathcal{A}}(x,t),C_{\mathcal{T}}(x,t),C_{\mathcal{V}}(x,t),D_{\mathcal{T}}(x),D_{\mathcal{A}}(x),D_{\mathcal{V}}(x),\\
&V_{\mathcal{T}}(x),V_{\mathcal{A}}(x),V_{\mathcal{V}}(x))-u)qdxdt\\
&+\int_0^T\int_{\mathcal{T}}\Bigg(\frac{\partial C_{\mathcal{T}}(x,t)}{\partial t}-\nabla(V_{\mathcal{T}}(x)C_{\mathcal{T}}(x,t))-\nabla\cdot(D_{\mathcal{T}}(x)\nabla C_{\mathcal{T}}(x,t))-k_1(x)C_{\mathcal{A}}(x,t)\\
&+(k_0+k_2)(x)C_{\mathcal{T}}(x,t)\Bigg)\mu(x,t)dxdt\\
&+\int_0^T\int_{\mathcal{A}}\Bigg(\frac{\partial C_{\mathcal{A}}(x,t)}{\partial t}-\nabla(V_{\mathcal{A}}(x)C_{\mathcal{A}}(x,t))-\nabla\cdot(D_{\mathcal{A}}(x)\nabla C_{\mathcal{A}}(x,t))-k_3(x)C_{\mathcal{V}}(x,t)\\
&+(k_0+k_1)(x)C_{\mathcal{A}}(x,t)\Bigg)\eta(x,t)dxdt\\
&+\int_0^T\int_{\mathcal{V}}\Bigg(\frac{\partial C_{\mathcal{V}}(x,t)}{\partial t}-\nabla(V_{\mathcal{V}}(x)C_{\mathcal{V}}(x,t))-\nabla\cdot(D_{\mathcal{V}}(x)\nabla C_{\mathcal{V}}(x,t))-k_2(x)C_{\mathcal{T}}(x,t)\\
&+(k_0+k_3)(x)C_{\mathcal{V}}(x,t)\Bigg)\gamma(x,t)dxdt
\end{aligned}
\tag{4.99}
$$

The optimality conditions for $k_1(x)$, $k_2(x)$, $k_3(x)$, $V_{\mathcal{T}}(x)$, $V_{\mathcal{A}}(x)$, $V_{\mathcal{V}}(x)$, $D_{\mathcal{T}}(x)$, $D_{\mathcal{A}}(x)$ and $D_{\mathcal{V}}(x)$ are

$$0 = \frac{\partial \mathcal{L}}{\partial k_1} = \alpha\big(\Lambda_{\mathcal{T}}(x)(k_1(x) - k_1^*) + \Lambda_{\mathcal{A}}(x)(k_1(x) - k_1^*)\big) - \xi\big(\Lambda_{\mathcal{T}}(x)\Delta k_1(x) + \Lambda_{\mathcal{A}}(x)\Delta k_1(x)\big)$$
$$- \int_0^T C_{\mathcal{A}}(x,t)\mu(x,t)dt + \int_0^T C_{\mathcal{A}}(x,t)\eta(x,t)dt \tag{4.100}$$

$$0 = \frac{\partial \mathcal{L}}{\partial k_2} = \alpha\big(\Lambda_{\mathcal{T}}(x)(k_2(x) - k_2^*) + \Lambda_{\mathcal{V}}(x)(k_2(x) - k_2^*)\big) - \xi\big(\Lambda_{\mathcal{T}}(x)\Delta k_2(x) + \Lambda_{\mathcal{V}}(x)\Delta k_2(x)\big)$$
$$+ \int_0^T C_{\mathcal{T}}(x,t)\mu(x,t)dt - \int_0^T C_{\mathcal{T}}(x,t)\gamma(x,t)dt \tag{4.101}$$

$$0 = \frac{\partial \mathcal{L}}{\partial k_3} = \alpha\big(\Lambda_{\mathcal{A}}(x)(k_3(x) - k_3^*) + \Lambda_{\mathcal{V}}(x)(k_3(x) - k_3^*)\big) - \xi\big(\Lambda_{\mathcal{A}}(x)\Delta k_3(x) + \Lambda_{\mathcal{V}}(x)\Delta k_3(x)\big)$$
$$- \int_0^T C_{\mathcal{V}}(x,t)\eta(x,t)dt + \int_0^T C_{\mathcal{V}}(x,t)\gamma(x,t)dt \tag{4.102}$$

$$0 = \frac{\partial \mathcal{L}}{\partial V_{\mathcal{T}}} = \int_0^T V_{\mathcal{T}}(x) \cdot \nabla\mu(x,t)\; dt + \alpha(V_{\mathcal{T}}(x) - V_{\mathcal{T}}^*) - \xi(\Lambda_{\mathcal{T}}(x)\Delta V_{\mathcal{T}}(x)) \tag{4.103}$$

$$0 = \frac{\partial \mathcal{L}}{\partial V_{\mathcal{A}}} = \int_0^T V_{\mathcal{A}}(x) \cdot \nabla\eta(x,t)\; dt + \alpha(V_{\mathcal{A}}(x) - V_{\mathcal{A}}^*) - \xi(\Lambda_{\mathcal{A}}(x)\Delta V_{\mathcal{A}}(x)) \tag{4.104}$$

$$0 = \frac{\partial \mathcal{L}}{\partial V_{\mathcal{V}}} = \int_0^T V_{\mathcal{V}}(x) \cdot \nabla\gamma(x,t)\; dt + \alpha(V_{\mathcal{V}}(x) - V_{\mathcal{V}}^*) - \xi(\Lambda_{\mathcal{V}}(x)\Delta V_{\mathcal{V}}(x)) \tag{4.105}$$

$$0 = \frac{\partial \mathcal{L}}{\partial D_{\mathcal{T}}} = \int_0^T \nabla C_{\mathcal{T}}(x) \cdot \nabla\mu(x,t)\; dt + \alpha(D_{\mathcal{T}}(x) - D_{\mathcal{T}}^*) - \xi(\Lambda_{\mathcal{T}}(x)\Delta D_{\mathcal{T}}(x)) \tag{4.106}$$

$$0 = \frac{\partial \mathcal{L}}{\partial D_{\mathcal{A}}} = \int_0^T \nabla C_{\mathcal{A}}(x) \cdot \nabla\eta(x,t)\; dt + \alpha(D_{\mathcal{A}}(x) - D_{\mathcal{A}}^*) - \xi(\Lambda_{\mathcal{A}}(x)\Delta D_{\mathcal{A}}(x)) \tag{4.107}$$

$$0 = \frac{\partial \mathcal{L}}{\partial D_{\mathcal{V}}} = \int_0^T \nabla C_{\mathcal{V}}(x) \cdot \nabla\gamma(x,t)\; dt + \alpha(D_{\mathcal{V}}(x) - D_{\mathcal{V}}^*) - \xi(\Lambda_{\mathcal{V}}(x)\Delta D_{\mathcal{V}}(x)) \tag{4.108}$$

5 Identifiability Analysis

This chapter is dedicated to a discussion of the identifiability of all physiological parameters in the system described by the parabolic differential equations presented in *Chapter 3* .

To prove the identifiability this chapter is based on the work of [**65**].

5.1 Statement of the problem

For this section, consider Figure 5.1 which represents a system for the parameter identification with a model. Consider also the system given by a parabolic differential equations (3.1), (3.2) and (3.3):

$$\frac{\partial C_{\mathcal{A}}}{\partial t} = \nabla \cdot (V_{\mathcal{A}}(x)C_{\mathcal{A}} + D_{\mathcal{A}}(x)\nabla C_{\mathcal{A}}) - (k_0(x) + k_1(x))C_{\mathcal{A}} + k_3(x)C_{\mathcal{V}}$$

$$\frac{\partial C_{\mathcal{T}}}{\partial t} = \nabla \cdot (V_{\mathcal{T}}(x)C_{\mathcal{T}} + D_{\mathcal{T}}(x)\nabla C_{\mathcal{T}}) - (k_0(x) + k_2(x))C_{\mathcal{T}} + k_1(x)C_{\mathcal{A}}$$

$$\frac{\partial C_{\mathcal{V}}}{\partial t} = \nabla \cdot (V_{\mathcal{V}}(x)C_{\mathcal{V}} + D_{\mathcal{V}}(x)\nabla C_{\mathcal{V}}) - (k_0(x) + k_3(x))C_{\mathcal{V}} + k_2(x)C_{\mathcal{T}}$$

Considering the inverse problem for the full model we want to identify all parameters $D_{\mathcal{A}}, D_{\mathcal{T}}, D_{\mathcal{V}}, V_{\mathcal{A}}, V_{\mathcal{T}}, V_{\mathcal{V}}, k_1, k_2$ and k_3 from the measurement $C_{\mathcal{A}}(x,t) + C_{\mathcal{T}}(x,t) + C_{\mathcal{V}}(x,t) = u(x,t)$.

5.2 One-Component Reaction-Diffusion Model

In order to gain a first understanding we can write:

$$\frac{\partial C_{\mathcal{A}}}{\partial t} = \nabla \cdot (V_{\mathcal{A}}(x)C_{\mathcal{A}} + D_{\mathcal{A}}(x)\nabla C_{\mathcal{A}}) - (k_0(x) + k_1(x))C_{\mathcal{A}} + f(x,t), \quad \forall x \in \Omega, \quad T > 0 \tag{5.1}$$

where $C_{\mathcal{A}} = C_{\mathcal{A}}(x,t)$ is twice differentiable, $f(x,t)$ is a input function and the boundary conditions given by (3.5). We consider also that the input functions can be measured, i.e, are known functions.

The output y of the measurement system is given by

$$y(x_p,t) = C_{\mathcal{A}}(x_p,t) \quad x_p \in \Omega_p, \; t \geq 0 \tag{5.2}$$

Consider that the equation below represents the model problem

$$\frac{\partial C_{\mathcal{A}_m}}{\partial t} = \nabla \cdot (V_{\mathcal{A}_m}(x) C_{\mathcal{A}_m} + D_{\mathcal{A}_m}(x) \nabla C_{\mathcal{A}_m}) - (k_0(x) + k_1(x)) C_{\mathcal{A}_m} + f(x,t) \tag{5.3}$$

with $x \in \Omega, t > 0$ and

$$y_m(x_p, t) = C_{\mathcal{A}_m}(x_p, t) \tag{5.4}$$

where $C_{\mathcal{A}_m}(x,t)$ is the state of the model and the subscript m denotes model quantities. The boundary condition for (5.3) takes the same form as in (3.15).

Definition 5.2.1 *(Identifiable Parameters) We shall call an unknown parameter identifiable if it can be determined uniquely in all points of the domain Ω by using the input-output relation of the system and the input-output data [**65**].*

If $D_{\mathcal{A}}(x) = D_{\mathcal{A}_m}(x), V_{\mathcal{A}}(x) = V_{\mathcal{A}_m}(x)$ and $k(x) = k_m(x)$, follow uniquely from the relation $e(x_p, t) = y(x_p, t) - y_m(x_p, t) = 0$, for all $x_p \in \Omega$, $t \geq 0$, $y(x_p, t)$ given by (5.2) and $y_m(x_p, t)$ by (5.4), thus $D_{\mathcal{A}}(x)$, $V_{\mathcal{A}}(x)$ and $k(x)$ are said to be identifiable,. When $e(x_p, t) = 0$, $\forall x_p \in \Omega$, $t \geq 0$ in the identification process of the Figure 5.1, the parameters are adjusted by some proper algorithm so that e is zero in $A(\Omega)$.

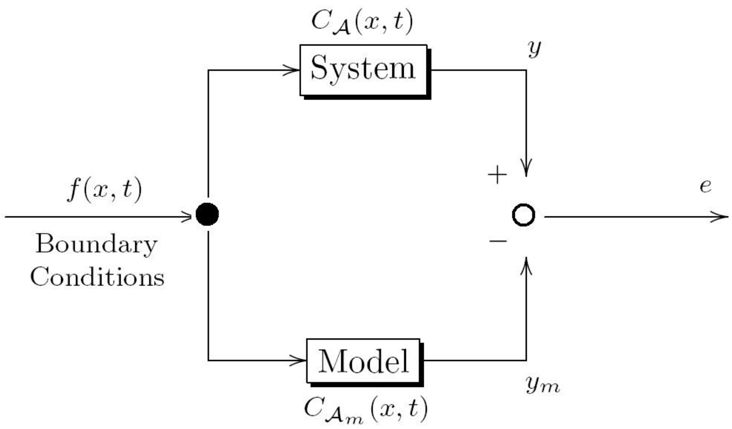

Figure 5.1: Parameter identification by using a model [**65**].

Assume that $C_{\mathcal{A}}(x,t)$ is measured at all points of $x \in \Omega$, $t \geq 0$ and define the difference variable $e(x,t) = C_{\mathcal{A}}(x,t) - C_{\mathcal{A}_m}(x,t)$, thus we have the Lemma 5.2.2, where the spatial one-dimensional case is considered:

Lemma 5.2.2 *The identity $e(x,t) = 0$ (equations (5.2), (5.4)) for all $x \in \Omega$ and $t \geq 0$ holds if and only if*

$$\frac{\partial}{\partial x}\left[(D_{\mathcal{A}}(x) - D_{\mathcal{A}_m}(x)) \frac{\partial C_{\mathcal{A}_m}}{\partial x}(x,t) + (V_{\mathcal{A}}(x) - V_{\mathcal{A}_m}(x)) C_{\mathcal{A}_m}(x,t)\right] + (k(x) - k_m(x)) C_{\mathcal{A}_m}(x,t) = 0 \tag{5.5}$$

with $x \in \Omega$ and $t > 0$.

Proof. For the proof of Lemma 5.2.2, consider the equations (5.1), (5.4) and (5.5).

$$\begin{aligned}\frac{\partial e}{\partial x} &= \frac{\partial}{\partial x}\left(D_{\mathcal{A}}\frac{\partial e}{\partial x} + V_{\mathcal{A}}e\right) + ke + \frac{\partial}{\partial x}\left((D_{\mathcal{A}} - D_{\mathcal{A}_m})\frac{\partial C_{\mathcal{A}_m}}{\partial x} + (V_{\mathcal{A}} - V_{\mathcal{A}_m})C_{\mathcal{A}_m}\right) + (k - k_m)C_{\mathcal{A}_m} \\ &= \frac{\partial}{\partial x}\left(D_{\mathcal{A}}\frac{\partial e}{\partial x} + V_{\mathcal{A}}e\right) + ke \quad \forall x \in \Omega \text{ and } t > 0\end{aligned} \tag{5.6}$$

The initial condition for (5.6) is given by $e(0) = u(0) - u_m(0) = 0$. Thus, due to the uniqueness of the solution, we have $e(x,t) = 0$ for all $x \in \Omega$ and $t \geq 0$.

5.2.1 Identifiability of $D_{\mathcal{A}}(x)$

It is assumed that $e(x,t) = 0 \ \forall \ x \in \Omega$, $\forall \ t \geq 0$, $V_{\mathcal{A}}(x)$ and $k_1(x)$ are known or both vanish.

All the results are represented in terms of the state of the model $C_{\mathcal{A}_m}$. However, since $e \equiv 0$, $C_{\mathcal{A}_m}$ may be replaced by the state of the system $C_{\mathcal{A}}$.

Let us define

$$\begin{aligned}E(t) &= \left\{x \in \Omega \middle| \frac{\partial C_{\mathcal{A}_m}}{\partial x}(x,t) = 0\right\} \\ G(t) &= \Omega - E(t)\end{aligned} \tag{5.7}$$

Proposition 5.2.3 *$D_{\mathcal{A}}$ is identifiable in $A(\Omega)$ if there exists some $t_1 > 0$ such that*

$$E(t_1) \neq \varnothing \tag{5.8}$$

and

$$\overline{G(t_1)} = \Omega \tag{5.9}$$

where $\varnothing$ is the empty set and $\overline{G}$ is the closure of G. The condition (5.9) especially may be replaced by

$$meas \ E(t_1) = 0 \tag{5.10}$$

with meas E being the measure of E.

Proof. Let be $q(x) = D_{\mathcal{A}}(x) - D_{\mathcal{A}_m}(x)$. By the assumption we obtain from (5.5)

$$\frac{\partial}{\partial x}\left[q(x)\frac{\partial C_{\mathcal{A}_m}}{\partial x}\right] = 0 \quad \text{for all} \quad x \in \Omega \quad \text{and all} \quad t > 0 \tag{5.11}$$

and

$$q(x)\frac{\partial C_{\mathcal{A}_m}}{\partial x} = c(t)$$

By condition (5.8), there exists t_1 such that $c(t_1) = 0$. From condition (5.9), the set $\{x \in \Omega | q(x) = 0\}$ is dense in Ω, since $q(x)$ is a continuous fuction in Ω. We conclude $q(x) = 0$ for all $x \in \Omega$, i.e., $D_{\mathcal{A}}(x)$ is identifiable. Condition (5.10) implies meas $G(t_1)$ = meas Ω, and consequently, meas $\overline{G(t_1)}$ = meas Ω. We have to show $\overline{G(t_1)} = \Omega$. For this, assume $\Omega - \overline{G(t_1)} \neq \varnothing$. Then, there exists an open

J such that $\Omega - \overline{G(t_1)} \supset J$. From $\Omega \supset \overline{G(t_1)} \cup J$ (J and $\overline{G(t_1)}$ are disjoint), we obtain meas $\Omega \geq$ meas $G(t_1)+$ meas J, which implies meas $J = 0$. (Contradiction).

Now another condition is given for the identifiability of $D_{\mathcal{A}}(x)$.

Proposition 5.2.4 *$D_{\mathcal{A}}$ is identifiable in $A(\Omega)$ if*

$$E(t) \neq \varnothing \quad for\ all \quad t > 0 \tag{5.12}$$

and

$$\overline{\bigcup_{t>0} G(t)} = \Omega \tag{5.13}$$

Proof. By (5.12) and Lemma (5.2.2), we obtain $q(x)\left(\frac{\partial C_{\mathcal{A}_m}}{\partial x}(x,t)\right) = 0$ for all $x \in \Omega$ and all $t > 0$, where $q(x) = D_{\mathcal{A}}(x) - D_{\mathcal{A}_m}(x)$. Set $M = \cup_{t>0} G(t)$. For any $x \in M$, there exists some $t(x) > 0$ such that $x \in G(t)$, i.e., $\left(\frac{\partial C_{\mathcal{A}_m}}{\partial x}\right)(x,t) \neq 0$. Thus, $q(x) = 0$ for all $x \in M$, and from condition (5.13) and the continuity for $q(x)$ it follows that $q(x) = 0$ for all $x \in \Omega$.

Note that the condition (5.12) is stricter than (5.8), while condition (5.13) is weaker than (5.9).

Proposition 5.2.5 *$D_{\mathcal{A}}$ is not identifiable if $\cup_{t>0} G(t)$ is not dense in Ω, especially if $\bigcap_{t>0} E(t)$ includes an open subset.*

Proof. We show that $D_{\mathcal{A}}(x_0) \neq D_{\mathcal{A}_m}(x_0)$ for some $x_0 \in \Omega$ even if $e(x,t) = 0$ for all $x \in \Omega$ and all $t \geq 0$ when $\cup_{t>0} G(t)$ is not dense in Ω. By the first condition, there exists an open subset J satisfying $\Omega - \overline{\cup_{t>0} G(t)} \supset J$. Take x_0 and $\epsilon > 0$ such that $J \supset B(x_0, \epsilon)$, where $B(x_0, \epsilon)$ ist one ball with center x_0 and radius ϵ and let $r(x)$ be a twice continuously differentiable function in Ω with support in $B(x_0, \epsilon)$ and $r(x_0) \neq 0$. Assume here $D_{\mathcal{A}}(x) = D_{\mathcal{A}_m}(x) + r(x)$. If $x \in B(x_0, \epsilon)$, then $\frac{\partial C_{\mathcal{A}_m}}{\partial x} = 0$ for all $t > 0$ since

$$x \in J \subset \ \Omega - \overline{\bigcup_{t>0} G(t)} \subset \ \Omega - \bigcup_{t>0} G(t) = \bigcap_{t>0} E(t)$$

and if $x \notin B(x_0, \epsilon)$, then $(D_{\mathcal{A}}(x) - D_{\mathcal{A}_m}(x))\left(\frac{\partial C_{\mathcal{A}_m}}{\partial x}\right) = 0$ for all $x \in \Omega$ and all $t > 0$ since $r(x) = 0$. Thus, by Lemma (5.2.2), $e(x,t) = 0$ for all $x \in \Omega$ and all $t \geq 0$, and $D_{\mathcal{A}}(x)$ is not identifiable. Moreover, if $\cap_{t>0} E(t)$ includes an open subset , $\cup_{t>0} G(t)$ is not dense in Ω.

Proposition 5.2.6 *If $E(t_1) = \varnothing$ for some t_1, then*

$$D_{\mathcal{A}}(x) - D_{\mathcal{A}_m}(x) = (D_{\mathcal{A}}(x_0) - D_{\mathcal{A}_m}(x_0)) exp \left[- \int_{x_0}^{x} \frac{\frac{\partial^2 C_{\mathcal{A}_m}}{\partial x^2}(s, t_1)}{\frac{\partial C_{\mathcal{A}_m}}{\partial x}(s, t_1)} ds \right] \tag{5.14}$$

for any x and $x_0 \in \Omega$.

Proof. By the assumption, (5.11) holds in this case, i.e.,

$$\frac{\partial C_{\mathcal{A}_m}}{\partial x} q'(x) + \frac{\partial^2 C_{\mathcal{A}_m}}{\partial x^2} q(x) = 0$$

The equation (5.14) is a solution of this differential equation under the condition $\left(\frac{\partial C_{\mathcal{A}_m}}{\partial x}\right)(x, t_1) \neq 0$.

Proposition 5.2.7 *If $E(t_1) = \varnothing$ for some $t_1 > 0$ and if $C_{\mathcal{A}_m}(x,t) = v_m(x) w_m(t)$ for all $x \in \Omega$ and $t \geq 0$, then $D_{\mathcal{A}}$ is not identifiable.*

Proof. $E(t_1) = \varnothing$ implies that $w_m(t_1) \neq 0$ and $\frac{\partial v_m}{\partial x}(x) \neq 0$ for any $x \in \Omega$. Let $D_{\mathcal{A}}(x) = D_{\mathcal{A}_m}(x) + \frac{1}{\left(\frac{\partial v_m(x)}{\partial x}\right)}$, then $D_{\mathcal{A}}(x) \neq D_{\mathcal{A}_m}(x)$ for all $x \in \Omega$, while

$$(D_{\mathcal{A}}(x) - D_{\mathcal{A}_m}(x)) \frac{\partial v_m(x)}{\partial x} w_m(t) = w_m(t)$$

for all $x \in \Omega$ and $t \geq 0$. Thus,

$$\frac{\partial}{\partial x}\left\{(D_{\mathcal{A}}(x) - D_{\mathcal{A}_m}(x)) \frac{\partial C_{\mathcal{A}_m}}{\partial x}\right\} = 0$$

for all $t > 0$ and, from Lemma (5.2.2), $e(x,t) = 0$ for all $x \in \Omega$ and all $t \geq 0$. Thus, $D_{\mathcal{A}}$ is not identifiable.

5.2.2 Identifiability of $k_1(x)$

We now study the identifiability of k_1 and to get a first idea we assume that $D_{\mathcal{A}}(x)$ and $V_{\mathcal{A}}(x)$ are both known, and that $e(x,t) = 0$ for all $x \in \Omega$ and all $t \geq 0$. Let us define

$$\begin{aligned} F(t) &= \{x \in \Omega | C_{\mathcal{A}_m}(x,t) = 0\} \\ H(t) &= \Omega - F(t) \end{aligned} \tag{5.15}$$

Proposition 5.2.8 *k_1 is identifiable if and only if*

$$\overline{\bigcup_{t>0} H(t)} = \Omega \tag{5.16}$$

Note that k_1 is not identifiable if $\bigcap_{t>0} F(t)$ includes an open subset.

Proof. By the assmption and Lemma (5.2.2), $e(x,t) = 0$ if and only if $(k_1(x) - k_{1_m}(x)) C_{\mathcal{A}_m}(x,t) = 0$. Certainly satisfied if the initial value $C_{\mathcal{A}_m}(x,0) > 0$ or $f > 0$. Necessity follows by proceeding similarly as in the proof of the proposition 5.2.5. The latter statement of the result is self -evident.

5.2.3 Identifiability of $V_{\mathcal{A}}(x)$

It is assumed that $e(x,t) = 0$ $\forall x \in \Omega$, $\forall t \geq 0$, $D_{\mathcal{A}}(x)$ and $k_1(x)$ are known or both vanish.

Let us define

$$I(t) = \left\{x \in \Omega \middle| C_{\mathcal{A}_m}(x,t) = 0\right\}$$

$$L(t) = \Omega - I(t) \tag{5.17}$$

Proposition 5.2.9 *$V_{\mathcal{A}}$ is identifiable in $A(\Omega)$ if there exists some $t_1 > 0$ such that*

$$I(t_1) \neq \varnothing \tag{5.18}$$

and

$$\overline{L(t_1)} = \Omega \tag{5.19}$$

where $\varnothing$ is the empty set and $\overline{L}$ is the closure of L.

Proof. By the assumption we obtain from (5.5)

$$\frac{\partial}{\partial x}\left[s(x)C_{\mathcal{A}_m}\right] = 0 \quad \text{for all} \quad x \in \Omega \quad \text{and all} \quad t > 0 \tag{5.20}$$

with $s(x) = V_{\mathcal{A}}(x) - V_{\mathcal{A}_m}(x)$, and

$$s(x)C_{\mathcal{A}_m} = d(t)$$

By condition (5.18), there exists t_1 such that $C_{\mathcal{A}_m=0}$. From condition (5.19), the set $\{x \in \Omega | s(x) = 0\}$ is dense in Ω, $s(x)$ is a continuous fuction in Ω). Thus $s(x) = 0$ for all $x \in \Omega$, i.e., $V_{\mathcal{A}}$ is identifiable.

Now another condition is given for the identifiable of $V_{\mathcal{A}}(x)$.

Proposition 5.2.10 *$V_{\mathcal{A}}$ is identifiable if*

$$I(t) \neq \varnothing \quad \textit{for all} \quad t > 0 \tag{5.21}$$

and

$$\overline{\bigcup_{t>0} L(t)} = \Omega \tag{5.22}$$

Proof. By (5.21) and Lemma (5.2.2), we obtain $s(x)\left(C_{\mathcal{A}_m}(x,t)\right) = 0$ for all $x \in \Omega$ and all $t > 0$, where $s(x) = V_{\mathcal{A}}(x) - V_{\mathcal{A}_m}(x)$. Set $P = \cup_{t>0} L(t)$. For any $x \in P$, there exists some $t(x) > 0$ such that $x \in L(t)$, i.e., $C_{\mathcal{A}_m}(x,t) \neq 0$. Thus, $s(x) = 0$ for all $x \in P$, and from condition (5.22) and the continuity for $s(x)$ it follows that $s(x) = 0$ for all $x \in \Omega$.

Proposition 5.2.11 *$V_{\mathcal{A}}$ is not identifiable if $\cup_{t>0} L(t)$ is not dense in Ω, especially if $\bigcap_{t>0} I(t)$ includes an open subset.*

Proof. We show that $V_{\mathcal{A}}(x_0) \neq V_{\mathcal{A}_m}(x_0)$ for some $x_0 \in \Omega$ even if $e(x,t) = 0$ for all $x \in \Omega$ and all $t \geq 0$ when $\cup_{t>0} L(t)$ is not dense in Ω. By the first condition for $V_{\mathcal{A}}$, there exists an open subset R satisfying $\Omega - \overline{\cup_{t>0} L(t)} \supset R$. Take x_0 and $\epsilon > 0$ such that $R \supset B(x_0, \epsilon)$, ($B(x_0, \epsilon)$ is one ball with center x_0 and radius ϵ) and let $t(x)$ be a twice continuously differentiable function in Ω with support in $B(x_0, \epsilon)$ and $t(x_0) \neq 0$. Assume here $V_{\mathcal{A}}(x) = V_{\mathcal{A}_m}(x) + t(x)$. If $x \in B(x_0, \epsilon)$, then $C_{\mathcal{A}_m} = 0$ for all $t > 0$ since

$$x \in R \subset \Omega - \overline{\bigcup_{t>0} L(t)} \subset \Omega - \bigcup_{t>0} L(t) = \bigcap_{t>0} I(t)$$

and if $x \notin B(x_0, \epsilon)$, then $(V_{\mathcal{A}}(x) - V_{\mathcal{A}_m}(x))C_{\mathcal{A}_m} = 0$ for all $x \in \Omega$ and all $t > 0$ since $t(x) = 0$. Thus, by Lemma (5.2.2), $e(x,t) = 0$ for all $x \in \Omega$ and all $t \geq 0$, and $V_{\mathcal{A}}$ is not identifiable. Moreover, if $\cap_{t>0} I(t)$ includes an open subset, $\cup_{t>0} L(t)$ is not dense in Ω.

Proposition 5.2.12 *If $I(t_1) = \varnothing$ for some t_1, then*

$$V_{\mathcal{A}}(x) - V_{\mathcal{A}_m}(x) = (V_{\mathcal{A}}(x_0) - V_{\mathcal{A}_m}(x_0))exp\left[-\int_{x_0}^{x} \frac{\frac{C_{\mathcal{A}_m}}{\partial x}(s,t_1)}{C_{\mathcal{A}_m}(s,t_1)}ds\right] \tag{5.23}$$

for any x and $x_0 \in \Omega$.

Proof. By the assumption, (5.20) holds in this case, i.e.,

$$s'(x)C_{\mathcal{A}_m} + s(x)\frac{\partial C_{\mathcal{A}_m}}{\partial x} = 0$$

The equation (5.23) is a solution of this differential equation under the condition $C_{\mathcal{A}_m}(x,t_1) \neq 0$.

The proposition 5.2.12 does not necessarily imply the nonidentifiability of parameter $V_{\mathcal{A}}(x)$.

Proposition 5.2.13 *If $I(t_1) = \varnothing$ for some $t_1 > 0$ and if $C_{\mathcal{A}_m}(x,t)$ is represented as $v_m(x)w_m(t)$, then $V_{\mathcal{A}}$ is not identifiable.*

Proof. $I(t_1) = \varnothing$ implies that $w_m(t_1) \neq 0$ and $\frac{\partial v_m}{\partial x}(x) \neq 0$ for any $x \in \Omega$. Let $V_{\mathcal{A}}(x) = V_{\mathcal{A}_m}(x) + \frac{1}{\left(\frac{\partial v_m(x)}{\partial x}\right)}$, then $V_{\mathcal{A}}(x) \neq V_{\mathcal{A}_m}(x)$ for all $x \in \Omega$, while

$$(V_{\mathcal{A}}(x) - V_{\mathcal{A}_m}(x))\frac{\partial v_m(x)}{\partial x}w_m(t) = w_m(t)$$

for all $x \in \Omega$ and $t \geq 0$. Thus,

$$\frac{\partial}{\partial x}\{(V_{\mathcal{A}}(x) - V_{\mathcal{A}_m}(x))C_{\mathcal{A}_m}\} = 0$$

for all $t > 0$ and, from Lemma (5.2.2), $e(x,t) = 0$ for all $x \in \Omega$ and all $t \geq 0$. Thus, $V_{\mathcal{A}}$ is not identifiable.

5.2.4 Identifiability of $V_{\mathcal{A}}(x), D_{\mathcal{A}}(x)$ and $k_1(x)$

Now we want to analyze the case where the known quantity is $C_{\mathcal{A}}(x,t)$ only, while the unknows are $V_{\mathcal{A}}(x)$, $D_{\mathcal{A}}(x)$ and $k_1(x)$. Fairly restrictive conditions will be required for the identifiability of all parameters.

Proposition 5.2.14 *If the functions $C_{\mathcal{A}}(x)$, $\left(\frac{\partial C_{\mathcal{A}_m}}{\partial x}\right)(x,t)$ and $\left(\frac{\partial^2 C_{\mathcal{A}_m}}{\partial x^2}\right)(x,t)$ are linearly independent as functions of t on a dense subset in Ω, then $V_{\mathcal{A}}, D_{\mathcal{A}}$ and k_1 are simultaneously identifiable.*

Proof. By setting

$$q_1(x) = D_{\mathcal{A}}(x) - D_{\mathcal{A}_m}(x)$$
$$q_2(x) = k_1(x) - k_{1_m}(x)$$
$$q_3(x) = V_{\mathcal{A}}(x) - V_{\mathcal{A}_m}(x)$$

we obtain from (5.5)

$$q_1(x)\frac{\partial^2 C_{\mathcal{A}_m}}{\partial x^2}(x,t) + q_1'(x)\frac{\partial C_{\mathcal{A}_m}}{\partial x}(x,t) + q_2(x)C_{\mathcal{A}_m}(x,t) + q_3(x)\frac{\partial C_{\mathcal{A}_m}}{\partial x}(x,t) + q_3(x)C_{\mathcal{A}_m}(x,t) = 0 \tag{5.24}$$

for all $x \in \Omega$ and all $t > 0$. From the assumption of linear independence, $q_1(x) = q_1'(x) = q_2(x) = q_3(x) = q_3'(x) = 0$ on some dense set in Ω, and again by continuity, $q_1(x) = q_2(x) = q_3(x) = 0$ for all $x \in \Omega$.

Proposition 5.2.15 *If $C_{\mathcal{A}_m}(x,t) = v_m(x)w_m(t)$, then $D_{\mathcal{A}}, V_{\mathcal{A}}$ and k_1 are not simultaneously identifiable. This statement holds especially at the steady state.*

Proof. For any function $v_m(x)$ which is twice continuously differentiable, we can select nonzero functions $q_1(x), q_2(x)$ and $q_3(x)$ which satisfy the following equation:

$$\frac{d}{dx}\left(q_1(x)\frac{dv_m}{dx}(x) + q_3(x)v_m(x)\right) + q_2(x)v_m(x) = 0 \quad \text{for all} \quad x \in \Omega$$

Multiplication by $w_m(t)$ yields

$$\frac{\partial}{\partial x}\left(q_1(x)\frac{\partial C_{\mathcal{A}_m}}{\partial x}(x,t) + q_3(x)C_{\mathcal{A}_m}(x,t)\right) + q_2(x)C_{\mathcal{A}_m}(x,t) = 0$$

for all $x \in \Omega$ and all $t > 0$. Since $q_1(x), q_2(x)$ and $q_3(x)$ are nonzero, $D_{\mathcal{A}}$, k_1 and $V_{\mathcal{A}}$ are not simultaneously identifiable from Lemma (5.2.2).

The above result implies, for example, in the case of the steady state, that it is not sufficient to consider only the difference e for the identification of $D_{\mathcal{A}}(x)$, $k_1(x)$ and $V_{\mathcal{A}}(x)$. However, if we have an a priori knowledge that shows $D_{\mathcal{A}}(x)$, $k_1(x)$ and $V_{\mathcal{A}}(x)$ to be constant, the result is obtained.

Now we study the most challenging case, where the known quantity is $C_{\mathcal{A}}(x,t)+C_{\mathcal{T}}(x,t)+C_{\mathcal{V}}(x,t)$ only, while the unknowns are the other parameters. Fairly restrictive conditions will be required for the identifiability of all parameters.

5.3 Two-Component Reaction-Diffusion Model

Now we analyze a simplified problem, but already quite realistic model ignoring the portion that represents the transport and considering only the differential equations that represent the radioactive concentration in artery and tissue.

Let $C_{\mathcal{A}_i} + C_{\mathcal{T}_i} = f$ (measurement) and $C_{\mathcal{T}_i} = 0$ for $t = 0$. Consider the system

$$\begin{aligned}\frac{\partial C_{\mathcal{A}_i}}{\partial t} &= \nabla\cdot(D_{\mathcal{A}_i}(x)\nabla C_{\mathcal{A}_i}(x,t)) - (k_{0_i}(x)+k_{1_i}(x))C_{\mathcal{A}_i}(x,t) + k_{3_i}(x)C_{\mathcal{T}_i}(x,t) = 0\\ \frac{\partial C_{\mathcal{T}_i}}{\partial t} &= \nabla\cdot(D_{\mathcal{T}_i}(x)\nabla C_{\mathcal{T}_i}(x,t)) - (k_{0_i}(x)+k_{3_i}(x))C_{\mathcal{T}_i}(x,t) + k_{1_i}(x)C_{\mathcal{A}_i}(x,t) = 0\end{aligned} \tag{5.25}$$

We consider also that

$$\begin{aligned}C_{\mathcal{A}}(x,t) &= C_{\mathcal{A}_1}(x,t) - C_{\mathcal{A}_2}(x,t)\\ C_{\mathcal{T}}(x,t) &= C_{\mathcal{T}_1}(x,t) - C_{\mathcal{T}_2}(x,t)\\ D_{\mathcal{A}}(x) &= D_{\mathcal{A}_1}(x)\\ D_{\mathcal{T}}(x) &= D_{\mathcal{T}_1}(x)\\ k_3(x) &= k_{3_1}(x)\\ k_0(x) &= k_{0_1}(x)\\ k_1(x) &= k_{1_1}(x)\end{aligned}$$

Thus, we have

$$\begin{aligned}&\partial_t C_{\mathcal{A}} + \nabla\cdot(D_{\mathcal{A}}(x)\nabla C_{\mathcal{A}}(x,t)) + k_3(x)C_{\mathcal{T}}(x,t) - (k_0(x)+k_1(x))C_{\mathcal{A}}(x,t)\\ &= \nabla\cdot((D_{\mathcal{A}_2}(x) - D_{\mathcal{A}_1}(x))\nabla C_{\mathcal{A}_2}(x,t)) + (k_{3_2}(x) - k_{3_1}(x))C_{\mathcal{T}_2}(x,t)\\ &- ((k_{0_2}(x)+k_{1_2}(x)) - (k_{0_1}(x)+k_{1_1}(x)))C_{\mathcal{A}_2}(x,t)\end{aligned} \tag{5.26}$$

$$\begin{aligned}&\partial_t C_{\mathcal{T}} + \nabla\cdot(D_{\mathcal{T}}(x)\nabla C_{\mathcal{T}}(x,t)) + k_1(x)C_{\mathcal{A}}(x,t) - (k_0(x)+k_3(x))C_{\mathcal{T}}(x,t)\\ &= \nabla\cdot((D_{\mathcal{T}_2}(x) - D_{\mathcal{T}_1}(x))\nabla C_{\mathcal{T}_2}(x,t)) + (k_{1_2}(x) - k_{1_1}(x))C_{\mathcal{A}_2}(x,t)\\ &- ((k_{0_2}(x)+k_{3_2}(x)) - (k_{0_1}(x)+k_{3_1}(x)))C_{\mathcal{T}_2}(x,t)\end{aligned} \tag{5.27}$$

We have also

$$C_{\mathcal{A}}(x,t) + C_{\mathcal{T}}(x,t) = 0 \tag{5.28}$$

and we consider at the beginning $C_{\mathcal{T}_i} = 0$ for $t = 0$, which implies $C_{\mathcal{T}} = 0$ for $t = 0$. Then we have

$$C_{\mathcal{A}} + C_{\mathcal{T}} = 0 \;\text{ for }\; t = 0 \Rightarrow C_{\mathcal{A}} = 0 \;\text{ for }\; t = 0$$

With the considerations made above, we obtain from (5.26), in the time $t = 0$

$$\partial_t C_{\mathcal{A}} = \nabla\cdot((D_{\mathcal{A}_2}(x) - D_{\mathcal{A}_1}(x))\nabla C_{\mathcal{A}_2}(x,0)) - ((k_{0_2}(x)+k_{1_2}(x)) - (k_{0_1}(x)+k_{1_1}(x)))C_{\mathcal{A}_2}(x,0) \tag{5.29}$$

and for the equation (5.27), considering $t = 0$ and $C_{\mathcal{T}_2}(0) = 0$

$$\partial_t C_{\mathcal{T}} = (k_{1_2}(x) - k_{1_1}(x))C_{\mathcal{A}_2}(x,0) \tag{5.30}$$

From the equations (5.29) and (5.30) we have

$$\partial_t(C_{\mathcal{A}} + C_{\mathcal{T}})\Big|_{t=0} = \nabla \cdot ((D_{\mathcal{A}_2}(x) - D_{\mathcal{A}_1}(x))\nabla C_{\mathcal{A}_2}(x,0)) \tag{5.31}$$

and the equation (5.28) implies that

$$\partial_t(C_{\mathcal{A}} + C_{\mathcal{T}}) = 0 \Rightarrow \nabla \cdot ((D_{\mathcal{A}_2}(x) - D_{\mathcal{A}_1}(x))\nabla C_{\mathcal{A}_2}(x,0)) = 0 \tag{5.32}$$

With appropriate initial value $C_{\mathcal{A}_2}(t = 0) = f(t = 0)$ it follows that $D_{\mathcal{A}_2}(x) = D_{\mathcal{A}_1}(x)$ (See Proposition 5.2.7). Analogous situation can be extended to the three-component model ignoring the portion that represents the transport.

5.4 Three-Component Reaction-Diffusion Model

Now we want to analyze the three-component model including the portion that represents the transport and considering the parabolic differential equations that represent the radioactive concentration in artery, tissue and vein.

Let be $C_{\mathcal{A}_i} + C_{\mathcal{T}_i} + C_{\mathcal{V}_i} = f$ (measurement) and $C_{\mathcal{T}_i} = C_{\mathcal{V}_i} = 0$ for $t = 0$. Let be now the system

$$\begin{aligned}
\frac{\partial C_{\mathcal{A}_i}}{\partial t} &= \nabla \cdot (D_{\mathcal{A}_i}(x)\nabla C_{\mathcal{A}_i}(x,t) + V_{\mathcal{A}_i}(x)C_{\mathcal{A}_i}(x,t)) - (k_{0_i}(x) + k_{1_i}(x))C_{\mathcal{A}_i}(x,t) + k_{3_i}(x)C_{\mathcal{V}_i}(x,t) = 0\\
\frac{\partial C_{\mathcal{T}_i}}{\partial t} &= \nabla \cdot (D_{\mathcal{T}_i}(x)\nabla C_{\mathcal{T}_i}(x,t) + V_{\mathcal{T}_i}(x)C_{\mathcal{T}_i}(x,t)) - (k_{0_i}(x) + k_{2_i}(x))C_{\mathcal{T}_i}(x,t) + k_{1_i}(x)C_{\mathcal{A}_i}(x,t) = 0\\
\frac{\partial C_{\mathcal{V}_i}}{\partial t} &= \nabla \cdot (D_{\mathcal{V}_i}(x)\nabla C_{\mathcal{V}_i}(x,t) + V_{\mathcal{V}_i}(x)C_{\mathcal{V}_i}(x,t)) - (k_{0_i}(x) + k_{3_i}(x))C_{\mathcal{V}_i}(x,t) + k_{2_i}(x)C_{\mathcal{T}_i}(x,t) = 0
\end{aligned} \tag{5.33}$$

We take into account the following considerations for $C_{\mathcal{A}}$, $C_{\mathcal{T}}$ and $C_{\mathcal{V}}$:

$$\begin{aligned}
C_{\mathcal{A}}(x,t) &= C_{\mathcal{A}_1}(x,t) - C_{\mathcal{A}_2}(x,t)\\
C_{\mathcal{T}}(x,t) &= C_{\mathcal{T}_1}(x,t) - C_{\mathcal{T}_2}(x,t)\\
C_{\mathcal{V}}(x,t) &= C_{\mathcal{V}_1}(x,t) - C_{\mathcal{V}_2}(x,t)
\end{aligned}$$

and for all others parameters:

$$\begin{aligned}
k_3(x) &= k_{3_1}(x)\\
k_2(x) &= k_{2_1}(x)\\
k_1(x) &= k_{1_1}(x)\\
k_0(x) &= k_{0_1}(x)\\
D_{\mathcal{A}}(x) &= D_{\mathcal{A}_1}(x)\\
D_{\mathcal{T}}(x) &= D_{\mathcal{T}_1}(x)\\
D_{\mathcal{V}}(x) &= D_{\mathcal{V}_1}(x)\\
V_{\mathcal{A}}(x) &= V_{\mathcal{A}_1}(x)\\
V_{\mathcal{T}}(x) &= V_{\mathcal{T}_1}(x)\\
V_{\mathcal{V}}(x) &= V_{\mathcal{V}_1}(x)
\end{aligned}$$

Thus making the appropriate replacements, we have

$$\begin{aligned}&\partial_t C_{\mathcal{A}} - \nabla\cdot(D_{\mathcal{A}}(x)\nabla C_{\mathcal{A}}(x,t) + V_{\mathcal{A}}(x)C_{\mathcal{A}}(x,t)) + k_3(x)C_{\mathcal{V}}(x,t) - (k_0(x)+k_1(x))C_{\mathcal{A}}(x,t)\\&= -\nabla\cdot((D_{\mathcal{A}_2}(x) - D_{\mathcal{A}_1}(x))\nabla C_{\mathcal{A}_2}(x,t) + (V_{\mathcal{A}_2}(x) - V_{\mathcal{A}_1}(x))C_{\mathcal{A}_2}(x,t)) + (k_{3_2}(x) - k_{3_1}(x))C_{\mathcal{V}_2}(x,t)\\&- ((k_{0_2}(x)+k_{1_2}(x)) - (k_{0_1}(x)+k_{1_1}(x)))C_{\mathcal{A}_2}(x,t)\end{aligned} \tag{5.34}$$

$$\begin{aligned}&\partial_t C_{\mathcal{T}} - \nabla\cdot(D_{\mathcal{T}}(x)\nabla C_{\mathcal{T}}(x,t) + V_{\mathcal{T}}(x)C_{\mathcal{T}}(x,t)) + k_1(x)C_{\mathcal{A}}(x,t) - (k_0(x)+k_2(x))C_{\mathcal{T}}(x,t)\\&= -\nabla\cdot((D_{\mathcal{T}_2}(x) - D_{\mathcal{T}_1}(x)\nabla C_{\mathcal{T}_2}(x,t) + (V_{\mathcal{T}_2}(x) - V_{\mathcal{T}_1}(x))C_{\mathcal{T}_2}(x,t)) + (k_{1_2}(x) - k_{1_1}(x))C_{\mathcal{A}_2}(x,t)\\&- ((k_{0_2}(x)+k_{2_2}(x)) - (k_{0_1}(x)+k_{2_1}(x)))C_{\mathcal{T}_2}(x,t)\end{aligned} \tag{5.35}$$

$$\begin{aligned}&\partial_t C_{\mathcal{V}} - \nabla\cdot(D_{\mathcal{V}}(x)\nabla C_{\mathcal{V}}(x,t) + V_{\mathcal{V}}(x)C_{\mathcal{V}}(x,t)) + k_2(x)C_{\mathcal{T}}(x,t) - (k_0(x)+k_3(x))C_{\mathcal{V}}(x,t)\\&= -\nabla\cdot((D_{\mathcal{V}_2}(x) - D_{\mathcal{V}_1}(x))\nabla C_{\mathcal{V}_2}(x,t) + (V_{\mathcal{V}_2}(x) - V_{\mathcal{V}_2}(x))C_{\mathcal{V}_2}(x,t)) + (k_{2_2}(x) - k_{2_1}(x))C_{\mathcal{T}_2}(x,t)\\&- ((k_{0_2}(x)+k_{3_2}(x)) - (k_{0_1}(x)+k_{3_1}(x)))C_{\mathcal{V}_2}(x,t)\end{aligned} \tag{5.36}$$

We have also

$$C_{\mathcal{A}}(x,t) + C_{\mathcal{T}}(x,t) + C_{\mathcal{V}}(x,t) = 0 \tag{5.37}$$

and we consider at the beginning $C_{\mathcal{T}_i} = C_{\mathcal{V}_i} = 0$ for $t = 0$, which implies $C_{\mathcal{T}} = C_{\mathcal{V}} = 0$ for $t = 0$. Then we have

$$C_{\mathcal{A}} + C_{\mathcal{T}} + C_{\mathcal{V}} = 0 \text{ for } t = 0 \Rightarrow C_{\mathcal{A}} = 0 \text{ for } t = 0$$

With the considerations made above, we obtain from (5.34), in the time $t = 0$

$$\begin{aligned}\partial_t C_{\mathcal{A}} &= -\nabla\cdot((D_{\mathcal{A}_2}(x) - D_{\mathcal{A}_1}(x))\nabla C_{\mathcal{A}_2}(x,0) + (V_{\mathcal{A}_2}(x) - V_{\mathcal{A}_1}(x))C_{\mathcal{A}_2}(x,0))\\&\quad- (k_{1_2}(x) + k_{1_1}(x))C_{\mathcal{A}_2}(x,0)\end{aligned} \tag{5.38}$$

and for the equation (5.35), considering $t = 0$ and $C_{\mathcal{T}_2}(0) = 0$

$$\partial_t C_{\mathcal{T}} = (k_{1_2}(x) - k_{1_1}(x))C_{\mathcal{A}_2}(x,0) \tag{5.39}$$

and finally, for the equation (5.36), with $t = 0$ and $C_{\mathcal{V}_2}(0) = 0$

$$\partial_t C_{\mathcal{V}} = 0 \tag{5.40}$$

From the equations (5.38), (5.39) and (5.40) we have

$$\partial_t(C_{\mathcal{A}} + C_{\mathcal{T}} + C_{\mathcal{V}})\Big|_{t=0} = -\nabla\cdot((D_{\mathcal{A}_2}(x) - D_{\mathcal{A}_1}(x))\nabla C_{\mathcal{A}_2}(x,0) + (V_{\mathcal{A}_2}(x) - V_{\mathcal{A}_1}(x))C_{\mathcal{A}_2}(x,0)) \tag{5.41}$$

and the equation (5.37) imply that

$$
\begin{aligned}
&C_{\mathcal{A}} + C_{\mathcal{T}} + C_{\mathcal{V}} = 0 \\
&\Rightarrow -\nabla \cdot ((D_{\mathcal{A}_2}(x) - D_{\mathcal{A}_1}(x))\nabla C_{\mathcal{A}_2}(x,0) + (V_{\mathcal{A}_2}(x) - V_{\mathcal{A}_1}(x))C_{\mathcal{A}_2}(x,0)) = 0
\end{aligned}
\tag{5.42}
$$

Assuming that $V_{\mathcal{A}}$ is known, one can identify $D_{\mathcal{A}}$.

6 Numerical solution

This Chapter is intended to a numerical discussion on the problem presented in *Chapter 3*. First we make a brief discussion involving the combination of the EM-algorithm and the parameter identification problem in a single algorithm as a way to clarify how one solves the problem. In *Section 6.2* we discuss the discretization of the set of differential equations which describe the problem in question. Therefore we present two methods that can be used to solve the optimization problem (4.76), the Gradient-Method and Forward-Backward Splitting and the idea of solving our problem numerically. Finally we want to discuss the process of convergence to the problem proposed in this work.

6.1 EM - Algorithm and Parameter Identification Problem

In this section we explain how the problem is treated numerically. Here we work with the EM-algorithm and the parameter identification problem together in each iteration, i.e., to solve the problem of minimizing (4.76) we need to know the value of $u_{k+\frac{1}{2}}$, so we need to calculate first the $k+\frac{1}{2}$-th step of the EM-algorithm:

$$u_{k+\frac{1}{2}} = \frac{u_k}{K^*1} K^* \left(\frac{f}{Ku_k} \right) \tag{6.1}$$

After solving the associated lagrangean functional we calculate all the parameters that composes the vector $p_{k+\frac{1}{2}}$. Finally the value of $G(p_{k+\frac{1}{2}}) = u_{k+1}$ is updated continuing the process and thus allowing the calculation of the next EM-iteration. The procedure is described in the Figure 6.1.

6.2 Discretization of the Differential Equations

We want to discuss in this section the discretization of the differential equations which describe the problem. For this, consider the following system, spatially dependent on x and y and temporal dependent on t:

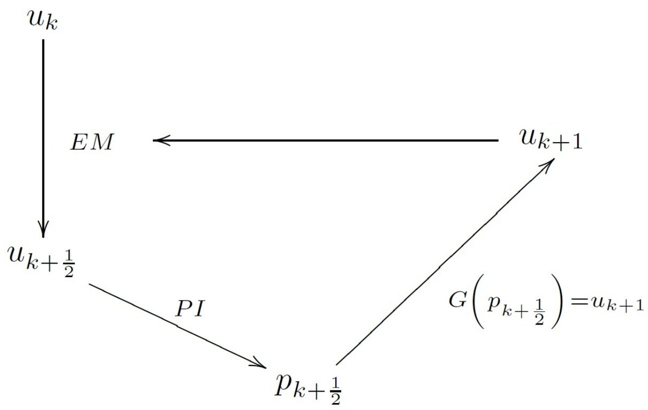

Figure 6.1: The EM - PI scheme [**6**]. The process starts in u_k. Then, using the EM-step, $u_{k+\frac{1}{2}}$ is estimated. Knowning $u_{k+\frac{1}{2}}$, we obtain the values of all biological parameters that compose $p_{k+\frac{1}{2}}$, within the parameter identification process. Using the image sequence generation functional G, we obtain u_{k+1} from those parameters. The next iterate for the EM algorithm is the image sequence u_{k+1}, instead of $u_{k+\frac{1}{2}}$.

$$\frac{\partial C}{\partial t} = \nabla((V(x)C) + (D(x)\nabla C)) + \begin{pmatrix} -diag(k_0+k_1) & k_3 & 0 \\ 0 & -diag(k_0+k_3) & k_2 \\ k_1 & 0 & -diag(k_0+k_2) \end{pmatrix} C \tag{6.2}$$

Where $C = \begin{pmatrix} C_{\mathcal{A}} \\ C_{\mathcal{V}} \\ C_{\mathcal{T}} \end{pmatrix}$, $D = \begin{pmatrix} D_{\mathcal{A}} \\ D_{\mathcal{V}} \\ D_{\mathcal{T}} \end{pmatrix}$ and $V = \begin{pmatrix} V_{\mathcal{A}} \\ V_{\mathcal{V}} \\ V_{\mathcal{T}} \end{pmatrix}$.

We discretize the first time derivative with the operator splitting method using the notation $C(t_k) = C^\tau(k)$. Then we obtain

$$(i) \qquad \frac{C^\tau\left(k+\frac{1}{3}\right) - C^\tau(k)}{\tau} = \frac{\partial}{\partial x}\left(D_x \frac{\partial C^\tau}{\partial x}\left(k+\frac{1}{3}\right) + V_x C^\tau\left(k+\frac{1}{3}\right)\right) \tag{6.3}$$

$$(ii) \qquad \frac{C^\tau\left(k+\frac{2}{3}\right) - C^\tau\left(k+\frac{1}{3}\right)}{\tau} = \frac{\partial}{\partial y}\left(D_y \frac{\partial C^\tau}{\partial y}\left(k+\frac{2}{3}\right) + V_y C^\tau\left(k+\frac{2}{3}\right)\right) \tag{6.4}$$

$$(iii) \qquad \frac{C^\tau(k+1) - C^\tau\left(k+\frac{2}{3}\right)}{\tau} = \begin{pmatrix} -diag(k_0+k_1) & k_3 & 0 \\ 0 & -diag(k_0+k_3) & k_2 \\ k_1 & 0 & -diag(k_0+k_2) \end{pmatrix} C^\tau(k+1) \tag{6.5}$$

The equations (6.3) and (6.4) can be discretized with the Scharfetter-Gummel Scheme [**31**]. We treat both equations separately and it remains to discretize the spatial derivative. For the x-scale we choose a grid $G_x = \{x_i = ih_x - 1 | i = 0, ..., 2N\}$ with the step size at the x-scale h_x and for y-scale, respectively $G_y = \{y_j = jh_y | j = 0, ..., M\}$ with the step size h_y.

Consider now only the equation (6.3). Note that

$$V_x^+ = 0.5(V_x(x_i, y_j) + V_x(x_{i+1}, y_j)), \quad \nabla W_x^+ = 0.5(\nabla W_x(x_i, y_j) + \nabla W_x(x_{i+1}, y_j)) \tag{6.6}$$

and

$$V_x^- = 0.5(V_x(x_i, y_j) + V_x(x_{i-1}, y_j)), \quad \nabla W_x^- = 0.5(\nabla W_x(x_i, y_j) + \nabla W_x(x_{i-1}, y_j)) \tag{6.7}$$

where $\nabla W_x = D_x^{-1} V_x$ $(D << V)$. Making the discretization of the equation with respect to x, assuming $j = \bar{j}$ and solving the equation with the implicit Euler method, we have (for details see **[31]**).

$$C_{\bar{j}}^{\tau}\left(k + \frac{1}{3}\right) = (I - \tau L_x)^{-1} C_{\bar{j}}^{\tau}(k) \tag{6.8}$$

with the matrix $L_x = (k_{i,j}^x)$, where we consider the following entries:

- For $V_x < 0$:

$$k_{i,i}^x = -\frac{V_x^+}{h_x \cdot \exp(\nabla W_x^+ \cdot hx) - hx} - \frac{V_x^- \cdot \exp(\nabla W_x^- \cdot hx)}{hx \cdot \exp(\nabla W_x^- \cdot hx) - hx} \tag{6.9}$$

$$k_{i+1,i}^x = \frac{V_x^+}{h_x \cdot \exp(\nabla W_x^+ \cdot hx) - hx} \tag{6.10}$$

$$k_{i-1,i}^x = \frac{V_x^- \cdot \exp(\nabla W_x^- \cdot hx)}{hx \cdot \exp(\nabla W_x^- \cdot hx) - hx} \tag{6.11}$$

- For $V_x \geq 0$:

$$k_{i,i}^x = -\frac{V_x^+}{h_x - \exp(-\nabla W_x^+ \cdot hx)} - \frac{V_x^- \cdot \exp(-\nabla W_x^- \cdot hx)}{hx - \exp(-\nabla W_x^- \cdot hx)} \tag{6.12}$$

$$k_{i+1,i}^x = \frac{V_x^+}{h_x - \exp(-\nabla W_x^+ \cdot hx)} \tag{6.13}$$

$$k_{i-1,i}^x = \frac{V_x^- \cdot \exp(-\nabla W_x^- \cdot hx)}{hx - \exp(-\nabla W_x^- \cdot hx)} \tag{6.14}$$

where V_x represents the velocity parameter in the x-direction ($V_{x\mathcal{A}}$ in artery, $V_{x\mathcal{T}}$ in tissue and $V_{x\mathcal{V}}$ in vein). Calculating this solution for all $\bar{j} = 1, \ldots, M-1$, we can find the solution matrix

$$C^{\tau}\left(k + \frac{1}{3}\right) = C_{\bar{j}=1}^{\tau}\left(k + \frac{1}{3}\right), \ldots, C_{\bar{j}=M-1}^{\tau}\left(k + \frac{1}{3}\right) = C_{i,j}^{\tau}\left(k + \frac{1}{3}\right) \tag{6.15}$$

for $i = 1, \ldots, 2N-1$ and $j = 1, \ldots, M-1$. For the initial data, we have

$$C_{0,\bar{j}}^{\tau} = \left(C_{i,j}^{\tau}(k)\right)_i, \quad \text{for } i = 1, \ldots, 2N-1 \tag{6.16}$$

We have then a solution $C_{\bar{j}}^{\tau}\left(k + \frac{1}{3}\right)$ for a fixed $\bar{j}$.

Similarly, considering now the equation (6.4), we want to make the discretization with respect to y. Note that

$$V_y^+ = 0.5(V_y(x_i, y_j) + V_y(x_i, y_{j+1})), \quad \nabla W_y^+ = 0.5(\nabla W_y(x_i, y_j) + \nabla W_y(x_i, y_j + 1)) \tag{6.17}$$

and

$$V_y^- = 0.5(V_y(x_i, y_j) + V_y(x_i, y_{j-1})), \quad \nabla W_y^- = 0.5(\nabla W_y(x_i, y_j) + \nabla W_y(x_i, y_{j-1})) \tag{6.18}$$

We assume now the other variable $i = \bar{i}$ as constant and compute a solution for $t = k + \frac{2}{3}$. Similarly applying the implicit Euler method we have (see [31])

$$C_{\bar{i}^\tau}\left(k + \frac{2}{3}\right) = (I - \tau L_y)^{-1} C_{\bar{i}}^\tau \left(k + \frac{1}{3}\right) \tag{6.19}$$

with the matrix $L_y = (k_{i,j}^y)$, where we consider the following entries:

- For $V_y < 0$:

$$k_{j,j}^y = -\frac{V_y^+}{h_y \cdot \exp\left(\nabla W_y^+ \cdot hy\right) - hy} - \frac{V_y^- \cdot \exp\left(\nabla W_y^- \cdot hy\right)}{hy \cdot \exp\left(\nabla W_y^- \cdot hy\right) - hy} \tag{6.20}$$

$$k_{j+1,j}^y = \frac{V_y^+}{h_y \cdot \exp\left(\nabla W_y^+ \cdot hy\right) - hy} \tag{6.21}$$

$$k_{j-1,j}^y = \frac{V_y^- \cdot \exp\left(\nabla W_y^- \cdot hy\right)}{hy \cdot \exp\left(\nabla W_y^- \cdot hy\right) - hy} \tag{6.22}$$

- For $V_y \geq 0$:

$$k_{j,j}^y = -\frac{V_y^+}{h_y - \exp\left(-\nabla W_y^+ \cdot hy\right)} - \frac{V_y^- \cdot \exp\left(-\nabla W_y^- \cdot hy\right)}{hy - \exp\left(-\nabla W_y^- \cdot hy\right)} \tag{6.23}$$

$$k_{j+1,j}^y = \frac{V_y^+}{h_y - \exp\left(-\nabla W_y^+ \cdot hy\right)} \tag{6.24}$$

$$k_{j-1,j}^y = \frac{V_y^- \cdot \exp\left(-\nabla W_y^- \cdot hy\right)}{hy - \exp\left(-\nabla W_y^- \cdot hy\right)} \tag{6.25}$$

Note that the initial conditions in this case are

$$C_{0,\bar{i}}^\tau = \left(C_{i,j}^\tau\left(k + \frac{1}{3}\right)\right)_j, \quad \text{for } j = 1, \ldots, M-1 \tag{6.26}$$

We have then a solution $C_{\bar{i}}^\tau\left(k + \frac{2}{3}\right)$ for a fixed $\bar{i}$. Calculating this solution for all $\bar{i} = 1, \ldots, 2N-1$ we can find the solution matrix

$$C^\tau\left(k + \frac{2}{3}\right) = \left(C_{\bar{i}=1}^\tau\left(k + \frac{2}{3}\right), \ldots, C_{\bar{i}=2N-1}^\tau\left(k + \frac{2}{3}\right)\right)^T = C_{i,j}^\tau\left(k + \frac{2}{3}\right) \tag{6.27}$$

for $i = 1, \ldots, 2N-1$ and $j = 1, \ldots, M-1$. Applying both systems alternately leads to a solution for all $i = 1, \ldots, 2N-1$ and $j = 1, \ldots, M-1$ at any time t. And the boundary values are given with the boundary conditions, hence we have a solution for every i, j (for more details see [31]).

Finally the equation (6.5) can be easily solved with a few simple calculations. The discretization of μ, η and γ was performed in the same way.

6.3 Gradient Method

To solve numerically the equation (4.99) taking into account the conditions of optimalily (4.88) - (4.94) and (4.100) - (4.108) we use the iterative gradient method.

This method is an algorithm widely used in the optimization problems to find a minimum (global or local).

Let F be a multivariable function differential. The method then consists in finding a search direction of a negative gradient of F at x:

$$d = -\nabla F(x^{(j)}) \tag{6.28}$$

from a starting point.

Through the discretization of (6.28) by the forward-differences, we obtain the iterative system below

$$x^{k+1}(x) = x^k - \tau \nabla F(x^{(j)}) \tag{6.29}$$

considering τ very small.

Following the same reasoning we obtain the following equations (6.30)-(6.43) which allow us to calculate the desired parameters (considering the spatially dependence on x and y and the temporal dependence on t, according to the examples presented in *Chapter 7*).

$$k_1^{k+1}(x,y) = k_1^k - \tau \frac{\partial \mathcal{L}}{\partial k_1}(p^k) \tag{6.30}$$

$$k_2^{k+1}(x,y) = k_2^k - \tau \frac{\partial \mathcal{L}}{\partial k_2}(p^k) \tag{6.31}$$

$$k_3^{k+1}(x,y) = k_3^k - \tau \frac{\partial \mathcal{L}}{\partial k_3}(p^k) \tag{6.32}$$

$$V_{x\mathcal{T}}^{k+1}(x,y) = V_{x\mathcal{T}}^k - \tau \frac{\partial \mathcal{L}}{\partial V_{x\mathcal{T}}}(p^k) \tag{6.33}$$

$$V_{y\mathcal{T}}^{k+1}(x,y) = V_{y\mathcal{T}}^k - \tau \frac{\partial \mathcal{L}}{\partial V_{y\mathcal{T}}}(p^k) \tag{6.34}$$

$$V_{x\mathcal{A}}^{k+1}(x,y) = V_{x\mathcal{A}}^k - \tau \frac{\partial \mathcal{L}}{\partial V_{x\mathcal{A}}}(p^k) \tag{6.35}$$

$$V_{y\mathcal{A}}^{k+1}(x,y) = V_{y\mathcal{A}}^k - \tau \frac{\partial \mathcal{L}}{\partial V_{y\mathcal{A}}}(p^k) \tag{6.36}$$

$$V_{x\mathcal{V}}^{k+1}(x,y) = V_{x\mathcal{V}}^k - \tau \frac{\partial \mathcal{L}}{\partial V_{x\mathcal{V}}}(p^k) \tag{6.37}$$

$$V_{y\mathcal{V}}^{k+1}(x,y) = V_{y\mathcal{V}}^k - \tau \frac{\partial \mathcal{L}}{\partial V_{y\mathcal{V}}}(p^k) \tag{6.38}$$

$$D_{x\mathcal{T}}^{k+1}(x,y) = D_{x\mathcal{T}}^k - \tau \frac{\partial \mathcal{L}}{\partial D_{x\mathcal{T}}}(p^k) \tag{6.39}$$

$$D_{y\mathcal{T}}^{k+1}(x,y) = D_{y\mathcal{T}}^k - \tau \frac{\partial \mathcal{L}}{\partial D_{y\mathcal{T}}}(p^k) \tag{6.40}$$

$$D_{x\mathcal{A}}^{k+1}(x,y) = D_{x\mathcal{A}}^{k} - \tau \frac{\partial \mathcal{L}}{\partial D_{x\mathcal{A}}}(p^k) \tag{6.41}$$

$$D_{y\mathcal{A}}^{k+1}(x,y) = D_{y\mathcal{A}}^{k} - \tau \frac{\partial \mathcal{L}}{\partial D_{y\mathcal{A}}}(p^k) \tag{6.42}$$

$$D_{x\mathcal{V}}^{k+1}(x,y) = D_{x\mathcal{V}}^{k} - \tau \frac{\partial \mathcal{L}}{\partial D_{x\mathcal{V}}}(p^k) \tag{6.43}$$

$$D_{y\mathcal{V}}^{k+1}(x,y) = D_{y\mathcal{V}}^{k} - \tau \frac{\partial \mathcal{L}}{\partial D_{y\mathcal{V}}}(p^k) \tag{6.44}$$

Having solved the equations above, we obtain the up of parameters that composes the vector p. Since these values represent physiological parameters, we want to limit numerically computed parameters to be physiological values, too. To obtain parameters k_1, k_2 and k_3 lying within a physiological range $[0, \varsigma]$, we use the projective gradient method:

$$k^{k+1} = \begin{cases} 1, & \text{if } \; k^k - \tau \frac{\partial \mathcal{L}}{\partial k}(p^k) > 1; \\ \varsigma, & \text{if } \; k^k - \tau \frac{\partial \mathcal{L}}{\partial k}(p^k) < \varsigma; \\ k^k - \frac{\partial \mathcal{L}}{\partial k}(p^k) & \text{else} \end{cases} \tag{6.45}$$

for τ reasonably small.

After we calculate the parameters that compose the vector p, we are able to upgrade the image $u_{k+1}(x,y,t)$ via

$$\begin{aligned} u_{k+1}(x,y,t) &= G(p(x,y)) \\ &= G(k_1(x,y), k_2(x,y), k_3(x,y), D_{\mathcal{T}}(x,y), D_{\mathcal{A}}(x,y), D_{\mathcal{V}}(x,y), V_{\mathcal{T}}(x,y), V_{\mathcal{A}}(x,y), V_{\mathcal{V}}(x,y)) \end{aligned} \tag{6.46}$$

that will used in the next EM-iteration step to find $u_{k+\frac{1}{2}}$, according to the following figure

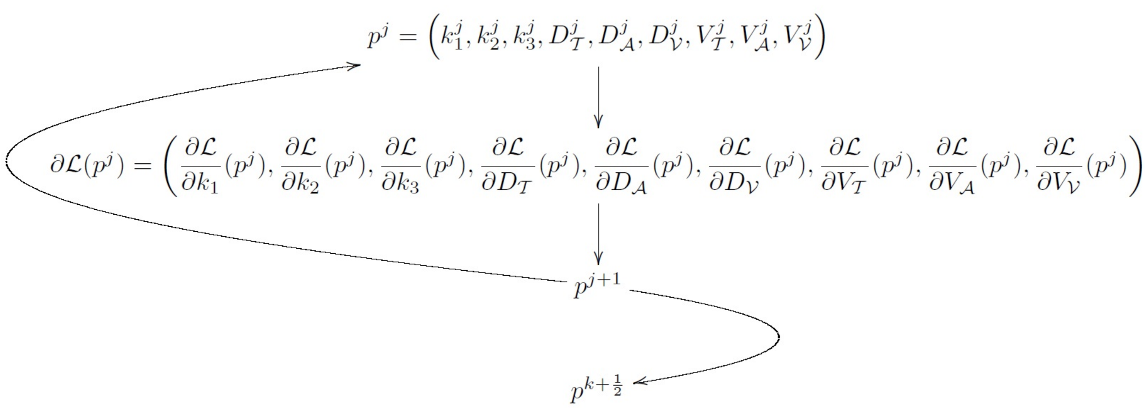

Figure 6.2: The scheme in the PI process. The j-th iterate is used to compute the $j+1$-th iterate from p^j and $\partial\mathcal{L}$. Processing iterates is stopped after m iterations until $|p^m - p^{m-1}| < \epsilon$ ($\epsilon > 0$ is a specified factor) is satisfied. This iteration is considered the optimal solution estimated $\tilde{p}$, fulfilling $\partial\mathcal{L}(\tilde{p}) = 0$ and being denoted $p_{k+\frac{1}{2}}$ building the base for the next EM-step.

Note that $V_{\mathcal{A}}^j$ represents both $V_{x\mathcal{A}}^j$ and $V_{y\mathcal{A}}^j$ (for the sake of simplicity) and the same also applies to the diffusion and velocity parameters.

Taking into account that the problem proposed here depends on various parameters that must be adjusted numerically in each iteration and it is very time consuming, we use another method that solves the minimization problem faster. This method, called Forward-Backward Splitting is presented in the next section.

6.4 Forward-Backward Splitting

As seen in chapter 4, we will apply the Forward-Backward Splitting method for all parameters that composes the vector p:

$$k_1^{k+1}(x,y) = k_1^k - \tau\frac{\partial\mathcal{G}}{\partial k_1}(p^k) - \tau\frac{\partial\mathcal{H}}{\partial k_1}(p^{k+1}) \tag{6.47}$$

$$k_1^{k+1} + \tau(2\alpha(k_1^{k+1} - k_1^*) - 2\xi\Delta k_1^{k+1}) = k_1^k - \tau\left(-\int_0^T C_{\mathcal{A}}\mu dt + \int_0^T C_{\mathcal{A}}\eta dt\right) \tag{6.48}$$

$$\begin{aligned}(1+2\alpha\tau)k_1^{k+1}(x,y) - 2\alpha\tau k_1^* - 2\xi\tau\Delta k_1^{k+1}(x,y) = k_1^k + \tau\int_0^T C_{\mathcal{A}}(x,y,t)\mu(x,y,t)dt \\ - \int_0^T C_{\mathcal{A}}(x,y,t)\eta(x,y,t)dt\end{aligned} \tag{6.49}$$

$$\begin{aligned}&(1+2\alpha\tau)k_1^{k+1}(x,y) - 2\xi\tau\left(\frac{k_{x+1,y} - 2k_{x,y} + k_{x-1,y}}{dx^2} + \frac{k_{x,y+1} - 2k_{x,y} + k_{x,y-1}}{dy^2}\right) \\ &= k_1^k(x,y) + \tau\int_0^T C_{\mathcal{A}}(x,y,t)\mu(x,y,t)dt - \tau\int_0^T C_{\mathcal{A}}(x,y,t)\eta(x,y,t)dt + 2\alpha\tau k_1^*\end{aligned} \tag{6.50}$$

$$\begin{aligned}(1+2\alpha\tau - 2\xi\tau B_x - 2\xi\tau B_y)k_1^{k+1}(x,y) = k_1^k(x,y) + \tau\int_0^T C_{\mathcal{A}}(x,y,t)\mu(x,y,t)dt \\ - \tau\int_0^T C_{\mathcal{A}}(x,y,t)\eta(x,y,t)dt + 2\alpha\tau k_1^*\end{aligned} \tag{6.51}$$

And, finally

$$\begin{aligned}&k_1^{k+1}(x,y) = (1+2\alpha\tau - 2\xi\tau B_x - 2\xi\tau B_y)^{-1} \\ &\qquad\left(k_1^k(x,y) + \tau\int_0^T C_{\mathcal{A}}(x,y,t)\mu(x,y,t)dt - \tau\int_0^T C_{\mathcal{A}}(x,y,t)\eta(x,y,t)dt + 2\alpha\tau k_1^*\right)\end{aligned} \tag{6.52}$$

In the language of numerical analysis,

$$\left(k_1^k(x,y) + \tau \int_0^T C_{\mathcal{A}}(x,y,t)\mu(x,y,t)dt - \tau \int_0^T C_{\mathcal{A}}(x,y,t)\eta(x,y,t)dt + 2\alpha\tau k_1^* \right)$$

gives a forward step with step size τ whereas $(1+2\alpha\tau - 2\xi\tau B_x - 2\xi\tau B_y)^{-1}$ gives a backward step. Similarly, for k_2 and k_3 we have

$$k_2^{k+1}(x,y) = (1+2\alpha\tau - 2\xi\tau B_x - 2\xi\tau B_y)^{-1} \left(k_2^k(x,y) - \tau \int_0^T C_{\mathcal{T}}(x,y)\mu(x,y)dt + \tau \int_0^T C_{\mathcal{T}}(x,y,t)\gamma(x,y,t)dt + 2\alpha\tau k_2^* \right) \tag{6.53}$$

$$k_3^{k+1}(x,y) = (1+2\alpha\tau - 2\xi\tau B_x - 2\xi\tau B_y)^{-1} \left(k_3^k(x,y,t) + \tau(x,y,t) \int_0^T C_{\mathcal{V}}(x,y,t)\eta(x,y,t)dt + \tau \int_0^T C_{\mathcal{V}}(x,y,t)\gamma(x,y,t)dt + 2\alpha\tau k_3^* \right) \tag{6.54}$$

And for the diffusion and velocity parameters we obtain

$$V_{\mathcal{T}}^{k+1}(x,y) = (1-\alpha\tau+\xi\tau B_x+\xi\tau B_y)^{-1} \left(V_{\mathcal{T}}^k(x,y) - \tau V_{\mathcal{T}}^k(x,y)\cdot\nabla \int_0^T \mu(x,y,t)dt + \alpha\tau V_{\mathcal{T}}^* \right) \tag{6.55}$$

$$V_{\mathcal{A}}^{k+1}(x,y) = (1-\alpha\tau+\xi\tau B_x+\xi\tau B_y)^{-1} \left(V_{\mathcal{A}}^k(x,y) - \tau V_{\mathcal{A}}^k(x,y,t)\cdot\nabla \int_0^T \eta(x,y,t)dt + \alpha\tau V_{\mathcal{A}}^* \right) \tag{6.56}$$

$$V_{\mathcal{V}}^{k+1}(x,y) = (1-\alpha\tau+\xi\tau B_x+\xi\tau B_y)^{-1} \left(V_{\mathcal{V}}^k(x,y) - \tau V_{\mathcal{V}}^k(x,y)\cdot\nabla \int_0^T \gamma(x,y,t)dt + \alpha\tau V_{\mathcal{V}}^* \right) \tag{6.57}$$

$$D_{\mathcal{T}}^{k+1}(x,y) = (1+\alpha\tau - \xi\tau B_x - \xi\tau B_y)^{-1} \left(D_{\mathcal{T}}^k(x,y) - \tau(\nabla D_{\mathcal{T}}^k(x,y) \int_0^T \nabla\mu(x,y,t)dt) + \alpha\tau D_{\mathcal{T}}^* \right) \tag{6.58}$$

$$D_{\mathcal{A}}^{k+1}(x,y) = (1+\alpha\tau - \xi\tau B_x - \xi\tau B_y)^{-1} \left(D_{\mathcal{A}}^k(x,y) - \tau(\nabla D_{\mathcal{A}}^k(x,y) \int_0^T \nabla\eta(x,y,t)dt) + \alpha\tau D_{\mathcal{A}}^* \right) \tag{6.59}$$

$$D_{\mathcal{V}}^{k+1}(x,y) = (1+\alpha\tau - \xi\tau B_x - \xi\tau B_y)^{-1} \left(D_{\mathcal{V}}^k(x,y) - \tau(\nabla D_{\mathcal{V}}^k(x,y) \int_0^T \nabla\gamma(x,y,t)dt) + \alpha\tau D_{\mathcal{V}}^* \right) \tag{6.60}$$

A good choice of τ defines a significant speedup, because the dependence on the ill-posedness of the operator K (the ill-conditioning of the matrix that represents the discretization of K) can make the iterative scheme very slow.

7

Results

In this chapter we present some computed test results on synthetic and real data, performed with MATLAB (The MathWorks^{TM}, Inc., Natick, MA). We emphasize here that the purpose of this chapter is to test both reconstruction of biological parameters involved as well as the behavior of real $H_2^{15}O$-PET-scan data qualitatively.

7.1 A Synthetic Data Example

We present here a synthetic data example and we illustrate the reconstruction of parameters. For this we use an image 79 x 159 pixels in domain Ω. For the radioactive concentration $C_{\mathcal{A}}$ in the artery we use the initial function

$$C_{\mathcal{A}}(x, y, 0) = \tau(1 - x^2)(N - y)y \tag{7.1}$$

with $N = 40$, being represented by the following figure:

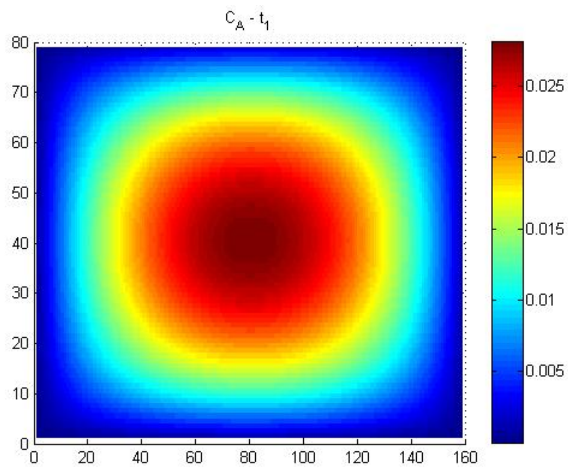

Figure 7.1: The radioactive concentration $C_{\mathcal{A}}$ in artery - t_1

The radioactive concentration in the tissue and in vein at the beginning are zero and the time step is $\tau = 10^{-5}$. The used method to solve numerically we use the Forward-Backward splitting (*Section*

6.4). The table below show the biological parameters involved and the corresponding regularization parameters (a-priori (α) and the gradient regularization (ξ)). The parameter $(\cdot)^*$ is related to the equation (4.95).

Parameter	Initial Value	$(\cdot)^*$	A-p. Regularization (α)	Gradient regularization (ξ)
k_1 (1/cm)	0.9	0.89	0.01287520644013148965	0.0008
k_2 (1/cm)	0.75	0.7	0.012867926470118801553	0.0001
k_3 (1/cm)	0.9	0.85	0.012876216264812848965	0.0001
$V_{x_\mathcal{A}}(cm/s)$	0.0001	0.1	0.001024495	0.0001
$V_{y_\mathcal{A}}(cm/s)$	700	15	1.1000	0.0001
$V_{x_\mathcal{T}}(cm/s)$	-50	-5	1.122098745999	0.0001
$V_{y_\mathcal{T}}(cm/s)$	0.0001	0.1	0.001024495	0.0001
$V_{x_\mathcal{V}}(cm/s)$	0.0001	0.1	0.001024495	0.0001
$V_{y_\mathcal{V}}(cm/s)$	700	15	1.1000000001	0.0001
$D_\mathcal{A}(cm^2/s)$	$3 * 10^{(-7)}$	$10^{(-3)}$	0.0003344	0.000444
$D_\mathcal{T}(cm^2/s)$	$3 * 10^{(-6)}$	$10^{(-2)}$	0.000344	0.000444
$D_\mathcal{V}(cm^2/s)$	$3 * 10^{(-7)}$	$10^{(-3)}$	0.0003344	0.000444

Table 7.1: Input data for the synthetic example

The parameters k_1, k_2 and k_3 are constants (with a small variation) in all pixels of the image, and their values of reconstruction are shown in the Table 7.2.

Parameter	Reconstruction of the parameter
k_1	$0.826394154400616 \pm 4 \cdot 10^{-10}$ (1/cm)
k_2	$0.688651340749675 \pm 3 \cdot 10^{-11}$ (1/cm)
k_3	$0.826346689791371 \pm 3 \cdot 10^{-11}$ (1/cm)

Table 7.2: Reconstruction of k_1, k_2 and k_3

The figures below show the exact reconstruction of all biological parameters. For all graphics below the direction y ist represented by u. In order to better visualize the radioactive flow in the artery and vein tissue the graphics have been plotted with the y axis on the horizontal, rotating the coordinate system.

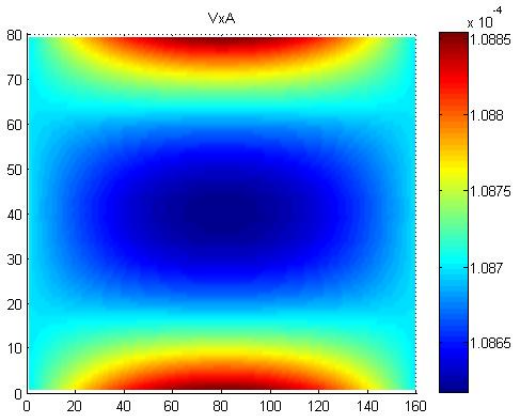

Figure 7.2: Reconstruction of $V_{x_\mathcal{A}}$

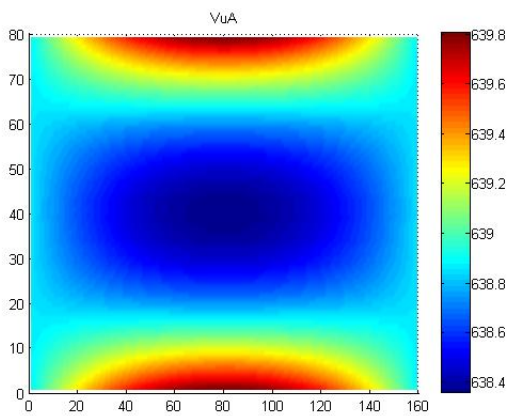

Figure 7.3: Reconstruction of $V_{y_\mathcal{A}}$

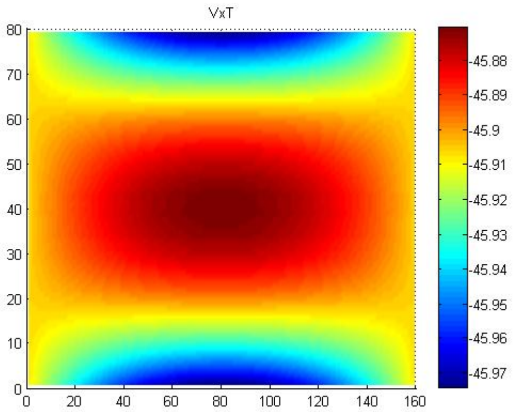

Figure 7.4: Reconstruction of $V_{x_{\mathcal{T}}}$

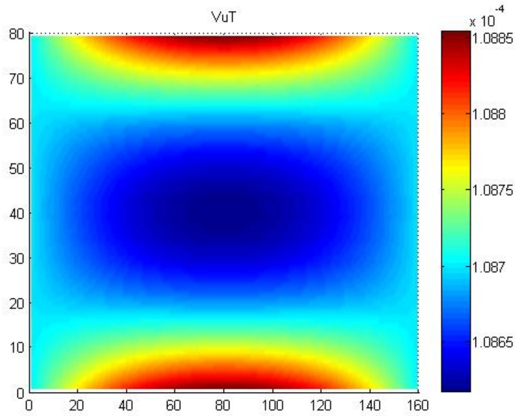

Figure 7.5: Reconstruction of $V_{y_{\mathcal{T}}}$

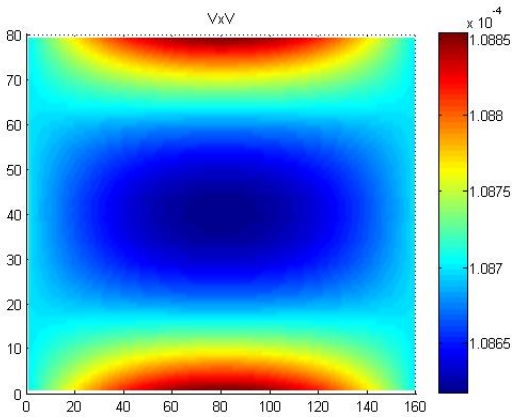

Figure 7.6: Reconstruction of $V_{x_{\mathcal{V}}}$

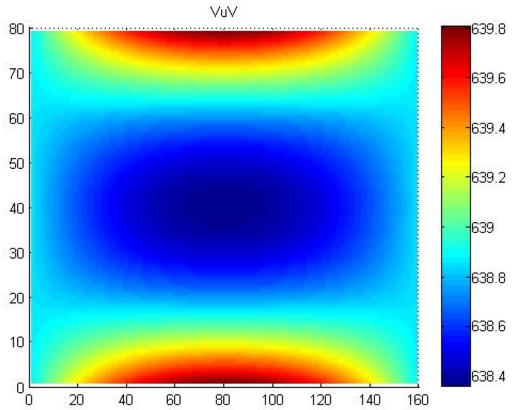

Figure 7.7: Reconstruction of $V_{y_{\mathcal{V}}}$

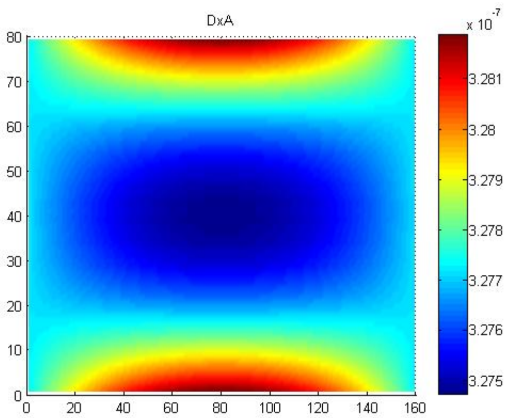

Figure 7.8: Reconstruction of $D_{x_{\mathcal{A}}}$

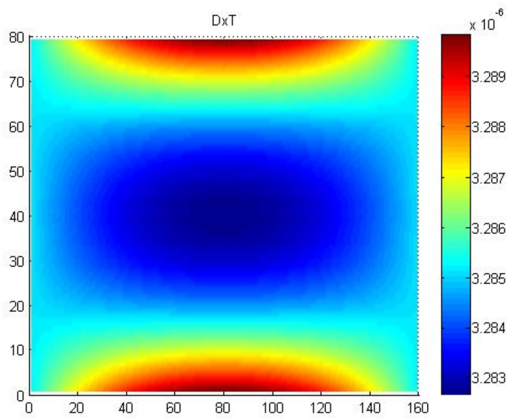

Figure 7.9: Reconstruction of $D_{x_{\mathcal{T}}}$

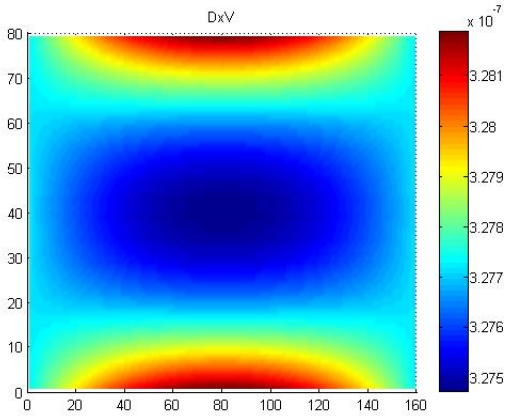

Figure 7.10: Reconstruction of $D_{x\mathcal{V}}$

The Figure 7.11 describes the behavior of blood flow that we want to reproduce i.e., the exchange of materials between artery, tissue and vein. It starts in the left ventricle of the heart, which it contracts and pumps blood to the largest artery in the body, the aorta. This blood passes through a network of small blood vessels called capillaries. The capillaries converge to small veins (venules) that will gradually uniting with each other, become veins and carry blood back to the heart.

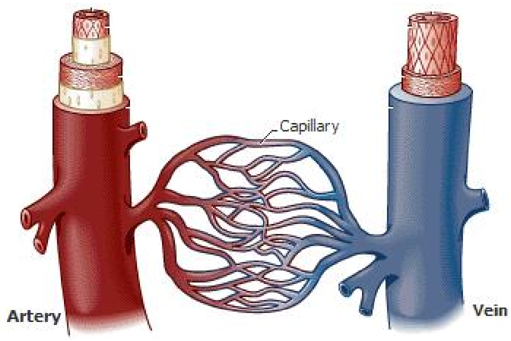

Figure 7.11: Exchange of materials. © 2007 Alexandre Wahl Hennigen

Based on this we present here the reconstructions that represent the radioactive concentrations in artery, tissue and vein for different times.

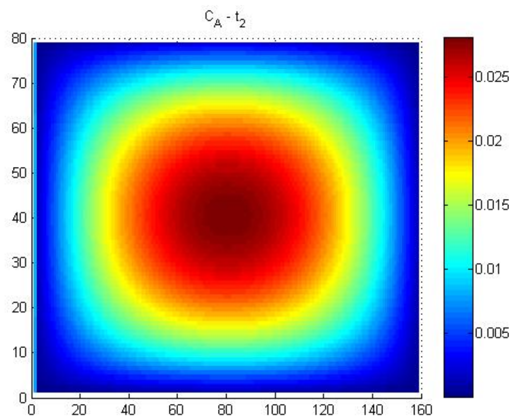

Figure 7.12: Reconstruction of $C_{\mathcal{A}} - t_2$

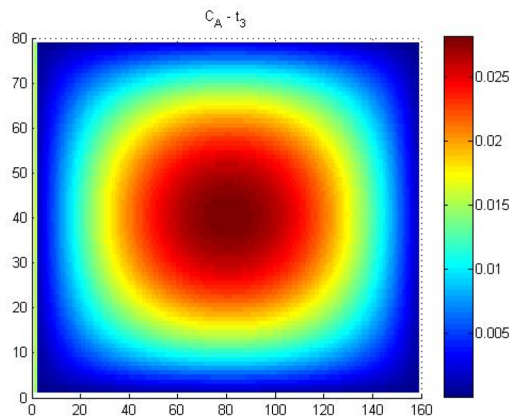

Figure 7.13: Reconstruction of $C_{\mathcal{A}} - t_3$

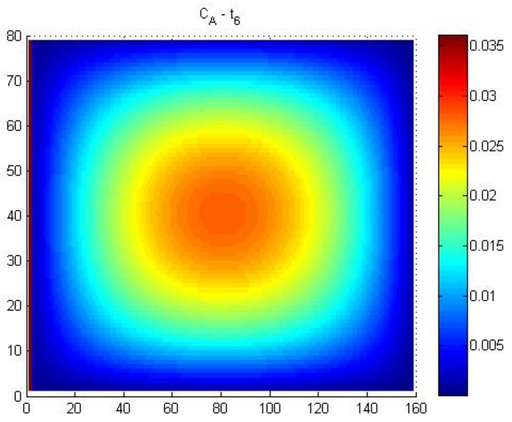

Figure 7.14: Reconstruction of $C_{\mathcal{A}} - t_6$

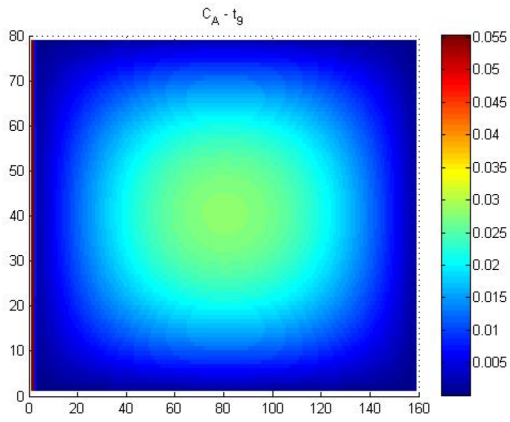

Figure 7.15: Reconstruction of $C_{\mathcal{A}} - t_9$

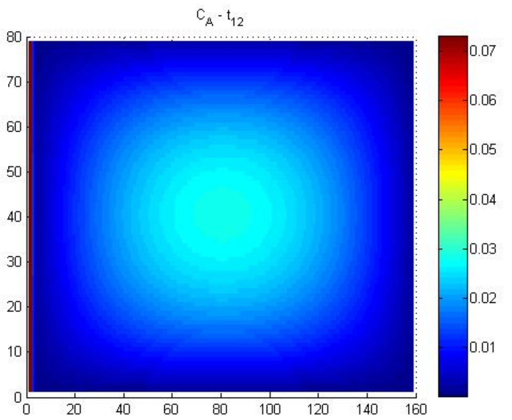

Figure 7.16: Reconstruction of $C_{\mathcal{A}} - t_{12}$

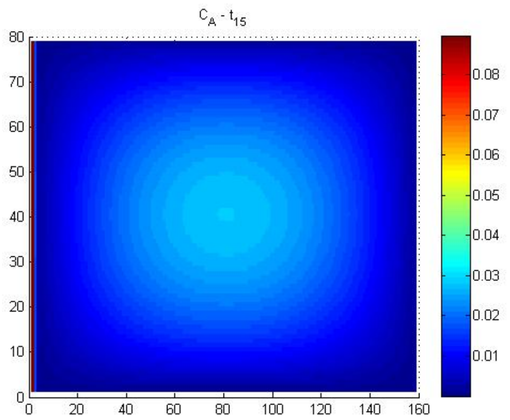

Figure 7.17: Reconstruction of $C_{\mathcal{A}} - t_{15}$

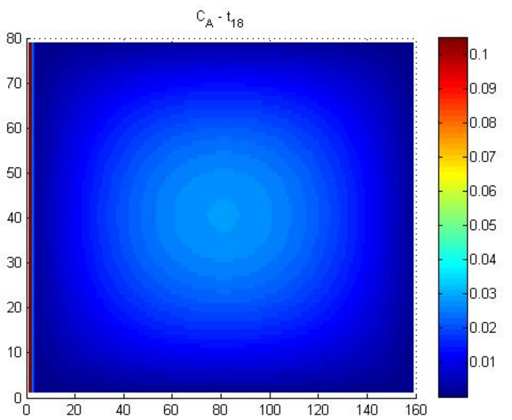

Figure 7.18: Reconstruction of $C_{\mathcal{A}} - t_{18}$

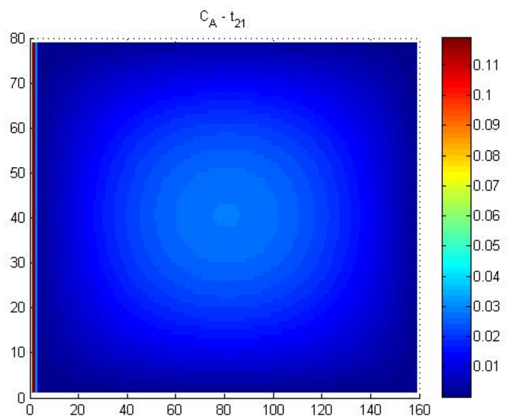

Figure 7.19: Reconstruction of $C_{\mathcal{A}} - t_{21}$

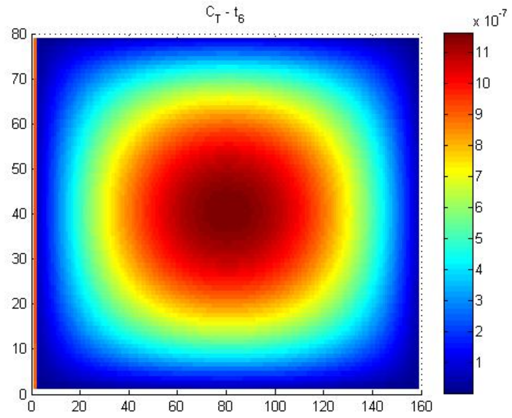

Figure 7.20: Reconstruction of $C_{\mathcal{T}} - t_6$

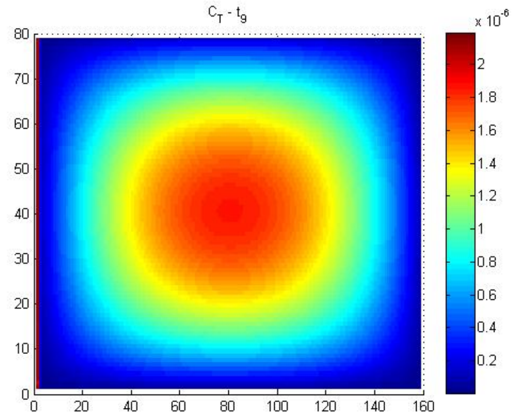

Figure 7.21: Reconstruction of $C_{\mathcal{T}} - t_9$

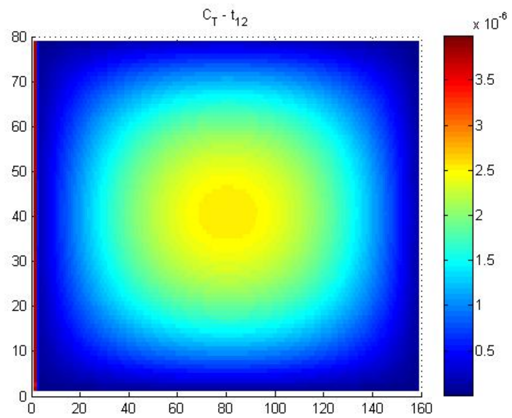

Figure 7.22: Reconstruction of $C_{\mathcal{T}} - t_{12}$

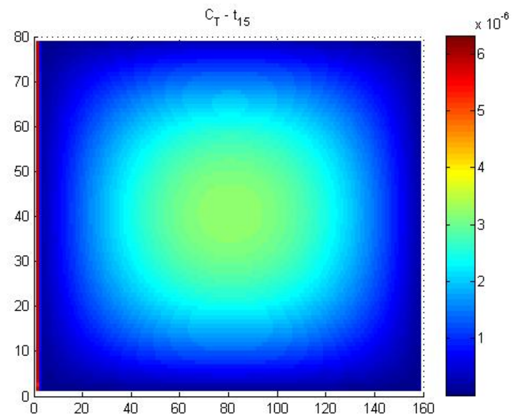

Figure 7.23: Reconstruction of $C_{\mathcal{T}} - t_{15}$

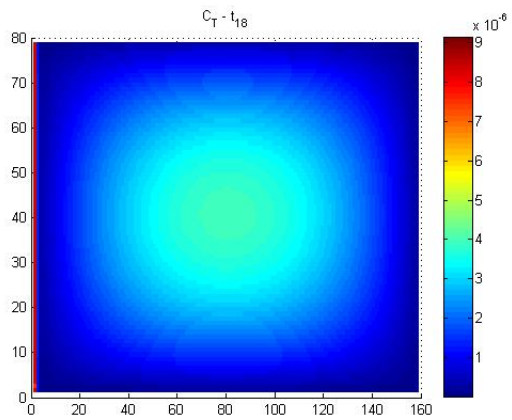

Figure 7.24: Reconstruction of $C_{\mathcal{T}} - t_{18}$

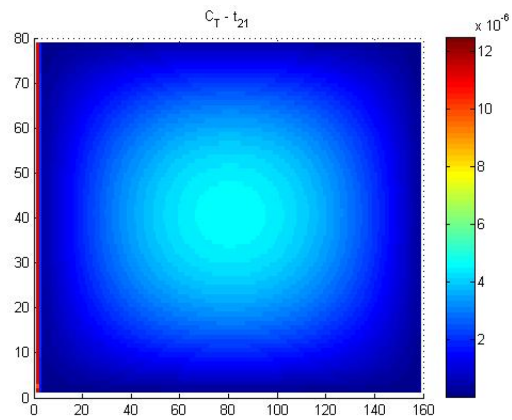

Figure 7.25: Reconstruction of $C_{\mathcal{T}} - t_{21}$

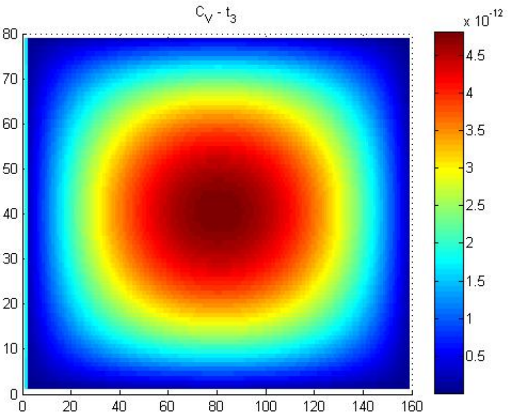

Figure 7.26: Reconstruction of $C_{\mathcal{V}} - t_3$

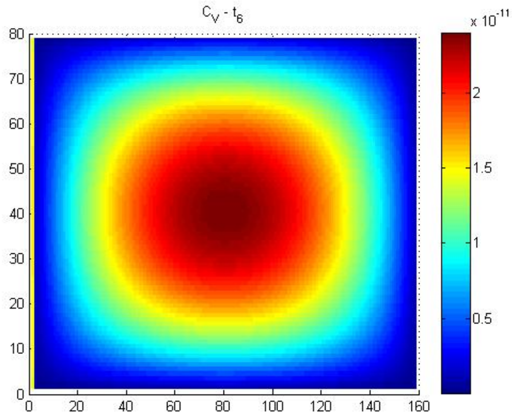

Figure 7.27: Reconstruction of $C_{\mathcal{V}} - t_6$

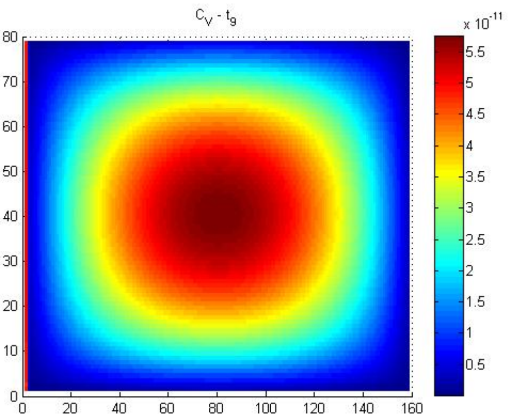

Figure 7.28: Reconstruction of $C_{\mathcal{V}} - t_9$

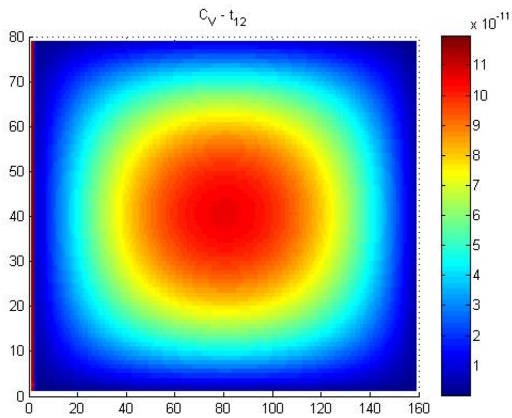

Figure 7.29: Reconstruction of $C_{\mathcal{V}} - t_{12}$

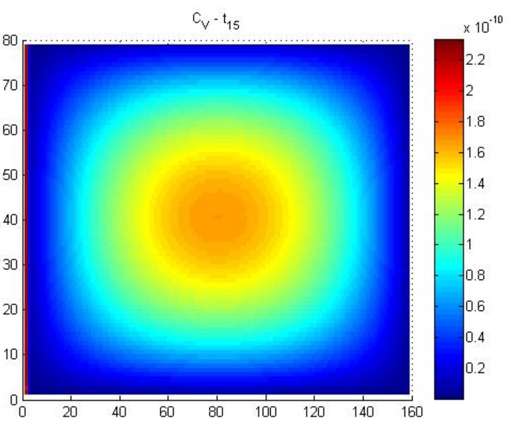

Figure 7.30: Reconstruction of $C_{\mathcal{V}} - t_{15}$

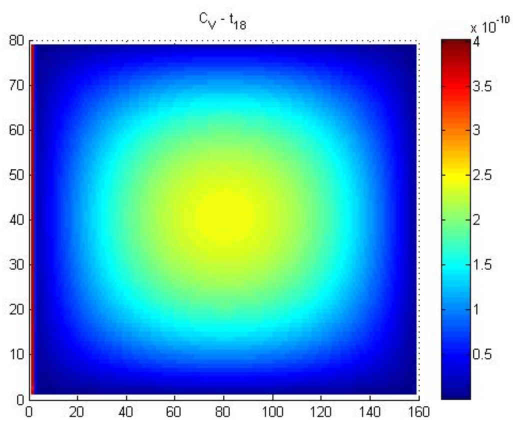

Figure 7.31: Reconstruction of $C_{\mathcal{V}} - t_{18}$

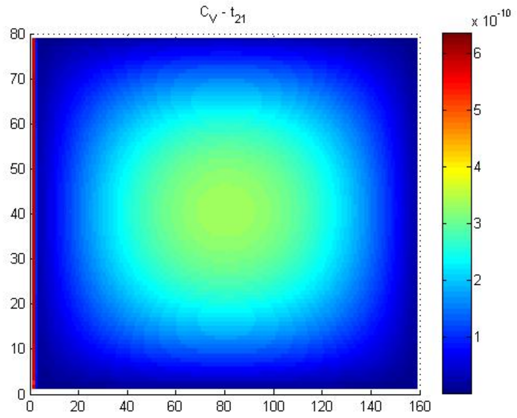

Figure 7.32: Reconstruction of $C_{\mathcal{V}} - t_{21}$

7.2 Parameter Identification on Exact Data - Error Analysis

For this section we performed a simple test using a matrix that represents the real PET-data (Figure 7.33) and generates an image 65 x 65 pixels. The objective of this test is purely evaluate the error scale in the reconstruction of physiological parameters involved. The used method to solve numerically we use the Forward-Backward splitting (*Section 6.4*). with $\tau = 10^{-4}$. The initial values and the respective regularization parameters are shown in Table 7.3. The reconstructed parameters are evaluated based on real parameters taken from **[69, 105]**.

Note that the margin of error is small, considering the fact that we are working with a ill-posed problem. The error is evaluated based on

$$\frac{||f - \tilde{f}||_{\infty}}{||f||_{\infty}}$$

where f denotes the exact parameter and $\tilde{f}$ denotes the parameter reconstruction, being $||\ \ ||_{\infty}$ the suprem-norm. Thus we obtain the following error values:

$$\frac{||k_1 - k_{1,rec}||_{L_\infty}}{||k_1||_{L_\infty}} = 0.013177662377619, \qquad \frac{||k_2 - k_{2,rec}||_{L_\infty}}{||k_2||_{L_\infty}} = 0.022069154633864$$

$$\frac{||k_3 - k_{3,rec}||_{L_\infty}}{||k_3||_{L_\infty}} = 0.017962700703776 \qquad \frac{||V_{x\mathcal{A}} - V_{x\mathcal{A},rec}||_{L_\infty}}{||V_{x\mathcal{A}}||_{L_\infty}} = 0.107200000000000$$

$$\frac{||V_{y\mathcal{A}} - V_{y\mathcal{A},rec}||_{L_\infty}}{||V_{y\mathcal{A}}||_{L_\infty}} = 0.042364570350000 \qquad \frac{||V_{x\mathcal{T}} - V_{x\mathcal{T},rec}||_{L_\infty}}{||V_{x\mathcal{T}}||_{L_\infty}} = 0.099845032204912$$

$$\frac{||V_{y\mathcal{T}} - V_{y\mathcal{T},rec}||_{L_\infty}}{||V_{y\mathcal{T}}||_{L_\infty}} = 0.10705351 \qquad \frac{||V_{x\mathcal{V}} - V_{x\mathcal{V},rec}||_{L_\infty}}{||V_{x\mathcal{V}}||_{L_\infty}} = 0.107253510$$

$$\frac{||V_{y\mathcal{V}} - V_{y\mathcal{V},rec}||_{L_\infty}}{||V_{y\mathcal{V}}||_{L_\infty}} = 0.042164507035 \qquad \frac{||D_{\mathcal{A}} - D_{\mathcal{A},rec}||_{L_\infty}}{||D_{\mathcal{A}}||_{L_\infty}} = 0.442795670666667$$

$$\frac{||D_{\mathcal{T}} - D_{\mathcal{T},rec}||_{L_\infty}}{||D_{\mathcal{T}}||_{L_\infty}} = 0.441155366666667 \qquad \frac{||D_{\mathcal{V}} - D_{\mathcal{V},rec}||_{L_\infty}}{||D_{\mathcal{V}}||_{L_\infty}} = 0.442829583333333$$

with $k_{1,rec}, k_{2,rec}, k_{3,rec}$, etc. denoting the computed reconstructions.

7.3 Parameter Identification for Real PET-System

We present now an example in order to analyze the reconstruction of the parameters for a specific case. Thus, we use an operator K (16512 x 4225) associated with the PET-real image given by the following figure:

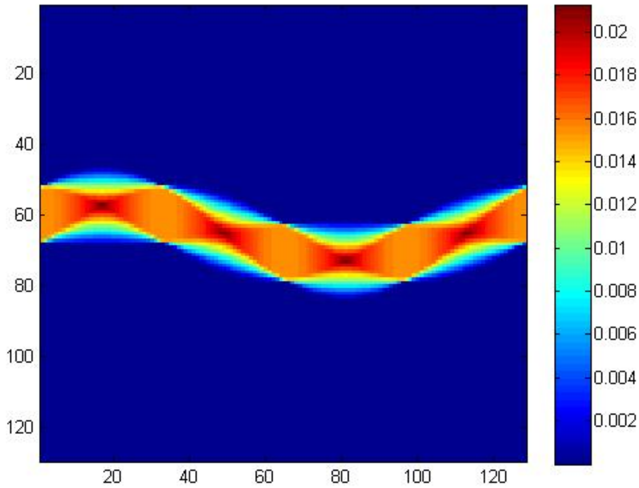

Figure 7.33: Synthetic image. Forward operator K from real PET scanner

By a given K we are able to produce an image that represents the behavior of real $H_2^{15}O$-PET-scan data. For this case we use an image 65 x 65 pixels, in domain Ω.

For the radioactive concentration $C_{\mathcal{A}}$ in the artery we use the initial function given by the equation (7.1) with $N = 50$ and the time step $\tau = 3 \cdot 10^{-5}$. The radioactive concentration in artery at the beginning can be visualized by the Figure 7.34.

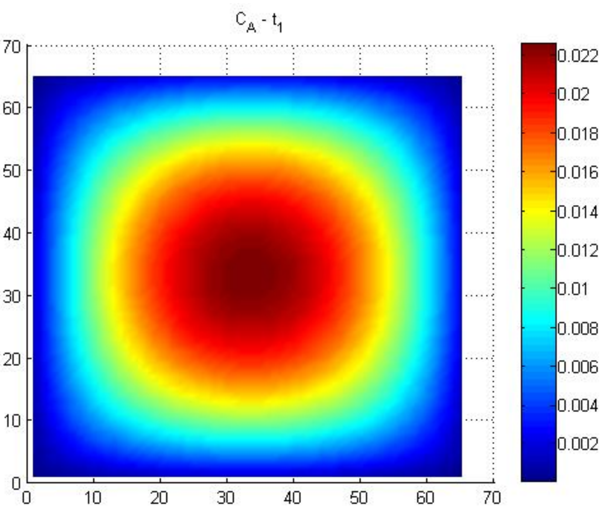

Figure 7.34: The radioactive concentration $C_{\mathcal{A}}$ in artery - t_1

As in the previous example, the radioactive concentration in the tissue and in vein at the beginning are zero and the used method to solve numerically we use the Forward-Backward splitting (*Section 6.4*). All the biological parameters involved are given by the following table.

Parameter	Initial Value	$(\cdot)^*$	A-p. Regularization (α)	Gradient regularization (ξ)
$k_1(*)(1/cm)$	0.9 (0)	0.89	0.017148965	0.0008
$k_2(*)(1/cm)$	0.75 (0)	0.7	0.015801553	0.0001
$k_3(1/cm)$	0.9	0.85	0.01648965	0.0001
$V_{x_\mathcal{A}}(cm/s)$	0.0001	0.1	0.001024495	0.0001
$V_{y_\mathcal{A}}(cm/s)$	700	15	1.1000	0.0001
$V_{x_\mathcal{T}}(cm/s)$	-50	-5	1.122098745999	0.0001
$V_{y_\mathcal{T}}(cm/s)$	0.0001	0.1	0.001024495	0.0001
$V_{x_\mathcal{V}}(cm/s)$	0.0001	0.1	0.001024495	0.0001
$V_{y_\mathcal{V}}(cm/s)$	700	15	1.1000000001	0.0001
$D_\mathcal{A}(cm^2/s)$	$3 * 10^{(-7)}$	$10^{(-3)}$	0.0003344	0.000444
$D_\mathcal{T}(cm^2/s)$	$3 * 10^{(-6)}$	$10^{(-2)}$	0.000344	0.000444
$D_\mathcal{V}(cm^2/s)$	$3 * 10^{(-7)}$	$10^{(-3)}$	0.0003344	0.000444

Table 7.3: Input data for a first real example

Here we also evaluate the behavior of radioactive flow when some interval of k_1 e k_2 is equal to zero and therefore, in the above table, the symbol $(*)$ refers to the fact that k_1 and k_2 are not considered constant across the region of interest. When $k_1 = k_2 = 0$ there is no exchange of materials from the artery to the tissue and from the tissue to the vein, and this means that the radioactive concentration (in this region) in the tissue and in the vein are zero.

The reconstruction of k_3 are always constant (therefore the figure is omitted) with value $0.80611044044 \pm 4 \cdot 10^{-9}/cm$. The following figures refer to the reconstruction of biological parameters for real PET-data:

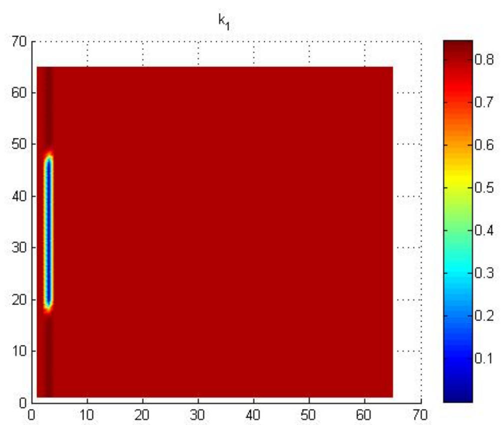

Figure 7.35: Reconstruction of k_1

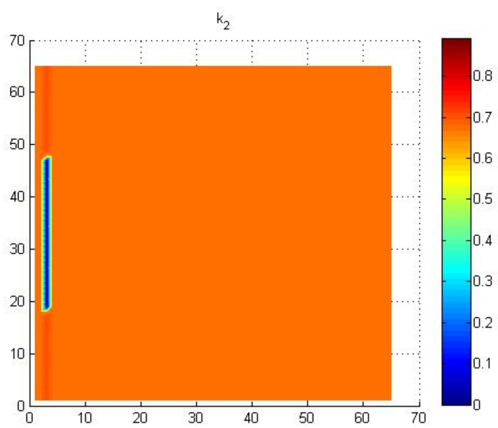

Figure 7.36: Reconstruction of k_2

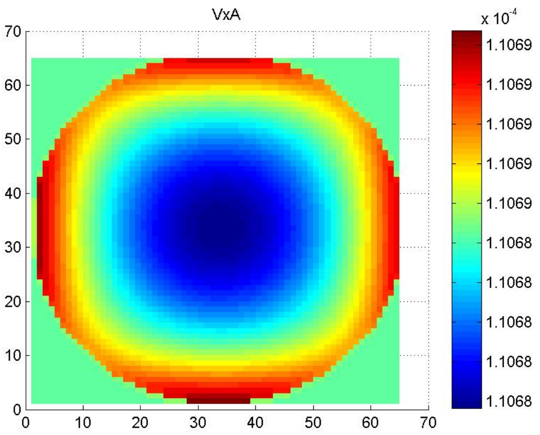

Figure 7.37: Reconstruction of $V_{x_{\mathcal{A}}}$

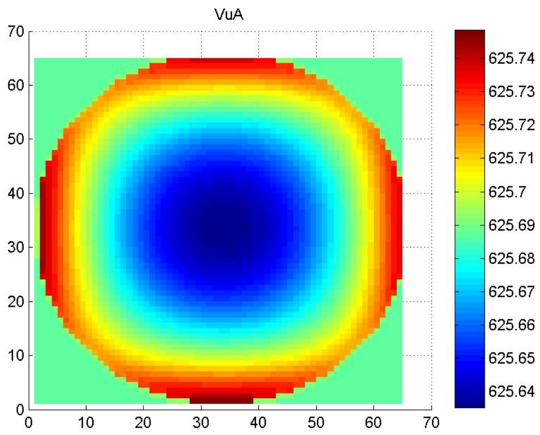

Figure 7.38: Reconstruction of $V_{y_{\mathcal{A}}}$

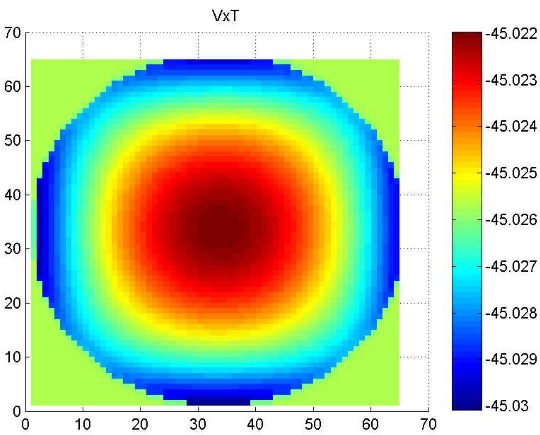

Figure 7.39: Reconstruction of $V_{x_{\mathcal{T}}}$

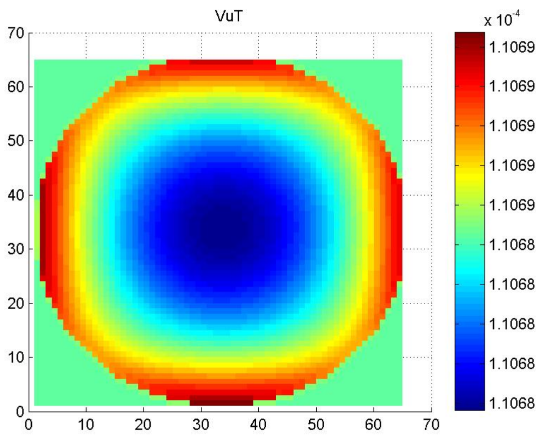

Figure 7.40: Reconstruction of $V_{y_{\mathcal{T}}}$

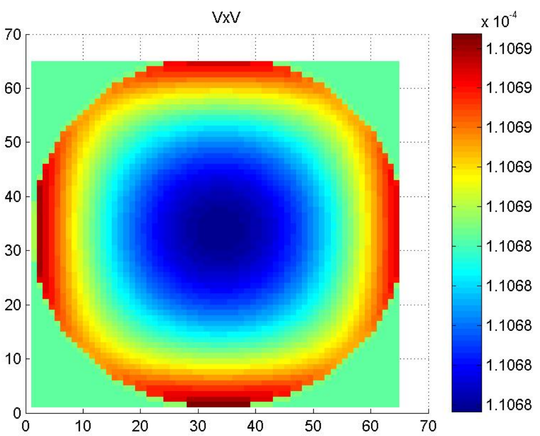

Figure 7.41: Reconstruction of $V_{x_{\mathcal{V}}}$

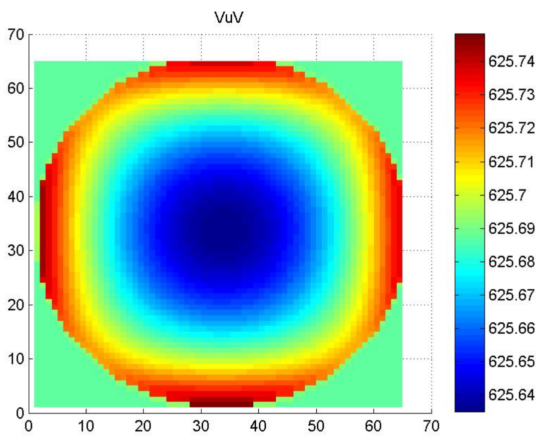

Figure 7.42: Reconstruction of $V_{y_{\mathcal{V}}}$

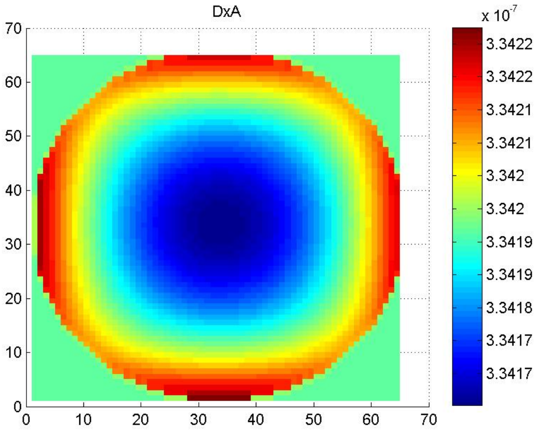

Figure 7.43: Reconstruction of $D_{x_{\mathcal{A}}}$

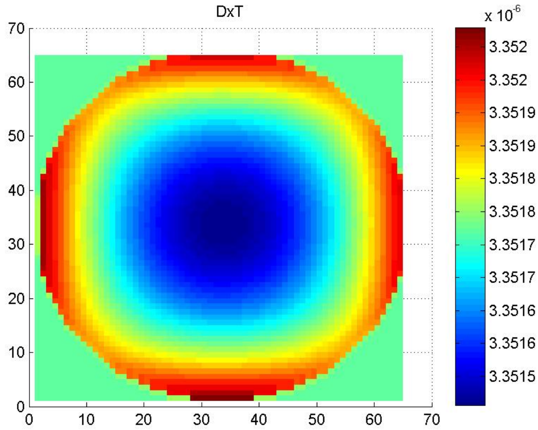

Figure 7.44: Reconstruction of $D_{x_{\mathcal{T}}}$

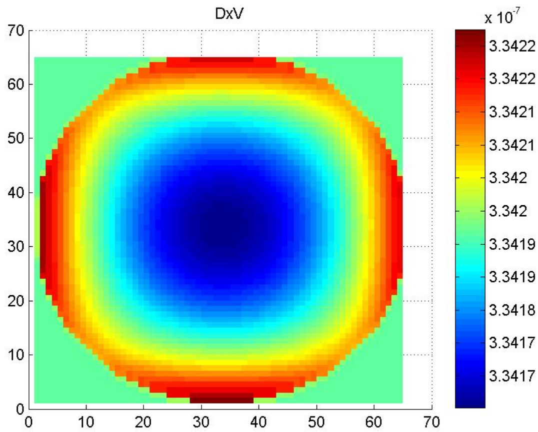

Figure 7.45: Reconstruction of $D_{x_{\mathcal{V}}}$

We want to introduce now, for the same example above, the reconstruction of some of these parameters (but with different regularization parameters) with u degraded by Poisson distributed noise in that f is calculated by $f = \gamma(Ku + n)$, for different values of γ:

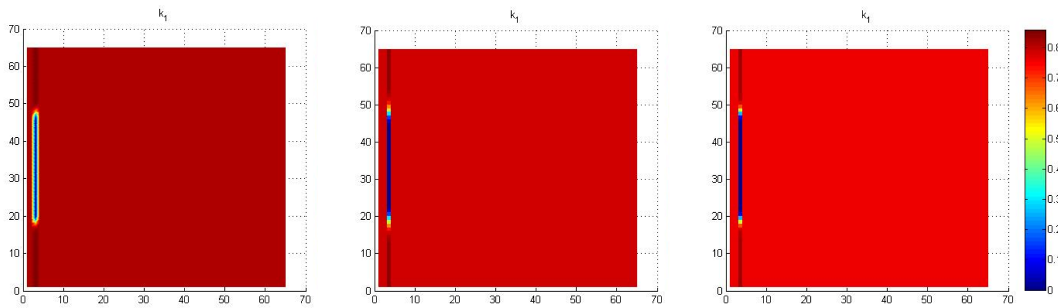

Figure 7.46: The figures above represent the reconstruction of k_1 for noise-free case (left) and k_1 degraded by Poisson noise with $\gamma = 5$ (middle) and $\gamma = 10$ (right), with n = 0.0055.

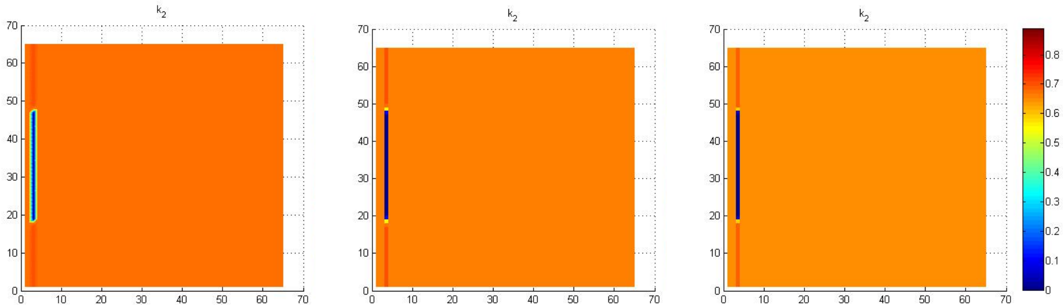

Figure 7.47: The figures above represent the reconstruction of k_2 for noise-free case (left) and k_2 degraded by Poisson noise with $\gamma = 5$ (middle) and $\gamma = 10$ (right), with n = 0.0055.

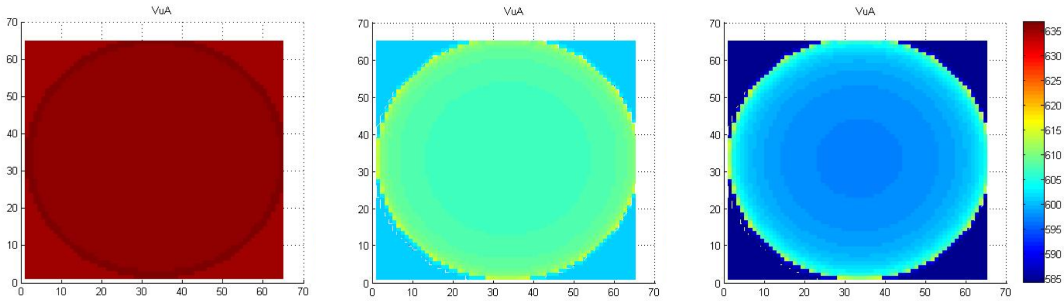

Figure 7.48: The figures above represent the reconstruction of $V_{y_{\mathcal{A}}}$ degraded by Poisson noise with $\gamma = 1$ (left), $\gamma = 5$ (middle) and $\gamma = 10$ (right), with n = 0.0055.

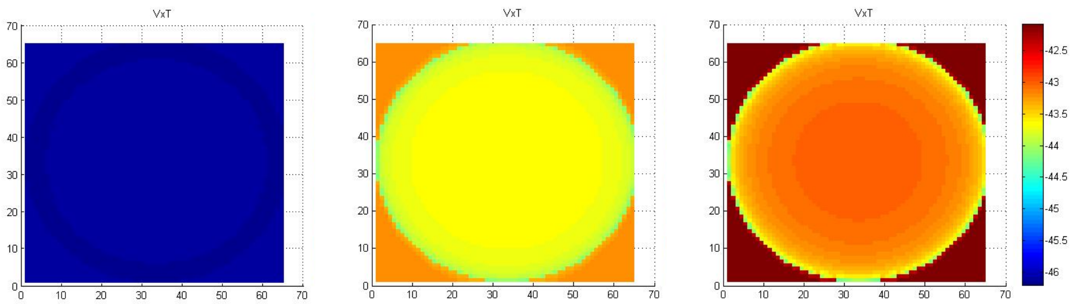

Figure 7.49: The figures above represent the reconstruction of $V_{x_{\mathcal{T}}}$ degraded by Poisson noise with $\gamma = 1$ (left), $\gamma = 5$ (middle) and $\gamma = 10$ (right), with n = 0.0055.

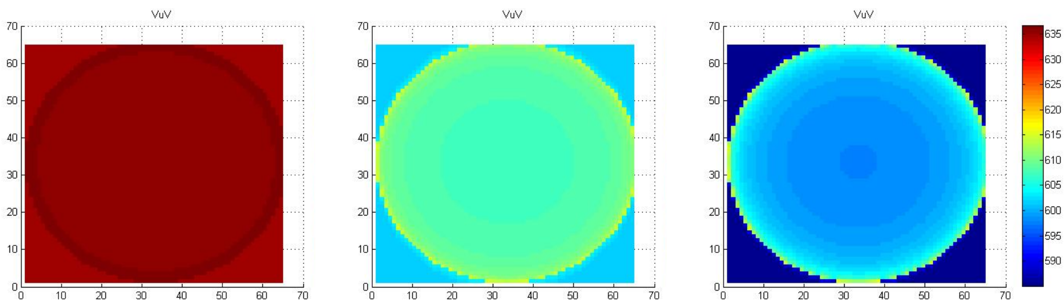

Figure 7.50: The figures above represent the reconstruction of $V_{y_{\mathcal{V}}}$ degraded by Poisson noise with $\gamma = 1$ (left), $\gamma = 5$ (middle) and $\gamma = 10$ (right), with n = 0.0055.

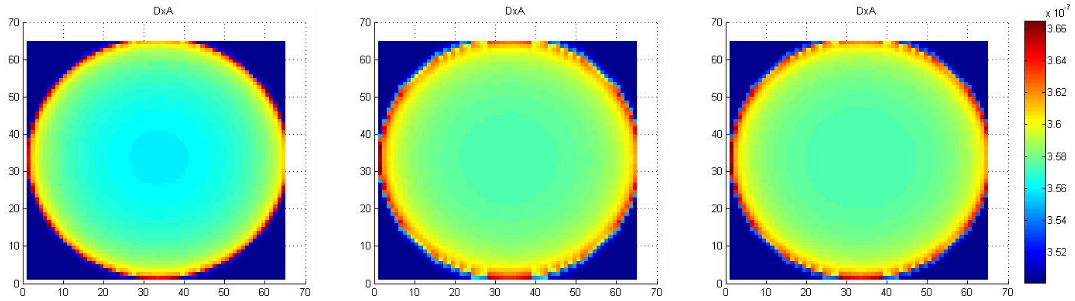

Figure 7.51: The figures above represent the reconstruction of $D_{\mathcal{A}}$ degraded by Poisson noise with $\gamma = 1$ (left), $\gamma = 5$ (middle) and $\gamma = 10$ (right), with n = 0.0055.

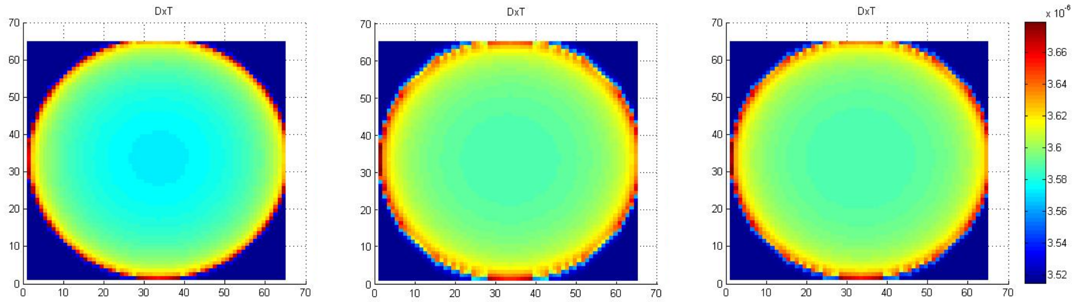

Figure 7.52: The figures above represent the reconstruction of $D_{\mathcal{T}}$ degraded by Poisson noise with $\gamma = 1$ (left), $\gamma = 5$ (middle) and $\gamma = 10$ (right), with n = 0.0055.

Finally, we present here the reconstructions that represent the radioactive concentrations in artery, tissue and vein for the example presented in beginning of this section, for different times:

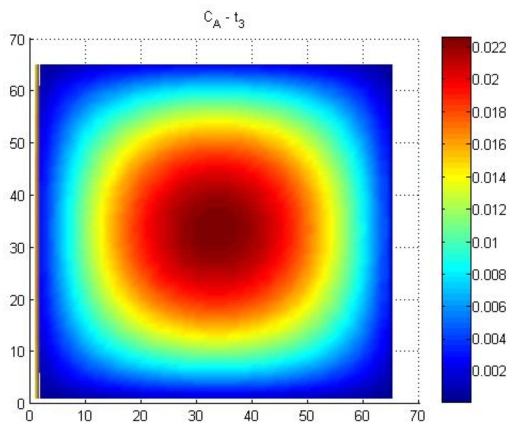

Figure 7.53: Reconstruction of $C_{\mathcal{A}} - t_3$

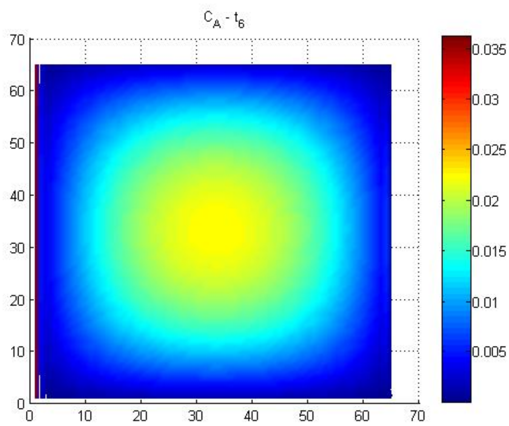

Figure 7.54: Reconstruction of $C_{\mathcal{A}} - t_6$

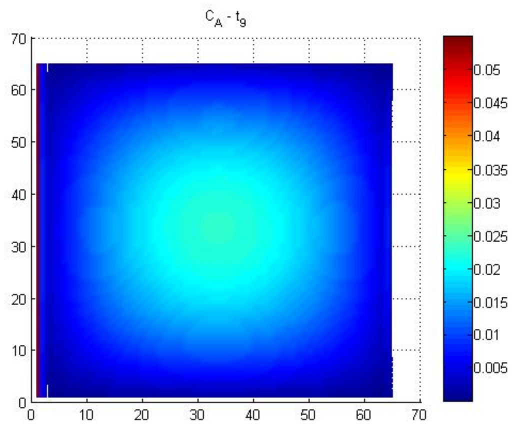

Figure 7.55: Reconstruction of $C_{\mathcal{A}} - t_9$

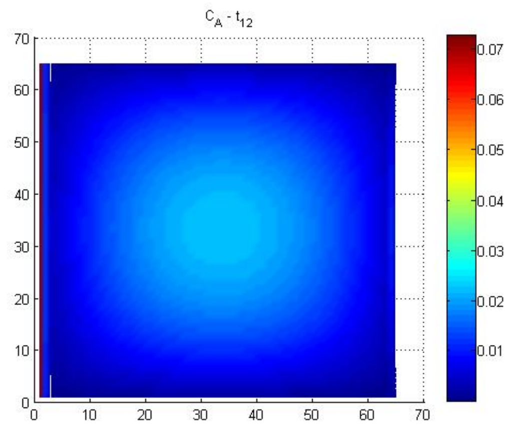

Figure 7.56: Reconstruction of $C_{\mathcal{A}} - t_{12}$

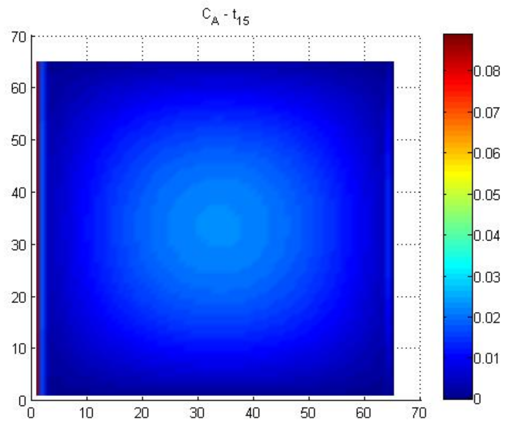

Figure 7.57: Reconstruction of $C_{\mathcal{A}} - t_{15}$

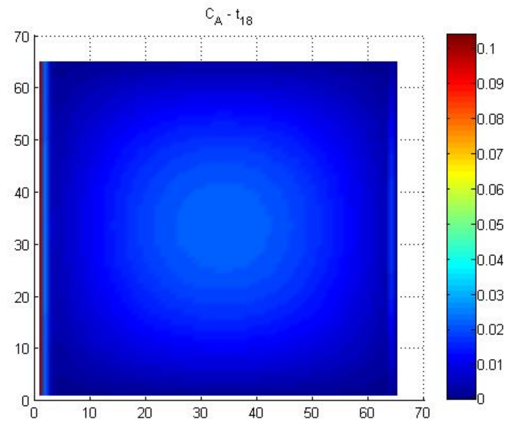

Figure 7.58: Reconstruction of $C_{\mathcal{A}} - t_{18}$

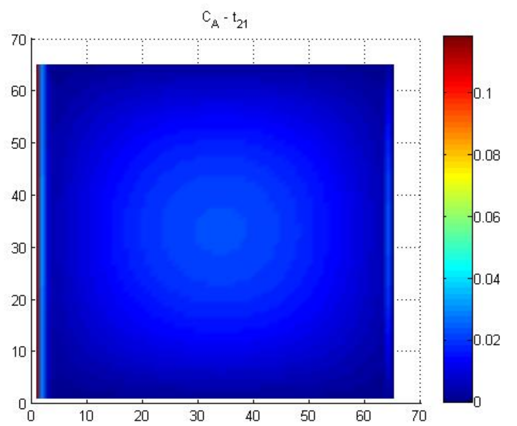

Figure 7.59: Reconstruction of $C_{\mathcal{A}} - t_{21}$

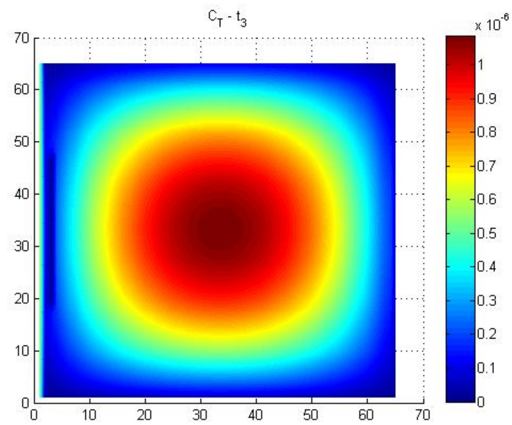

Figure 7.60: Reconstruction of $C_{\mathcal{T}} - t_3$

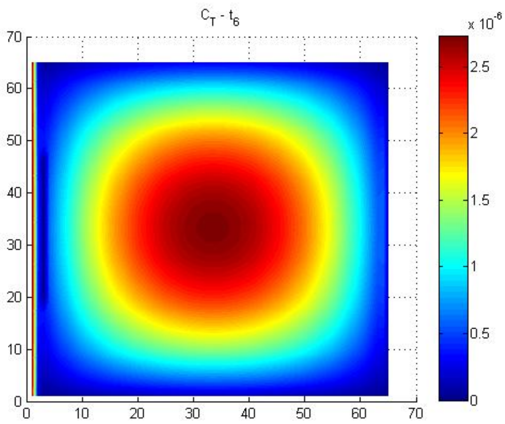

Figure 7.61: Reconstruction of $C_{\mathcal{T}} - t_6$

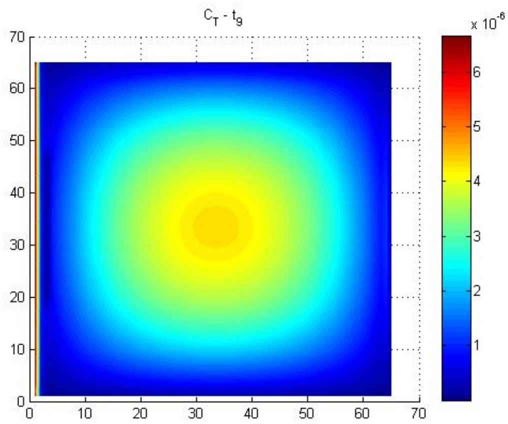

Figure 7.62: Reconstruction of $C_{\mathcal{T}} - t_9$

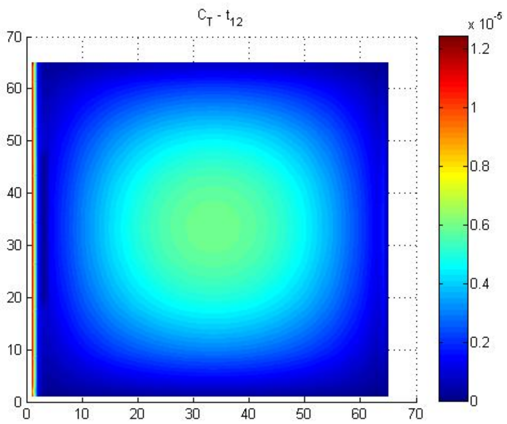

Figure 7.63: Reconstruction of $C_{\mathcal{T}} - t_{12}$

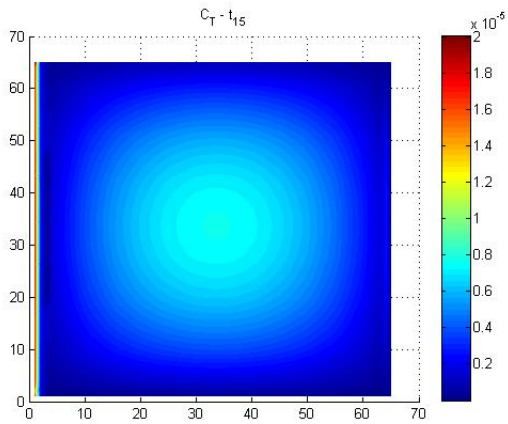

Figure 7.64: Reconstruction of $C_{\mathcal{T}} - t_{15}$

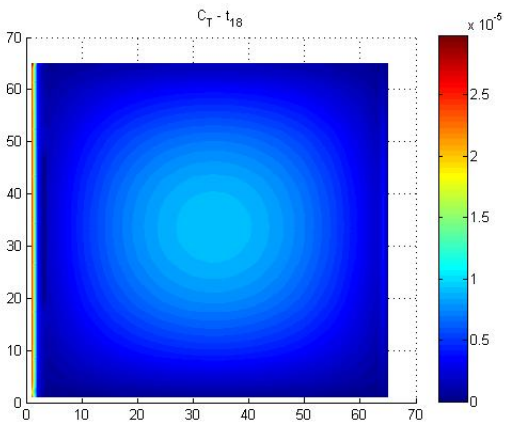

Figure 7.65: Reconstruction of $C_{\mathcal{T}} - t_{18}$

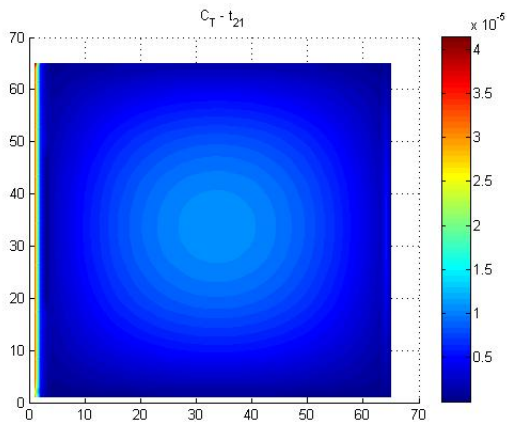

Figure 7.66: Reconstruction of $C_{\mathcal{T}} - t_{21}$

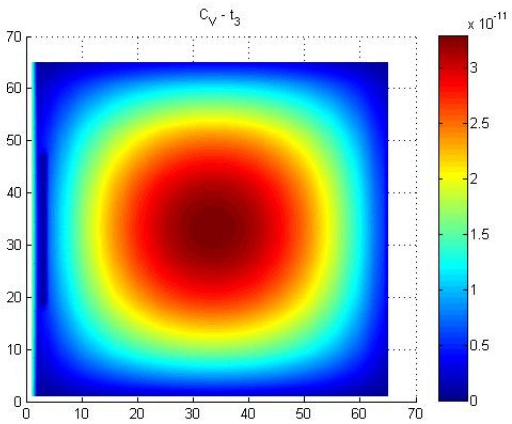

Figure 7.67: Reconstruction of $C_{\mathcal{V}} - t_3$

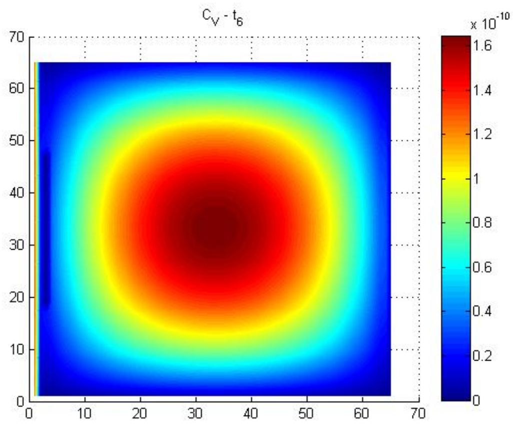

Figure 7.68: Reconstruction of $C_{\mathcal{V}} - t_6$

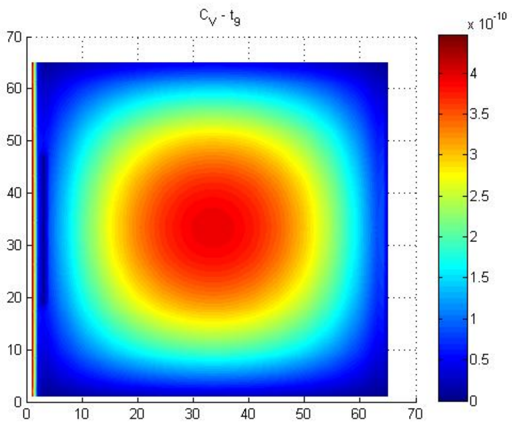

Figure 7.69: Reconstruction of $C_{\mathcal{V}} - t_9$

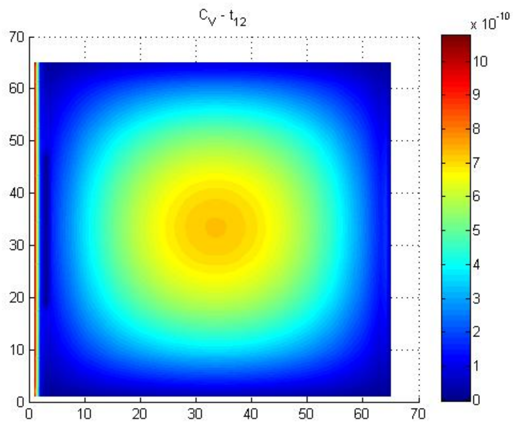

Figure 7.70: Reconstruction of $C_{\mathcal{V}} - t_{12}$

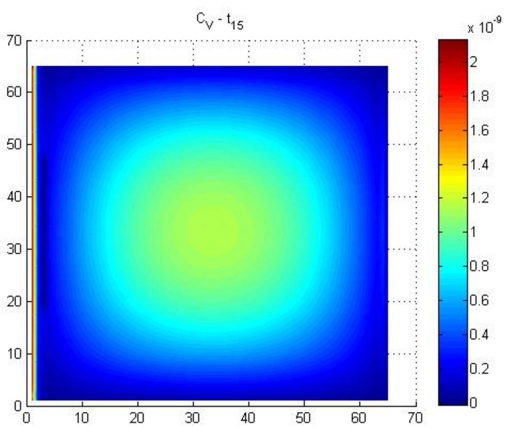

Figure 7.71: Reconstruction of $C_{\mathcal{V}} - t_{15}$

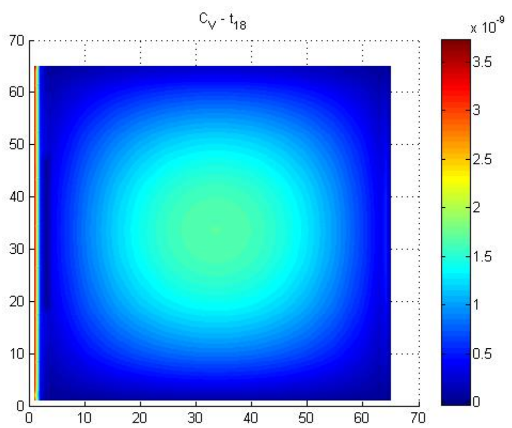

Figure 7.72: Reconstruction of $C_{\mathcal{V}} - t_{18}$

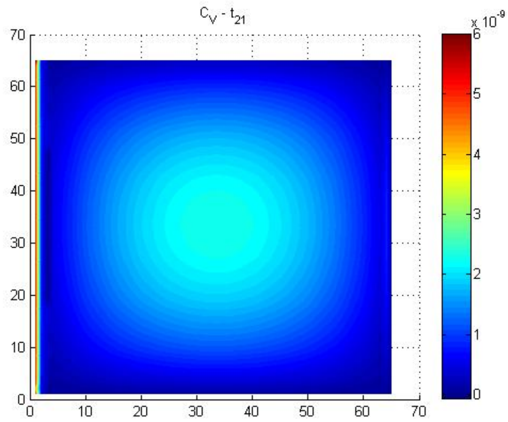

Figure 7.73: Reconstruction of $C_{\mathcal{V}} - t_{21}$

Thus we are able to produce the graphics for $u = C_{\mathcal{A}} + C_{\mathcal{T}} + C_{\mathcal{V}}$ as follows:

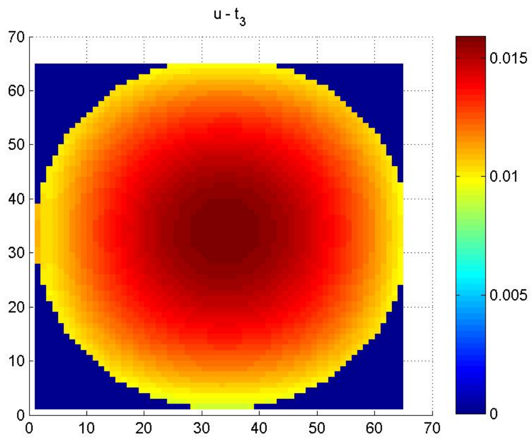

Figure 7.74: Reconstruction of $u - t_3$

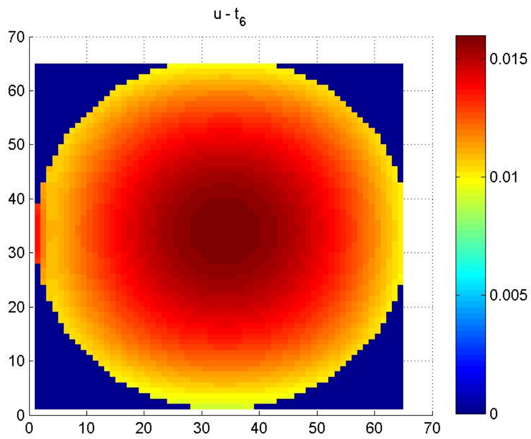

Figure 7.75: Reconstruction of $u - t_6$

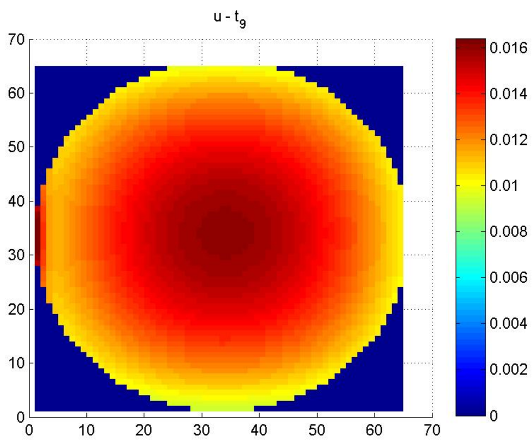

Figure 7.76: Reconstruction of $u - t_9$

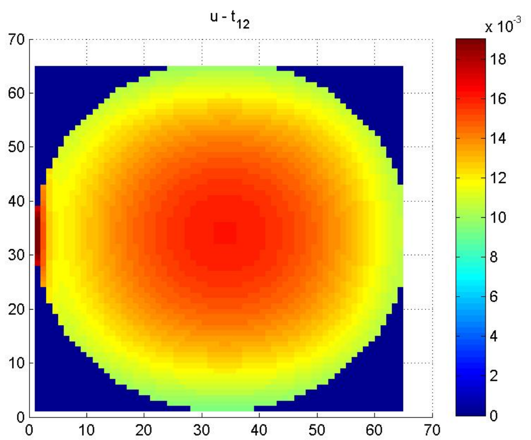

Figure 7.77: Reconstruction of $u - t_{12}$

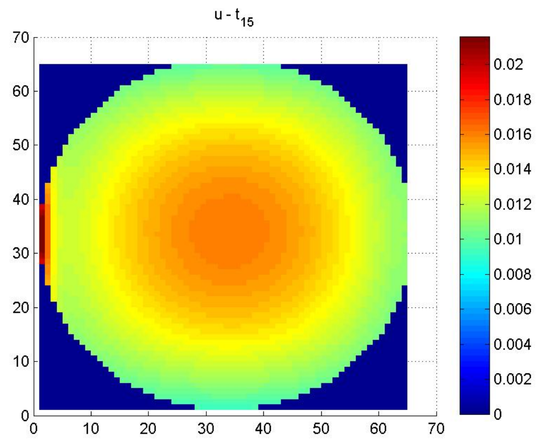

Figure 7.78: Reconstruction of $u - t_{15}$

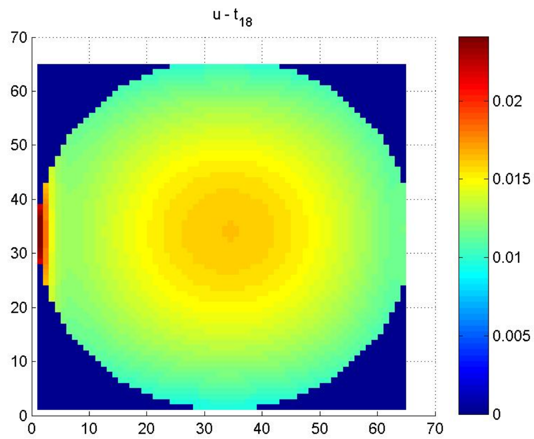

Figure 7.79: Reconstruction of $u - t_{18}$

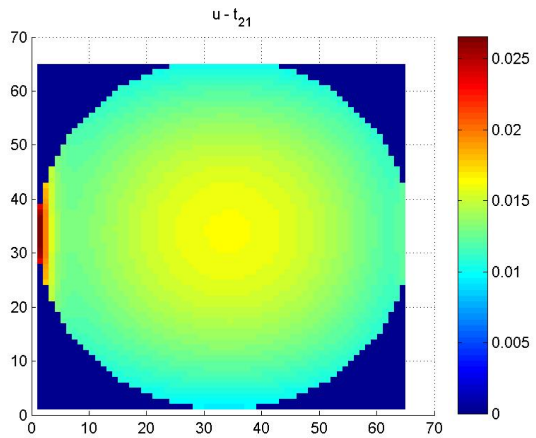

Figure 7.80: Reconstruction of $u - t_{21}$

Note that as the operator K has values equal to zero (outside the circle bounded by K), exactly in this region we can not reconstruct the image u, therefore u equals zero.

7.3.1 Second Example of Parameter Identification on Real PET-System

As a third and final example of this work, we will use again the operator K that represents the real PET-matrix presented above, but with the aim of analyzing a new case considering different input values for k_1, k_2 and k_3. The input values can be visualized in the Table 7.4.

For the radioactive concentration $C_{\mathcal{A}}$ in the artery we use the initial function given by the equation (7.1), with $N = 50$ and the time step $\tau = 3 \cdot 10^{-5}$ in domain Ω. The used method to solve numerically we use the Forward-Backward splitting (*Section 6.4*). The radioactive concentration in artery at the beginning can be visualized by the Figure 7.34. The reconstruction of k_3 are always constant (therefore the figure is omitted) with value $0.010686812999361 \pm 4 \cdot 10^{-8} 1/cm$.

Parameter	Initial Value	$(\cdot)^*$	A-p. Regularization (α)	Gradient regularization (ξ)
$k_1(*)(1/cm)$	0.9 (0)	0.89	0.017148965	0.0008
$k_2(*)(1/cm)$	0.75 (0)	0.7	0.016801553	0.0001
$k_3(1/cm)$	0.01	0.85	0.051822197678965	0.0001
$V_{x_\mathcal{A}}(cm/s)$	0.0001	0.1	0.001024495	0.0001
$V_{y_\mathcal{A}}(cm/s)$	700	15	1.1000	0.0001
$V_{x_\mathcal{T}}(cm/s)$	-50	-5	1.122098745999	0.0001
$V_{y_\mathcal{T}}(cm/s)$	0.0001	0.1	0.001024495	0.0001
$V_{x_\mathcal{V}}(cm/s)$	0.0001	0.1	0.001024495	0.0001
$V_{y_\mathcal{V}}(cm/s)$	700	15	1.1000000001	0.0001
$D_\mathcal{A}(cm^2/s)$	$3*10^{(-7)}$	$10^{(-3)}$	0.0003344	0.000444
$D_\mathcal{T}(cm^2/s)$	$3*10^{(-6)}$	$10^{(-2)}$	0.000344	0.000444
$D_\mathcal{V}(cm^2/s)$	$3*10^{(-7)}$	$10^{(-3)}$	0.0003344	0.000444

Table 7.4: Input data

The following figures refer to the reconstruction of biological parameters for real PET-data:

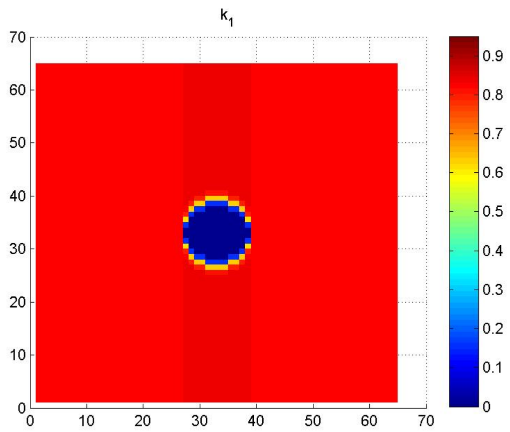

Figure 7.81: Reconstruction of k_1

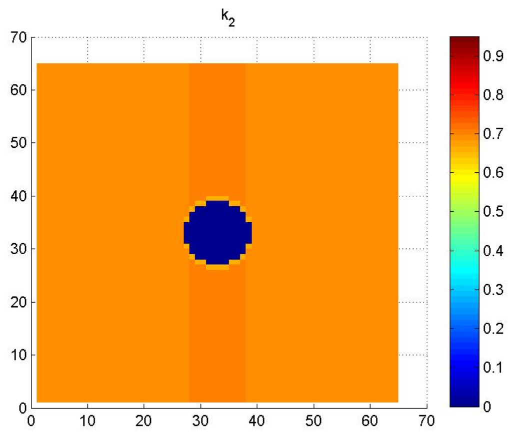

Figure 7.82: Reconstruction of k_2

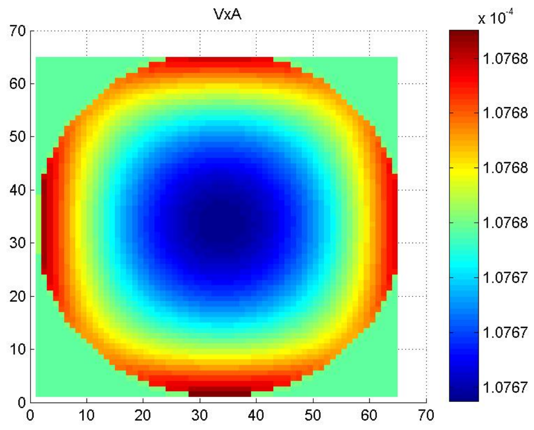

Figure 7.83: Reconstruction of $V_{x_\mathcal{A}}$

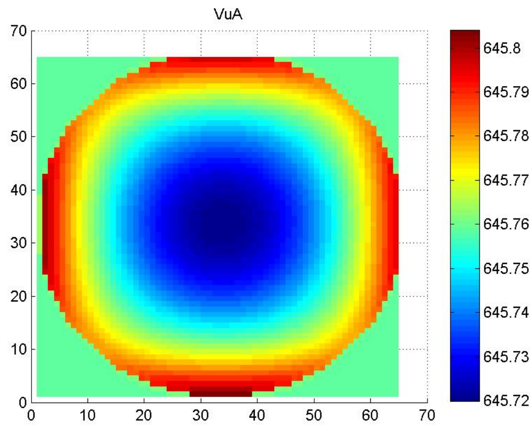

Figure 7.84: Reconstruction of $V_{y_\mathcal{A}}$

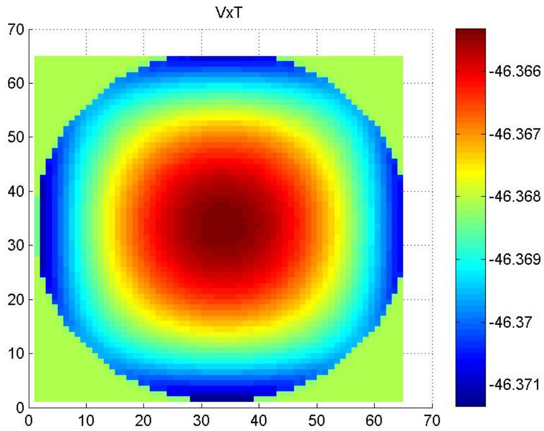

Figure 7.85: Reconstruction of $V_{x_{\mathcal{T}}}$

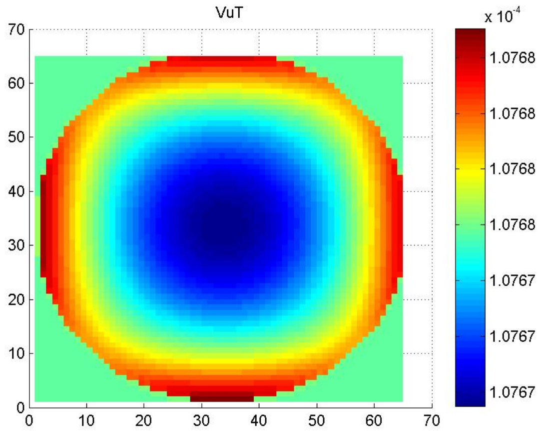

Figure 7.86: Reconstruction of $V_{y_{\mathcal{T}}}$

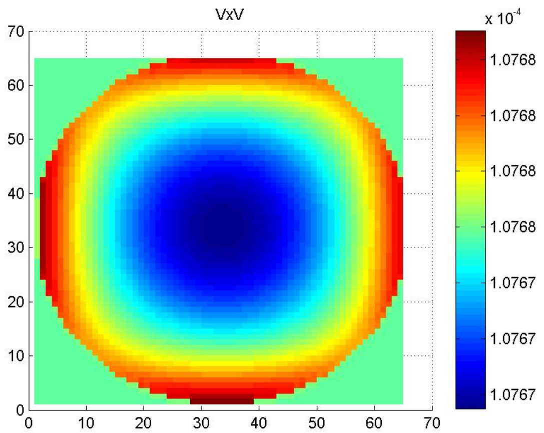

Figure 7.87: Reconstruction of $V_{x_{\mathcal{V}}}$

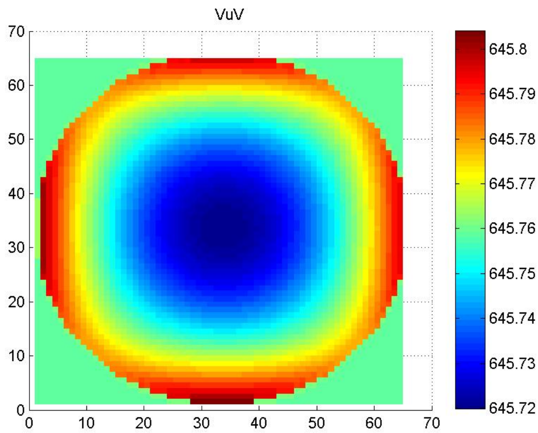

Figure 7.88: Reconstruction of $V_{y_{\mathcal{V}}}$

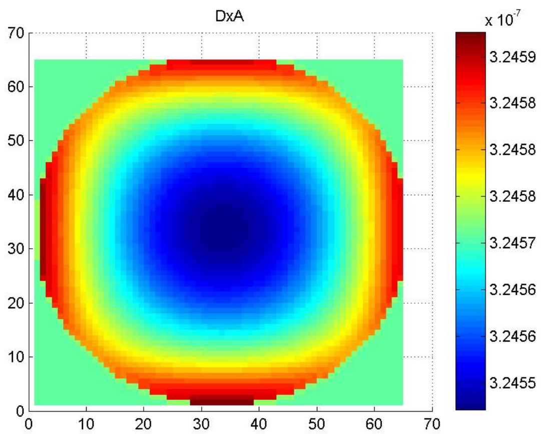

Figure 7.89: Reconstruction of $D_{x_{\mathcal{A}}}$

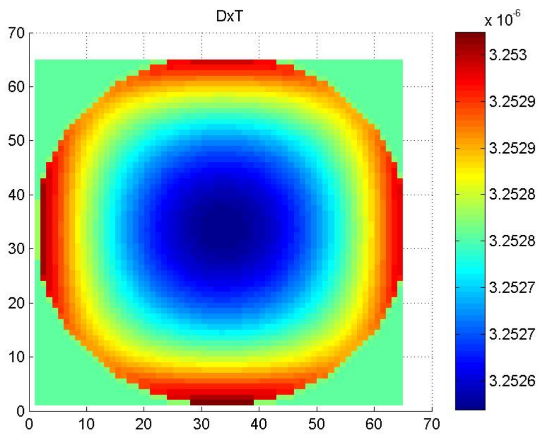

Figure 7.90: Reconstruction of $D_{x_{\mathcal{T}}}$

And the radioactive concentrations in tissue, vein and u:

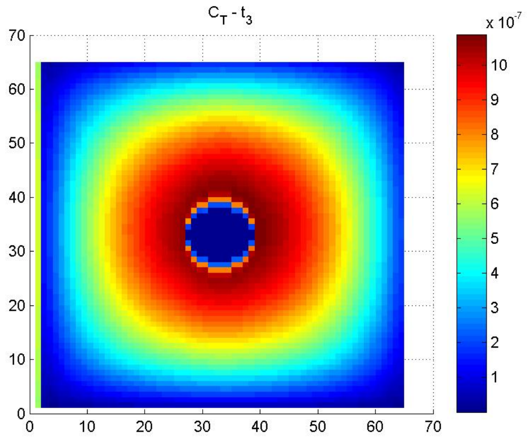

Figure 7.91: Reconstruction of $C_{\mathcal{T}} - t_3$

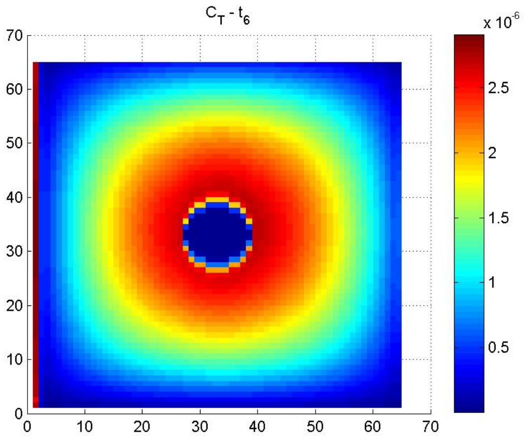

Figure 7.92: Reconstruction of $C_{\mathcal{T}} - t_6$

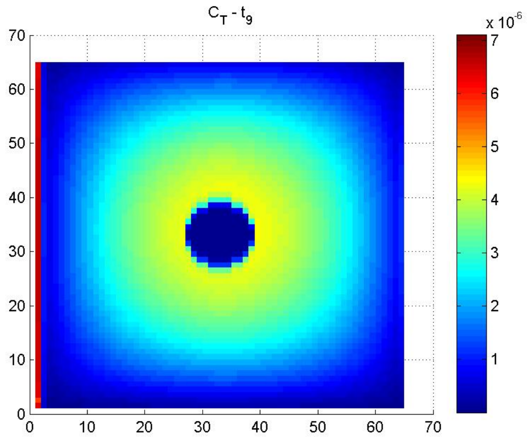

Figure 7.93: Reconstruction of $C_{\mathcal{T}} - t_9$

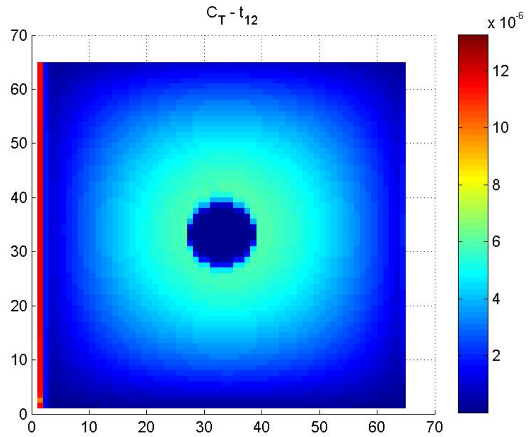

Figure 7.94: Reconstruction of $C_{\mathcal{T}} - t_{12}$

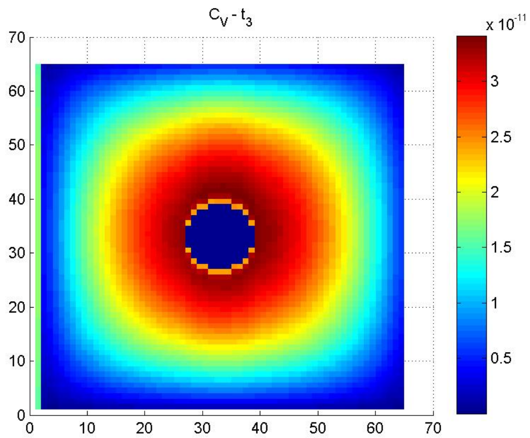

Figure 7.95: Reconstruction of $C_{\mathcal{V}} - t_3$

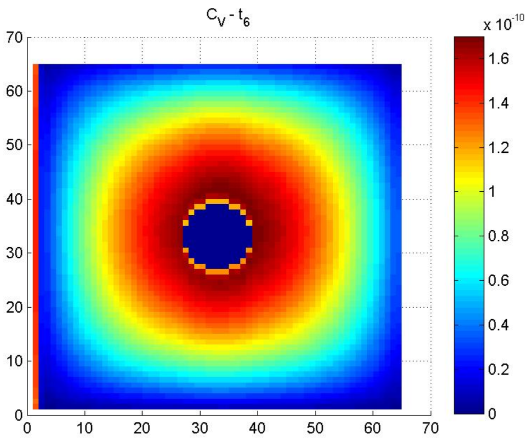

Figure 7.96: Reconstruction of $C_{\mathcal{V}} - t_6$

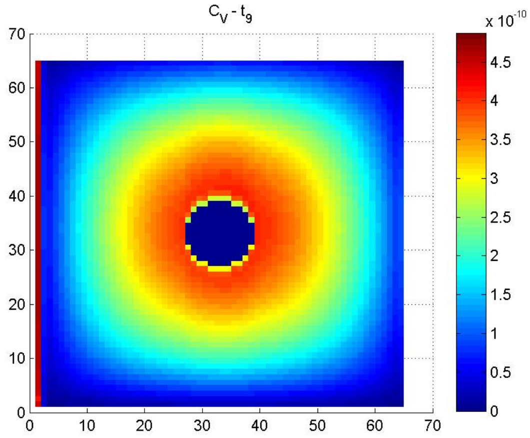

Figure 7.97: Reconstruction of $C_{\mathcal{V}} - t_9$

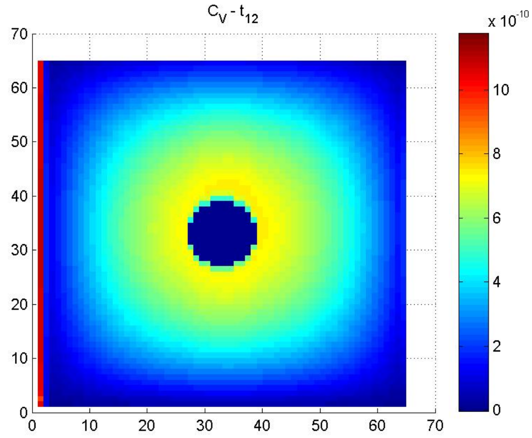

Figure 7.98: Reconstruction of $C_{\mathcal{V}} - t_{12}$

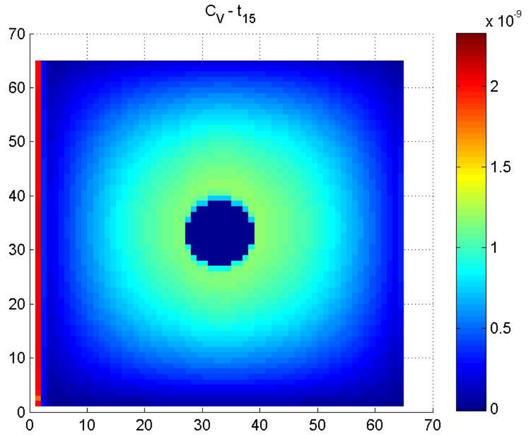

Figure 7.99: Reconstruction of $C_{\mathcal{V}} - t_{15}$

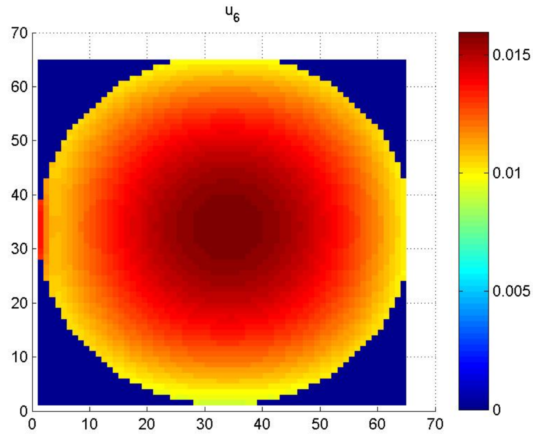

Figure 7.100: Reconstruction of $u - t_2$

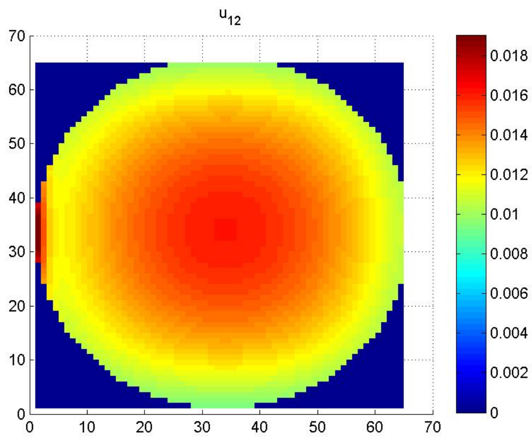

Figure 7.101: Reconstruction of $u - t_{12}$

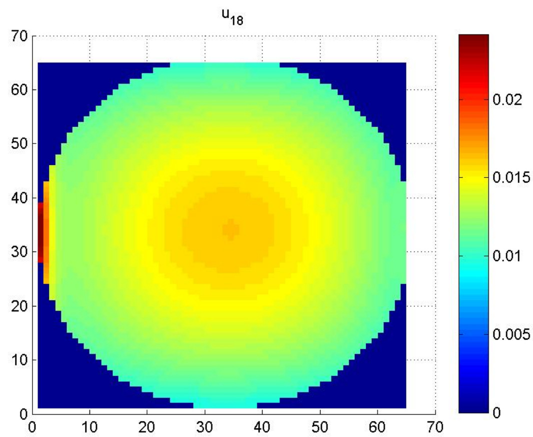

Figure 7.102: Reconstruction of $u - t_{18}$

As we can see, the fact that k_1 and k_2 are equal to zero exactly in the center is reflected in the graphics that represent the radioactive concentrations in tissue and vein, which remains zero in the same place.

Bibliography

[1] R. Acar and C. R. Vogel. Analysis of bounded variation penalty methods for ill-posed problems. *Inverse Problems*, 10:1217–1229, 1994.

[2] J. Y. Ahn, D. S. Lee, S. Kim, G. J. Cheon, J. S. Yeo, S. Shin, J. Chung, and M. C. Lee. Quantification of regional myocardial blood flow using dynamic $H_2^{15}O$ PET and factor analysis. *J. Nucl. Med*, 42(5):782–787, 2001.

[3] H. W. Alt. *Lineare Funktionalanalysis*, volume 35. Springer, Berlin, 1999.

[4] G. Aubert and P. Kornprobst. *Mathematical Problems in Image Processing: Partial Differential Equations and the Calculus of Variations.* Vol. 147 of Applied Mathematical Sciences. Springer-Verlag, New York, 2002.

[5] H. T. Banks and K. Kunisch. *Estimation Techniques for Distributed Parameter Systems.* BirkhÄauser, Boston, 1989.

[6] M. Benning. *A Nonlinear Variational Method for Improved Quantification of Myocardial Blood Flow Using Dynamic $H_2^{15}O$ PET.* Münster, Jun 2008.

[7] M. Benning. *Singular Regularization of Inverse Problems.* Münster, May 2011.

[8] M. Benning and M. Burger. Error estimates for general fidelities. *Electronic Transactions on Numerical Analysis*, 38:44–68, 2011.

[9] M. Benning, P. Heins, and M. Burger. A solver for dynamic pet reconstruction based on forward-backward splitting. *In AIP ICNAAM Conference Proceedings*, pages 1967–1970, 2010.

[10] M. Benning, T. Kösters, F. Wübbeling, K. Schäfers, and M. Burger. A nonlinear variational method for improved quantification of myocardial blood flow using dynamic $H_2^{15}O$ PET. *IEEE Nuclear Science Symposium Conference*, pages 4472–4477, 2008.

[11] S. R. Bergmann, K. A. Fox, and A. L. Rand. Quantification of regional myocardial blood flow in vivo with $H_2^{15}O$. *Circulation*, 70:724–733, 1984.

[12] M. Bertero and P. Boccacci. *Introduction to inverse problems in imaging.* Institute of Physics Publishing, Bristol, 1998.

[13] J. M. Borwein and A. S. Lewis. Convergence of best entropy estimates. *SIAM J. Optim.*, 1(2):191–205, 1991.

[14] J. M. Borwein and A. S. Lewis. *Convex Analysis and Nonlinear Optimization: Theory and Examples (CMS Books in Mathematics)*. Springer, 2nd edition, November 2005.

[15] C. Brune. *4D Imaging in Tomography and Optical Nanoscopy*. Münster, July 2010.

[16] C. Brune, A. Sawatzky, F. Wubbeling, T. Kosters, and M. Burger. Forward backward EM-TV methods for inverse problems with poisson noise. *unpublished*, pages 1–59, 2011.

[17] M. Burger. Parameter identification. *Lecture Notes*, 2005.

[18] M. Burger. Numerik partieller differentialgleichungen. *Lecture Notes*, 2006/2007.

[19] M. Burger. Inverse problems. *Lecture Notes*, 2007/2008.

[20] M. Burger and C. Brune. Variationsmethoden in der biomedizinischen bildgebung. *Lecture Notes. 51*, 2010.

[21] M. Burger, E. Resmerita, and L. He. Error estimation for bregman iterations and inverse scale space methods in image restoration. *Computing*, 81:109–135, 2007.

[22] I. Buvat. Quantification in emission tomography: Challenges, solutions, and performance. *Nuclear Instruments and Methods in Physics Research*, 571:10–13, 2007.

[23] G. Carrero, D. McDonald, E. Crawford, G. Vries, and M. J. Hendzel. Using FRAP and mathematical modeling to determine the in vivo kinetics of nuclear proteins. *Academic Press*, 29:14–28, 2003.

[24] R. E. Carson. *Tracer Kinetic Modeling in PET. In: D. Bailey et al., Positron Emission Tomography - Basic Sciences*. Springer, London, 2005.

[25] R. E. Carson and K. Lange. A statistical model for positron emission tomography. *Journal of the American Statistical Association*, 80(389):20–22, 1985.

[26] M. Castelani, A. Colombo, R. Giordano, E. Pusineri, C. Canzi, V. Longari, E. Piccaluga, S. Palatresi, L. Dellavedova, D. Soligo, P. Rebulla, and P. Gerundini. The role of PET with ^{13}N-ammonia and ^{18}F-FDG in the assessment of myocardial perfusion and metabolism in patients with recent AMI and intracoronary stem cell injection. *The Journal of Nuclear Medicine*, 51(12):1908–1916, 2010.

[27] J. M. Chadam and H.-M. Yin. Determination of an unknown function in a parabolic equation with an overspecified condition. *Mathematical Methods in the Applied Sciences*, 13:421–430, 1990.

[28] G. H-G. Chen and R. T. Rockafellar. Convergence rates in forward-backward splitting. *SIAM J. Optimization*, 7(2):1–25, 1997.

[29] E. Clarkson and M. A. Kupinski. Global comportmental pharmacokinetic models for spatiotemporal SPECT and PET imaging. *SIAM J. Imaging Sciences*, 2(1):203–225, 2009.

[30] D. Colton, R. Ewing, and W. Rundell. *Inverse Problems in Partial Differential Equations*. SIAM, Philadelphia, 1992.

[31] K. Daniel. *Agenten-basierte Modelle und Fokker-Planck-Gleichungen für Finanzmärkte.* Münster, Aug 2008.

[32] R. Dautray, J.-L. Lions, and M. Artola. *Mathematical Analysis and Numerical Methods for Science and Technology: Volume 5: Evolution Problems I.* Springer-Verlag, Berlin Heidelberg New York, 2000. 739.

[33] H. F. de Campos Velho. Inverse problems: Basic concepts and applications (invited short course). *Bulletim of the Brazilian Society for Computing and Applied Mathematics, Série III (special issue: Proceedings of the IV Meeting on Computational Modeling),IPRJ-UERJ, Nova Friburgo (RJ), Brazil*, 2002.

[34] A. P. Dempster, N. M. Laird, and D. B. Rubin. Maximum likelihood from incomplete data via the EM algorithm. *Journal of the Royal Statistical Society*, 39:1–38, 1977.

[35] P. P. B. Eggermont. Maximum entropy regularization for fredholm integral equations of the first kind. *SIAM Journal on Mathematical Analysis*, 24:1557–1576, 1993.

[36] I. Ekeland and R. Temam. *Convex analysis and variational problems.* Corrected Reprint Edition. SIAM, 1999.

[37] H. W. Engl, M. Hanke, and A. Neubauer. *Regularization of Inverse Problems.* Kluwer Academic Publishers, paperback edition 2000 edition, Netherlands, 1996.

[38] H. W. Engl and W. Rundell. *Inverse Problems in Diffusion Processes.* SIAM, Philadelphia, 1994.

[39] L. Eriksson, C. Bohm, M. Kesselberg, G. Blomqvist, J. Litton, L. Widen, M. Bergstrom, K. Ericson, and T. Greitz. A four ring positron camera system for emission tomography of the brain. *IEEE Trans. Nucl. Sci*, 29:539–543, 1982.

[40] L. C. Evans. *Partial Differential Equations: Second Edition (Graduate Studies in Mathematics).* Providence, RI, American Math. Soc., 2. ed., 2010.

[41] M. Fiechtera, C. Gebharda, J. R. Ghadria, T. A. Fuchsa, A. P. Pazhenkottila, R. N. Nkouloua, B. A. Herzoga, U. Altorfera, O. Gaemperlia, and P. A. Kaufmann. Myocardial perfusion imaging with ^{13}N-ammonia PET is a strong predictor for outcome. *International Journal of Cardiology*, pages 1–4, 2012.

[42] O. Forster. *Analysis III: Integralrechnung im $\mathbb{R}^n$ mit Anwendungen.* Vieweg, 1981.

[43] S. S. Gambhir, C. L. Keppenne, P. K. Banerjee, and M. E. Phelps. A new method to estimate parameters of linear compartmental models using artificial neural networks. *Phys Med Biol*, 43:1659–1678, 1998.

[44] S. M. Gorelick, G. Liu, and C. Zheng. Quantifying mass tranfer in permeable media containing conductive dendritic networks. *Geophysical Research Letters*, 32:1–4, 2005.

[45] A. Griesbaum, B. Kaltenbacher, and B. Vexler. Efficient computation of the tikhonov regularization parameter by goal-oriented adaptive discretization. *Inverse Problems*, 24:1–20, 2008.

[46] C. W. Groetsch. *Inverse problems in the mathematical sciences.* Vieweg Mathematics for Scientists and Engineers. Friedr. Vieweg and Sohn, Braunschweig, 1993.

[47] G. T. Gullberg, B. W. Reutter, A. Sitek, J. S. Maltz, and T. F. Budinger. Dynamic single photon emission computed tomographybasic principles and cardiac applications. *Physics in Medicine and Biology*, 55(20):R111, 2010.

[48] J. Hadamard. Sur les problèmes aux dérivés partielles et leur signification physique. *Princeton University Bulletin*, 13:49–52, 1902.

[49] J. Hadamard. *Lectures on Cauchy's problem in linear partial differential equations.* Dover Publications, New York, 1953.

[50] W. Han, W. Cong, and G. Wang. Mathematical theory and numerical analysis of bioluminescence tomography. *Inverse Problems*, 22:1659–1675, 2006.

[51] M. Hinze, R. Pinnau, M. Ulbrich, and S. Ulbrich. *Optimization with PDE Constraints. Mathematical Modelling: Theory and Applications*, volume 23. Springer, Netherlands, 2010.

[52] J.-B. Hiriart-Urruty and C. Lemaréchal. *Convex Analysis and Minimization Algorithms I, vol. 305 of Grundlehren der mathematischen Wissenschaften (Fundamental Principles of Mathematical Sciences).* Springer Verlag, Berlin, 1993.

[53] H. Iida, I. Kanno, A. Takahashi, S. Miura, M. Murakami, K. Takahashi, Y. Ono, F. Shishido, A. Inugami, and N. Tomura. Measurement of absolute myocardial blood flow with $H_2^{15}O$ and dynamic positron-emission tomography: strategie for quantification in relation to the partial-volume effect. *Circulation*, 78(1):104–115, 1988.

[54] V. Isakov. *Inverse Source Problems.* AMS, Providence, 1990.

[55] V. Isakov. *Inverse Problems in Partial Differential Equations.* Springer, New York, 1998.

[56] A. N. Iusem. Convergence analysis for a multiplicatively relaxed em algorithm. *Mathematical Methods in the Applied Sciences*, 14:573–593, 1991.

[57] B. Kaltenbacher. A projection-regularized newton method for non-linear ill-posed problems and its application to parameter identification problems with finite element discretization. *SIAM J.Numer.Anal*, 37(6):1885–1908, 2000.

[58] B. Kaltenbacher. Parameter identification in partial differential equations. *Lecture Notes*, 2005/2006.

[59] B. Kaltenbacher, A. Neubauer, and O. Scherzer. *Iterative Regularization Methods for Nonlinear Ill-posed Problems.* De Gruyter, Berlin, New York, 2008.

[60] M. E. Kamasak, C. A. Boumann, E. D. Morris, and K. Sauer. Direct reconstruction of kinetic parameter images from dynamic PET data. *IEEE Transactions on Medical Imaging*, 24:636–650, 2005.

[61] H. Kasumba, S. L. Keeling, and M. Müller. Decay estimate addendum to: Revision of the theory of tracer transport and the convolution model of DCE-MRI. *SFB-Report*, 22:1–9, 2010.

[62] C. Katoh, K. Morita, T. Shiga, N. Kubo, K. Nakada, and N. Tamaki. Improvement of algorithm for quantification of regional blood flow using ^{15}O-water with PET. *J. Nucl. Med.*, 45(11):1908–1916, 2004.

[63] S. L. Keeling, R. Bammer, and R. Stollberger. Revision of the theory of tracer transport and the convolution model of dynamic contrast enhanced magnetic resonance imaging. *Journal of Mathematical Biology*, 55(3):389–411, 2007.

[64] A. Kirsch. *An introduction to the mathematical theory of inverse problems.* Springer-Verlag, New York, 1996.

[65] S. Kitamura and S. Nakagiri. Identifiability of spatially-varying and constant parameters in distributed systems of parabolic type. *SIAM J. Control and Optimization*, 15(5):785–802, 1977.

[66] J. Krivokapich, G. T. Smith, S. C. Huang, E. J. Hoffman, O. Ratib, M. E. Phelps, and H. R. Schelbert. 13N-ammonia myocardial imaging at rest with exercise in normal volunteers. quantification of absolute myocardial perfusion with dynamic positron emission tomography. *Circulation*, 80:1328–1337, 1989.

[67] W. G. Kuhle, G. Porenta, S. C. Huang, D. Buxton, S. S. Gambhir, H. Hansen, M. E. Phelps, and H. R. Schelbert. Quantification of regional myocardial blood flow using 13N ammonia and reoriented dynamic positron emission tomographic imaging. *Circulation*, 86:1004–1017, 1992.

[68] L. Lüdermann, G. Sreenivasa, R. Michel, C. Rosner, M. Plotkin, R. Felix, P. Wust, and H. Amthauer. Corrections of arterial input function for dynamic $H_2^{15}O$ PET to assess perfusion of pelvic tumours: arterial blood sampling versus image extraction. *Phys. Med. Biol.*, 51:2883–2900, 2006.

[69] J. R. Levick. *An introduction to cardiovascular physiology.* Hodder Arnold, London, 2010.

[70] J. Libertini. Determining tumor blood flow parameters from dynamic images measurements. *Journal of Physics: Conference Series*, 135:1–7, 2008.

[71] G. Lindblad. Entropy, information and quantum measurements. *Communications in Mathematical Physics*, 33:305–322, 1973.

[72] L. Ljung. *System Identification: Theory for the user.* PTR Prentice Hall, Upper Saddle River, 2nd edition, 1999.

[73] D. A. Lorenz. Convergence rates and source conditions for tikhonov regularization with sparsity constraints. *J. Inverse Ill-Posed Problems*, 16:463–478, 2008.

[74] A. K. Louis. *Inverse problems in medicine.* Teubner, Stuttgart, 1989.

[75] B. A. Mair, D. R. Gilland, and J. Sun. Estimation of images and nonrigid deformations in gated emission ct. *IEEE Transactions on Medical Imaging*, 25(9):1130–1144, 2006.

[76] E. Meyer. Simultaneos correction for tracer arrival delay and dispersion in CFB measurements by the $H_2^{15}O$ autoradiographic method and dynamic PET. *J. Nucl. Med*, 30(6):1069–1078, 1989.

[77] M. Mintun, M. Raichle, M. Kilbourn, G. Wooten, and M. Welch. A quantitative model for the in vivo assessment of drug binding sites with positron emission tomography. *Ann Neurol*, 15:217–227, 1984.

[78] M. Mintun, M. Raichle, W. Martin, and P. Herscovitch. Brain oxygen utilization measured with $O - 15$ radiotracers and positron emission tomography. *J Nucl Med*, 25:177–187, 1984.

[79] J. Modersitzki. *Numerical Methods for Image Registration (Numerical Mathematics and Scientific Computation).* Oxford University Press, Oxford, 2004.

[80] O. Muzik, R. S. Beanlands, G. D. Hutchins, T. J. Magner, N. Nguyen, and M. Schwaiger. Validation of nitrogen-13-ammonia tracer kinetic model for quantification of myocardial blood flow using PET. *J. Nucl. Med*, 34:83–91, 1993.

[81] F. Natterer. *The mathematics of computerized tomography.* SIAM Monographs on Mathematical Modeling and Computation, Philadelphia, 2001.

[82] F. Natterer and F. Wubbeling. *Mathematical Methods in Image Reconstruction.* SIAM Monographs on Mathematical Modeling and Computation, Philadelphia, 2001.

[83] A. Neubauer. On converse and saturation results for tikhonov regularization of linear ill-posed problems. *SIAM J. Numer. Anal*, 34:517–527, 1997.

[84] M. E. Phelps, E. J. Hoffman, S. C. Huang, and D. E. Kuhl. Ecat: A new computerized tomographic imaging system for positron-emitting radiopharmaceuticals. *J. Nucl. Med*, 19:635–647, 1978.

[85] K. P.Schäfers, T. J. Spinks, P. G. Camici, P. M. Bloomfield, C. G. Rhodes, M. P. Law, C. S. R. Baker, and O. Rimoldi. Absolute quantification of myocardial blood flow with $H_2^{15}O$ and 3-dimensional PET: An experimental validation. *J. Nucl. Med.*, 43(8):1031–1040, 2002.

[86] R. Raffard, K. Amonlirdviman, J. D. Axelrod, and C. J. Tomlin. Automatic parameter identification via the adjoint method, with application to understanding planar cell polarity. *45th IEEE Conference on Decision and Control*, pages 13–18, 2006.

[87] A. Rahmim, Y. Zhou, and D. F. Wong. Direct 4d parametric image reconstruction with plasma input and reference tissue models in reversible binding imaging. *IEEE Nuclear Science Symposium Conference Record*, pages 2516–2522, 2009.

[88] M. Renardy and R. C. Rogers. *An Introduction to Partial Differential Equations.* Springer, Berlin, 1993.

[89] E. Resmerita. Regularization of ill-posed problems in banach spaces: Convergence rates. *Inverse Problems*, 21(4):1303, 2005.

[90] E. Resmerita and R. S. Anderssen. Joint additive kullback-leibler residual minimization and regularization for linear inverse problems. *Mathematical Methods in the Applied Sciences*, 30:1527–1544, 2007.

[91] E. Resmerita, H. W. Engl, and A. N. Iusem. The expectation-maximization algorithm for ill-posed integral equations: a convergence analysis. *Inverse Problems*, 23:2575–2588, 2007.

[92] R. T. Rockafellar and R. J. B. Wets. *Variational Analysis.* Springer-Verlag, New York, 1997.

[93] A. Sawatzky. *(Nonlocal) Total Variation in Medical Imaging.* Münster, July 2011.

[94] A. Sawatzky, C. Brune, F. Wübbeling, T. Kösters, K. P. Schäfers, and editors M. Burger. Accurate EM-TV algorithm in PET with low SNR. *2008 IEEE Nuclear Science Symposium Conference Record*, November 2008. DOI: 10.1109/NSSMIC.2008.4774392.

[95] A. Sawatzky, D. Tenbrinck, X. Jiang, and M. Burger. A variational framework for region-based segmentation incorporating physical noise models. CAM Report 11-81, UCLA, december 2011. (Revised: August 2012).

[96] K. P. Schäfers, T. J. Spinks, P. G. Camici, P. M. Bloomfield, C. G. Rhodes, M. P. Law, C. S. R. Baker, and O. Rimoldi. Absolute quantification of myocardial blood flow with $H_2^{15}O$ and 3-dimensional PET: An experimental validation. *J Nucl Med*, 43(8):1031–1040, 2002.

[97] L. A. Shepp and Y. Vardi. Maximum likelihood reconstruction for emission tomography. *IEEE Trans. Med. Imaging*, 1:113–122, 1982.

[98] P. T. Siegrist, L. Husmann, M. Knabenhans, O. Gaemperli, I. Valenta, T. Hoefflinghaus, H. Scheffel, P. Stolzmann, H. Alkadhi, and P. A. Kaufmann. ^{13}N-ammonia myocardial perfusion imaging with a PET/CT scanner: impact on clinical decision making and cost-effectiveness. *Eur J Nucl Med Mol Imaging*, 35:889–895, 2008.

[99] G. T. Smith, U. Liu, and B. R. Upadhyaya. Quantitative myocardial blood flow determined by dynamic PET scanning and neural network analysis. *Radiology*, 177:148, 1990.

[100] J. M. Sullivan, W. J. Taylor, W. C. Elliott, and R. Gorlin. Regional myocardial blood flow. *The Journal of Clinical Investigation*, 46(9):1402–1412, 1967.

[101] A. Tarantola. *Inverse problem theory and methods for model parameter estimation.* Society for Industrial and Applied Mathematics (SIAM), Philadelphia, 2005.

[102] Y. Vardi, L. A. Shepp, and L. Kaufman. A statistical model for positron emission tomography. *J. Am. Stat. Assoc*, 80:8–20, 1985.

[103] C. Vogel. *Computational Methods for Inverse Problems.* SIAM, Philadelphia, 2002.

[104] H. Watabe, Y. Ikoma, M. Naganawa, and M. Shidahara. PET kinetic analysis - comportmental model. *Annals of Nuclear Medicine*, 20(9):583–588, 2006.

[105] M. N. Wernick and J. N. Aarsvold. *Emission Tomography: The Fundamentals of PET and SPECT.* Elsevier Academic Press, 2004.

[106] G.-Z. Yang, R. Merrifield, S. Masood, and P. J. Kilner. Flow and myocardial interaction: an imaging perspective. *Phil. Trans. R. Soc. B*, 362:1329–1341, 2007.

[107] K. Yosida. *Functional Analysis.* Springer, Berlin, 1980.

[108] E. Zeidler. *Nonlinear Functional Analysis and Its Applications III: Variational Methods and Optimization.* Springer, Berlin, 1984.

[109] G. L. Zeng, G. T. Gullberg, and R. H. Huesman. Using linear time-invariant system theory to estimate kinetic parameters directly from projection measurements. *IEEE Transactions on Nuclear Science*, 42:2339–2346, 1995.